

Utah State University

DigitalCommons@USU

---

All Graduate Theses and Dissertations

Graduate Studies

---

12-2022

## Relativistic, Continuum Drift-Kinetic Capability in the NIMROD Plasma Fluid Code

Tyler Markham  
*Utah State University*

Follow this and additional works at: <https://digitalcommons.usu.edu/etd>



Part of the [Physics Commons](#)

---

### Recommended Citation

Markham, Tyler, "Relativistic, Continuum Drift-Kinetic Capability in the NIMROD Plasma Fluid Code" (2022). *All Graduate Theses and Dissertations*. 8683.  
<https://digitalcommons.usu.edu/etd/8683>

This Dissertation is brought to you for free and open access by the Graduate Studies at DigitalCommons@USU. It has been accepted for inclusion in All Graduate Theses and Dissertations by an authorized administrator of DigitalCommons@USU. For more information, please contact [digitalcommons@usu.edu](mailto:digitalcommons@usu.edu).



RELATIVISTIC, CONTINUUM DRIFT-KINETIC CAPABILITY IN THE NIMROD

PLASMA FLUID CODE

by

Tyler Markham

A dissertation submitted in partial fulfillment  
of the requirements for the degree

of

DOCTOR OF PHILOSOPHY

in

Physics

Approved:

---

Eric D. Held, Ph.D.  
Major Professor

---

Andrew Spencer, Ph.D.  
Committee Member

---

Jeong-Young Ji, Ph.D.  
Committee Member

---

Oscar Varela, Ph.D.  
Committee Member

---

Nghiem Nguyen, Ph.D.  
Committee Member

---

D. Richard Cutler, Ph.D.  
Vice Provost of Graduate Studies

UTAH STATE UNIVERSITY  
Logan, Utah

2022

Copyright © Tyler Markham 2022

All Rights Reserved

## ABSTRACT

Relativistic, Continuum Drift-Kinetic Capability in the NIMROD Plasma Fluid Code

by

Tyler Markham, Doctor of Philosophy

Utah State University, 2022

Major Professor: Eric D. Held, Ph.D.

Department: Physics

A "runaway" electron is an electron that, through a self-reinforcing process, accelerates to relativistic speeds. At multiple points during tokamak discharges, relativistic runaway electron (RE) beams can form. RE beams pose a serious risk in the form of severe damage to plasma facing components in ITER and future burning plasma reactors. Early RE studies used simplified geometric and transport models, but enabled feedback on the overall plasma evolution. This feedback is important for understanding the evolution of the RE current column. The work in this thesis is an important step toward self-consistently evolving an RE distribution in the plasma fluid code NIMROD. While the long-term goal is to predict RE particle and heat loads on plasma facing components in NIMROD simulations of ITER, this work seeks to verify several 2D phase-space benchmarks involving the linear and nonlinear relativistic Coulomb collision operators. Completing these benchmarks required implementation of the hefty, nonlinear Beliaev-Budker collision operator in NIMROD. In order to motivate this, we first demonstrate the need for the nonlinear operator by presenting the 2D phase space evolution of a low-density RE population according to the approximate, linearized collision operator. We show that the linear operator does not conserve momentum or energy for cases involving a diffuse, relativistic population relaxing back to a non-relativistic background plasma. Other important RE physics in the kinetic

equation, like the electric field acceleration and synchrotron radiation reaction force, is also presented. After a discussion of our implementation of the Braams-Karney differential formulation of the Beliaev-Budker operator, we show NIMROD simulations that exhibit the correct 2D phase-space evolution. In particular, we show successful benchmarking of the NIMROD and NORSE codes for the case of thermodynamic equilibrium.

(106 pages)

## PUBLIC ABSTRACT

Relativistic, Continuum Drift-Kinetic Capability in the NIMROD Plasma Fluid Code

Tyler Markham

A "runaway" electron is an electron that, through a self-reinforcing process, accelerates to relativistic speeds. At multiple points during tokamak discharges, relativistic runaway electron (RE) beams can form. RE beams pose a serious risk in the form of severe damage to plasma facing components in ITER and future burning plasma reactors. Early RE studies used simplified geometric and transport models, but enabled feedback on the overall plasma evolution. This feedback is important for understanding the evolution of the RE current column. The work in this thesis is an important step toward self-consistently evolving an RE distribution in the plasma fluid code NIMROD. While the long-term goal is to predict RE particle and heat loads on plasma facing components in NIMROD simulations of ITER, this work seeks to verify several 2D phase-space benchmarks involving the linear and nonlinear relativistic Coulomb collision operators. In particular, we show successful benchmarking of the NIMROD and NORSE codes for the case of thermodynamic equilibrium.

## ACKNOWLEDGMENTS

I would like to thank my friends Trevor, Zoe, and Josh for helping to keep me afloat when things seemed at their worst. I would also like to thank Dr. Held, Dr. Spencer, and Dr. Ji. Without Dr. Held I would not even be in the position to get my PhD. He has always been there as a support system for me and I truly value him as an advisor and friend. Dr. Spencer has taken so much of his time in order to help me grow and understand NIMROD and various numerical techniques and has always welcomed me every time I bothered him in his office. Lastly, I am grateful for Dr. Ji always pushing me to do things the right way instead of the easy way.

Tyler Markham

## CONTENTS

	Page
ABSTRACT . . . . .	iii
PUBLIC ABSTRACT . . . . .	v
ACKNOWLEDGMENTS . . . . .	vi
LIST OF FIGURES . . . . .	ix
1 INTRODUCTION . . . . .	1
2 SPECIAL RELATIVITY FRAMEWORK . . . . .	5
2.1 Relativistic Mechanics and Electromagnetism . . . . .	5
2.2 Lorentz Boosts and Einstein's Velocity Addition . . . . .	11
3 RELATIVISTIC SINGLE-PARTICLE DESCRIPTION OF A PLASMA . . . . .	18
3.1 Relativistic Lagrangian of a Charged Particle . . . . .	18
3.2 Conjugate Momenta and the Relativistic Hamiltonian . . . . .	21
3.3 Non-Canonical Hamiltonian Theory for Single-Particle Motion . . . . .	23
4 RELATIVISTIC KINETIC THEORY AND THERMODYNAMICS . . . . .	30
4.1 Relativistic Boltzmann Equation . . . . .	30
4.2 The Maxwell-Jüttner Distribution and First Law of Thermodynamics . . . . .	35
4.3 The Beliaev-Budker Operator . . . . .	42
5 TEST PARTICLE OPERATOR IN NIMROD . . . . .	45
5.1 The Sandquist and Papp Operators . . . . .	45
5.2 NIMROD Implementation . . . . .	50
5.3 Results . . . . .	56
6 BRAAHMS-KARNY FORMULATION IN NIMROD . . . . .	63
6.1 Braams-Karney Differential Formulation . . . . .	63
6.2 NIMROD Implementation . . . . .	72
6.3 Results . . . . .	76
7 CONCLUSION . . . . .	81
References . . . . .	83
APPENDICES . . . . .	86
A DISCRETIZATION OF COUPLING MATRICES . . . . .	87
A.1 Linear DKE and Papp Operator Coupling . . . . .	87
A.2 Beliaev-Budker Operator Coupling . . . . .	88
B BRAAMS-KARNEY POTENTIALS . . . . .	90
B.1 BK Potentials and Their First and Second Derivatives . . . . .	90



CURRICULUM VITAE ..... 94

## LIST OF FIGURES

	Page
Figure 1.1 Poincare plots of magnetic field lines in ITER simulation at 1.30 ms.	1
Figure 1.2 Ratio of runaway growth rate calculated by Rosenbluth's Monte Carlo code. Here $Z$ is the effective atomic ion number for the background plasma.	3
Figure 5.1 2D phase-space representation of $\tilde{f}_e^{\text{MJ}} \equiv f_e^{\text{MJ}}/N_M$ for $z_e = 1$ (left) and $z_e = 100$ (right). The parallel flow parameter $s_{V\parallel} = 0$ for both cases. The normalization coefficient $N_M$ is defined in (4.44). The 1D FE grid in $\xi$ and the collocation grid in $s$ is overlayed on the MJ distribution to give an indication of normalized momentum-space resolution. . . . .	56
Figure 5.2 Collisional relaxation of $m_e^3 f_e$ with 30 time-steps at $\Delta\tilde{t} = 10^{-3}$ and 7 time-steps at $\Delta\tilde{t} = 10^{-2}$ . The 2D normalized momentum space contour plots (read from left to right and top to bottom) show the distribution at four different times. Here $N_s = 40$ , $N_\xi = 7$ , $\mathcal{M}_\xi = 3$ , $z_e = 10$ , $z_B = 100$ , $s_{V\parallel} = 0.65$ , $\tilde{E}_\parallel = 0$ , $\alpha = 0$ , $\beta = 10^{-4}$ , and $n_B = 10^{19}\text{m}^{-3}$ . . . . .	57
Figure 5.3 Convergence test for the case in Figure 5.2. This case is run for more time-steps in order to show fluid parameters evolving to the bulk population in equilibrium. Here (left-arrow) plots the average kinetic energy for different values of $N_s$ , while (right-arrow) plots the RE number density normalized by the number density of the bulk population for the same $N_s$ values. . . . .	58
Figure 5.4 Collisional relaxation of a double MJ distribution with 20 time-steps at $\Delta\tilde{t} = 10^{-4}$ and 5 time-steps at $\Delta\tilde{t} = 10^{-3}$ . Here $N_s = 40$ , $N_\xi = 7$ , $\mathcal{M}_\xi = 3$ , $z_e = 51$ , $z_B = 510$ , $s_{V\parallel} = 0.65$ , $\tilde{E}_\parallel = 0$ , $\alpha = 0$ , $\beta = 10^{-3}$ , and $n_B = 10^{19}\text{m}^{-3}$ . . . . .	59
Figure 5.5 Evolution of unshifted ( $s_{V\parallel} = 0$ ) MJ distribution over 30 time-steps at $\Delta\tilde{t} = 10^{-1}$ . Here $N_s = 40$ , $N_\xi = 7$ , $\mathcal{M}_\xi = 3$ , $z_e = 51$ , $z_B = 510$ , $s_{V\parallel} = 0$ , $\tilde{E}_\parallel = 2.25$ , $\alpha = 0.2$ , $\beta = 10^{-3}$ , and $n_B = 10^{19}\text{m}^{-3}$ . . . . .	60
Figure 5.6 Three 1D ( $s_\perp = 0$ ) slices of the case from Figure 5.5 with two slightly modified and one un-modified. These cases are ( $\tilde{E}_\parallel = 2.25, \alpha = 0$ ) in red, ( $\tilde{E}_\parallel = 0, \alpha = 0.2$ ) in blue, and ( $\tilde{E}_\parallel = 2.25, \alpha = 0.2$ ) in purple. . . . .	61

Figure 5.7 Convergence test for the purely synchrotron term in Figure 5.6. This case is run for more time-steps in order to show fluid parameters evolving to the bulk population in equilibrium. Here (left-arrow) plots the average kinetic energy for different values of  $N_S$  (shown as np), while (right-arrow) plots the RE number density normalized by the number density of the bulk population for the same  $N_s$  values. . . . . 62

Figure 6.1  $\Upsilon$  and  $\Pi$  potentials calculated using  $\tilde{f}_e^{(0)}$  for  $l = 0$  such that  $s_{V\parallel} = 0$  and  $z_e = 51$ . Blue dots are values of the potential calculated using NIMROD and red lines are the potentials using Mathematica’s capabilities. Here  $N_s = 40$ ,  $N_\xi = 7$ , and  $\mathcal{M}_\xi = 1$ . . . . . 77

Figure 6.2 First derivatives of potentials from Figure 6.1. . . . . 78

Figure 6.3 Second derivatives of potentials from Figure 6.1. . . . . 79

Figure 6.4 Equilibrium benchmark for case in Figure 6.1 with  $\Delta\tilde{t} = 1$  over 60 time-steps. Here  $\tilde{E}_\parallel = 0$ ,  $\alpha = 0$ , and  $n_{ERe} = 10^{19}m^{-3}$ . Number density is shown in blue, while the kinetic energy is shown in red. . . . . 80

# CHAPTER 1

## INTRODUCTION

A “runaway” electron (RE) is an electron that, through a self-reinforcing process, accelerates to high speeds. At multiple points throughout tokamak operation, relativistic RE beams can form. Thermal quenching in tokamak plasmas lead to rapidly decreasing temperature and increased resistivity. Under normal tokamak operating conditions, the electric-field used to drive toroidal current does not lead to substantial RE generation. However, due to the rapid change in the plasma’s resistivity from the thermal quench, large inductive electric fields are generated. Introduction of such large inductive fields can cause a substantial fraction of the electrons in the plasma to “runaway”. Additionally, the increased resistivity drives tearing modes and large magnetic islands, as can be seen in Figure 1.1 (Izzo et al., 2011). This then leads to field-line stochasticity. As a result, REs can then run along the magnetic field to the inner wall of the tokamak.

Due to the potentially catastrophic consequences that high-energy REs can have on plasma facing components during tokamak operation, a great deal of research has gone into studying the mechanism(s) by which they are produced. In 1959, Dreicer proposed that

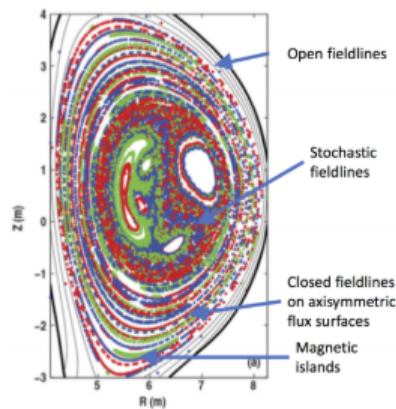


**Figure 1.1:** Poincare plots of magnetic field lines in ITER simulation at 1.30 ms.

there existed a critical electric field (often referred to as the Dreicer field) given by

$$E_D \equiv \frac{n_e e^3 \ln \Lambda}{4\pi \epsilon_0^2 m_e v_{Te}^2}, \quad (1.1)$$

where  $n_e$  is the electron number density,  $e$  is the elementary charge,  $\ln \Lambda$  is the Coulomb logarithm,  $\epsilon_0$  is the permittivity of free space,  $m_e$  is the mass of an electron, and  $v_{Te}$  is the electron thermal velocity (Dreicer, 1959). The Dreicer field is described as the electric-field past which the electric-force acting on an electron is greater than the collisional friction force. However, this critical electric-field is derived using non-relativistic mechanics, hence it is not ideal for REs that can take on relativistic speeds. Relativistic corrections to the critical field were made by Connor & Hasties (CH) who derived

$$E_{CH} \equiv \left(\frac{v_{Te}}{c}\right)^2 E_D, \quad (1.2)$$

where  $c$  is the speed of light (Connor & Hastie, 1975). Upon inspection of (1.2), the CH critical electric-field is very closely related to the Dreicer field. One thing it provides, that the Dreicer field does not, is a lower limit on the critical field. This explains why REs were not always generated according to the Dreicer mechanism. Moreover, it provides a mechanism by which REs can rejoin the bulk population.

Additionally, any process that excites even a small population of electrons can cause the RE population to grow exponentially through an avalanche process. Electron avalanche can occur in tokamak plasmas when electrons collide with neutral atoms. This collision causes impact ionization, which in turn can generate more REs. As seen in Figure 1.2, Rosenbluth showed that prior predictions of avalanche growth rates are underestimates for low electric-fields (Rosenbluth & Putvinski, 1997).

Currently the world's largest tokamak, the International Thermonuclear Experimental Reactor (ITER), is under construction in southern France. Expected power output for ITER is 500 MW, core with a core temperature of 150 million degrees Celsius and a plasma radius of 6.2 m (ITER, n.d.). Given the fact that RE generation is predicted to be more

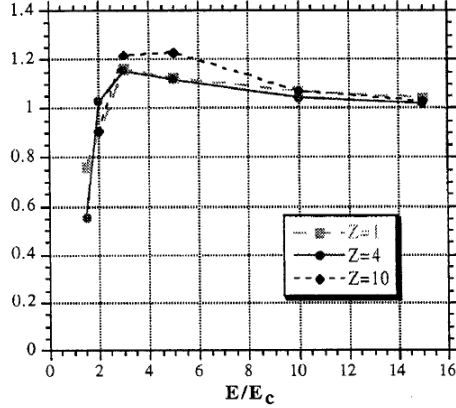


**Figure 1.2:** Ratio of runaway growth rate calculated by Rosenbluth’s Monte Carlo code. Here  $Z$  is the effective atomic ion number for the background plasma.

likely in larger tokamaks like ITER, further study into the evolution REs, and the conditions under which they form, is an important topic of study for disruption mitigation.

Early attempts to model REs used simple geometric and transport models, but enabled feedback of the RE current on the overall plasma evolution. This feedback is important for understanding the evolution of the RE current column so that better techniques can be developed to prevent RE current columns from hitting the wall. Much of the research to date has progressed by either simplifying momentum-space or physical-space dynamics. In this thesis, we shall simplify the physical-space dynamics.

While the long-term goal of this research is to predict RE particle and heat loads on plasma facing components in NIMROD simulations of ITER, this thesis seeks to verify several 2D phase-space benchmarks involving the linear and nonlinear relativistic Coulomb collision operators. NIMROD is a multi-fluid extended magnetohydrodynamics (MHD) code used in simulations of the macroscopic stability of magnetic fusion energy experiments like tokamaks (Sovinec et al., 2004). In order to motivate our RE work, in Chapters 2, 3, and 4, we first build the theory required to describe the relativistic Boltzmann equation, which is then simplified to the Beliaev-Budker operator for the small momentum transfer limit. The need for the nonlinear operator is then motivated in Chapter 5 by presenting the 2D phase space evolution of a low-density RE population according to the approximate, linearized collision operator. We show that the linear operator does not conserve momentum or

energy for cases involving a diffuse, relativistic population relaxing back to a non-relativistic background plasma. Verification of other important RE physics in the kinetic equation, like the electric field acceleration and synchrotron radiation reaction force, is also presented. After a discussion of our implementation of the Braams-Karney differential formulation of the Beliaev-Budker operator in Chapter 6, we show NIMROD simulations that exhibit the correct 2D phase-space evolution. In particular, we show successful bench-marking of the NIMROD and NORSE codes for the case of thermodynamic equilibrium. We conclude in Chapter 7 with a discussion of future work on building a successful coupling of RE physics in the NIMROD code.

CHAPTER 2  
SPECIAL RELATIVITY FRAMEWORK

### 2.1 Relativistic Mechanics and Electromagnetism

Since the ultimate goal is to provide a kinetic description of the plasma using a single-particle distribution function defined in a 6D phase-space, we first look to define the four-vector analogues to  $\mathbf{x}$  and  $\mathbf{p}$ . In 4D position space the square of the length of a line element in Cartesian coordinates in the lab-frame is given by

$$\begin{aligned} dx^\mu dx_\mu &= -c^2 dt^2 + dx^2 + dy^2 + dz^2 \\ &= \eta_{\mu\nu} dx^\mu dx^\nu, \end{aligned} \tag{2.1}$$

where  $x^\mu \doteq (ct, x^i)$  is the four-position. The rank two tensor  $\eta_{\mu\nu}$  is known as the Minkowski metric, which is the metric for 4D Cartesian coordinates. In general, we denote any arbitrary metric by  $g_{\mu\nu}$ . In this thesis, we shall assume the Einstein summation convention for repeated indices. Additionally, unless stated otherwise, Greek indices will range from 0-3 and roman indices will range from 1-3.

Next, we define the proper-time  $\tau$  as the time experienced by an observer traveling at the same speed, and located at the same position, as the origin of the particle's reference frame, or  $dx^\mu dx_\mu = -c^2 d\tau^2$ . Using this expression, (2.1), and the invariance of (2.1), the relationship between proper-time and time can be shown to be given by

$$\begin{aligned} d\tau &= \sqrt{1 - \frac{1}{c^2} \left( \left( \frac{dx}{dt} \right)^2 + \left( \frac{dy}{dt} \right)^2 + \left( \frac{dz}{dt} \right)^2 \right)} dt \\ &= \sqrt{1 - \frac{v^2}{c^2}} dt \\ &\equiv \frac{dt}{\gamma}. \end{aligned} \tag{2.2}$$



Additionally, it should be noted that the proper-time is a scalar, i.e. it does not transform under any coordinate transformation. This concept is more easily understood by considering the general form of proper-time differential:

$$d\tau = \frac{1}{c} \sqrt{-g_{\mu\nu} dx^\mu dx^\nu}. \quad (2.3)$$

As can be seen in (2.3), the right-hand-side (RHS) is comprised of three tensors with all indices contracted, which implies  $d\tau$  is a scalar and therefore does not transform. However, if we further assume that we are unconcerned about transforming our time coordinate, and restrict all transformations to be time-independent transformations such that the transformation on the spatial coordinates are curvilinear, then  $g_{00} = -1$  and  $x^0 = ct$  in all coordinate transformations under this constraint. Applying this constraint, (2.3) reduces to

$$\begin{aligned} d\tau &= \frac{1}{c} \sqrt{-g_{00} dx^0 dx^0 - g_{ij} dx^i dx^j} \\ &= \sqrt{1 - \frac{1}{c^2} g_{ij} v^i v^j} dt \\ &= \sqrt{1 - \frac{v^2}{c^2}} dt \\ &= \frac{dt}{\gamma}. \end{aligned} \quad (2.4)$$

Note that this is simply a consequence of the invariance of three-vector magnitudes in 3D position space under spatial curvilinear transformations. Ergo, the relationship between time and proper-time still holds under these types of transformations. However, a 4D curvilinear analogue would require the time component to transform as well. As a result, it is important to note that throughout this thesis, when we say that something is invariant under “curvilinear transformations”, we are only referring to the time independent transformations of the spatial components normally used in 3D position space. The only instance in which we will transform the time coordinate will be under a Lorentz transformation, which will be discussed in more detail in a later section.

Now that we have established our approach, we define a few more parameters. The general prescription to convert 3D non-relativistic vectors defined by time-derivatives to the 4D relativistic ones is to “upgrade” derivatives with respect time to derivatives with respect to  $\tau$  and replace three-vectors with their four-vector equivalents. For example, the four-velocity  $u^\mu$  is given by

$$u^\mu \equiv \frac{dx^\mu}{d\tau} \doteq (\gamma c, \gamma v^i). \quad (2.5)$$

This procedure ensures that the resulting vector is in fact a four-vector and is therefore covariant. Following this procedure we can also define the four-momentum and four-force (sometimes referred to as the Minkowski force)  $p^\mu$  and  $K^\mu$  by

$$p^\mu \equiv m u^\mu \quad (2.6)$$

$$K^\mu \equiv \frac{dp^\mu}{d\tau}, \quad (2.7)$$

where  $m$  is the mass. A direct consequence of this “upgrade” is that the magnitudes of the four-vector analogues are invariant under *any* transformation. Using the example of the four-velocity again, it can be seen that in Cartesian coordinates:

$$u^\mu u_\mu = -\gamma^2 c^2 + \gamma^2 v^2 \quad (2.8)$$

$$= -c^2 \left( \frac{1 - \frac{v^2}{c^2}}{1 - \frac{v^2}{c^2}} \right) \quad (2.9)$$

$$= -c^2. \quad (2.10)$$

Note that  $u^\mu u_\mu = -c^2$  is a coordinate independent statement since  $c$  is a scalar. This is due entirely to the tensorial nature of  $x^\mu$  and the the invariance of  $\tau$ .

With basic definitions out of the way, we turn our attention to electromagnetism in special relativity. First, we define the Faraday tensor  $F_{\mu\nu}$  as

$$F_{\mu\nu} \equiv 2\nabla_{[\mu} A_{\nu]}, \quad (2.11)$$

where  $A^\mu \doteq (\Phi/c, A^i)$  is the four-vector potential,  $\nabla_\mu$  is the covariant derivative with respect to  $x^\mu$ ,  $\Phi$  is the electrostatic potential, and  $A^i$  is the three-vector potential. The brackets around the indices in (2.11) denote the anti-symmetric part of the tensor over the enclosed indices. Technically, the Faraday tensor is defined in terms of the covariant derivative  $\nabla_\mu$ , which when operating on an arbitrary four-vector  $V_\nu$  and an arbitrary rank two tensor  $V_{\mu\nu}$  is given by

$$\nabla_\mu V_\nu \equiv \partial_\mu V_\nu - \Gamma_{\mu\nu}^\lambda V_\lambda \quad (2.12)$$

$$\nabla_\mu V_{\nu\lambda} \equiv \partial_\mu V_{\nu\lambda} - \Gamma_{\mu\nu}^\rho V_{\rho\lambda} - \Gamma_{\mu\lambda}^\rho V_{\nu\rho}, \quad (2.13)$$

where  $\Gamma_{\mu\nu}^\lambda$  is the connection.

We can simplify the expression in (2.11) by assuming a metric compatible connection, or a connection that satisfied the the condition:

$$\nabla_\mu g_{\nu\lambda} = \partial_\mu g_{\nu\lambda} - \Gamma_{\mu\nu}^\rho g_{\rho\lambda} - \Gamma_{\mu\lambda}^\rho g_{\nu\rho} = 0. \quad (2.14)$$

Since the metric is always symmetric, solving for  $\Gamma_{\mu\nu}^\lambda$  yields the Christoffel connection

$$\Gamma_{\mu\nu}^\lambda = \frac{1}{2} g^{\lambda\rho} (\partial_\mu g_{\nu\rho} + \partial_\nu g_{\rho\mu} - \partial_\rho g_{\mu\nu}), \quad (2.15)$$

which is symmetric in its two lower indices by construction. By choosing this connection, (2.11) reduces to

$$F_{\mu\nu} = 2\partial_{[\mu} A_{\nu]}. \quad (2.16)$$

At this point, we need to now relate (2.11) to the relativistic version of Maxwell's equations. In Cartesian coordinates, the spacetime and spatial components of the Faraday

tensor in the Lorenz gauge are given by

$$F_{0i} = -\frac{E_i}{c} \quad (2.17)$$

$$F_{ij} = \varepsilon_{ijk} B^k, \quad (2.18)$$

where  $\varepsilon_{ijk}$  is the 3D Levi-Chevita symbol and  $B^i \equiv \varepsilon^{ijk} \partial_j A_k$ . While (2.17) is invariant under curvilinear transformations, (2.18) is not, since the Levi-Chevita symbol is not a tensor. Hence, by the Principle of General Covariance (PGC) we must find the tensor analogue to  $\varepsilon_{ijk}$ . Luckily this is easily done by noting that  $\varepsilon_{ijk}$  transforms as a tensor density.

Following Carroll's procedure (Carroll, 1997) for constructing the Levi-Chevita tensor for the 3D case, the 3D Levi-Chevita tensors (in its raised and lowered forms) is given by

$$\epsilon_{ijk} \equiv \sqrt{|g|} \varepsilon_{ijk} \quad (2.19)$$

$$\epsilon^{ijk} \equiv \frac{1}{\sqrt{|g|}} \varepsilon^{ijk}, \quad (2.20)$$

where  $g \doteq \det(g_{\mu\nu})$ . For curvilinear transformations,  $\sqrt{|g|} = h_1 h_2 h_3$ , with the  $h_i$ 's defined as the corresponding curvilinear scale-factors. With Levi-Chevita tensor now defined, the last thing to do is to upgrade (2.18) and the definition of the magnetic field to

$$F_{ij} = \epsilon_{ijk} B^k \quad (2.21)$$

$$B^k \equiv \epsilon^{ijk} \partial_j A_k. \quad (2.22)$$

The covariant forms of Maxwell's equations are given by

$$\nabla_\nu F^{\mu\nu} = \mu_0 J^\mu \quad (2.23)$$

$$\nabla_{[\mu} F_{\nu\lambda]} = 0, \quad (2.24)$$

such that  $\mu_0$  is the magnetic permeability in a vacuum,  $J^\mu \doteq (\rho c, J^i)$  is the four-vector

current density,  $\rho$  is the lab-frame volumetric charge density, and  $J^i$  is the 3-vector current density. Utilizing (2.21) and (2.22) to unpack the  $\mu = 0$  component of (2.23) yields

$$\begin{aligned}\mu_0 \rho c &= \partial_\nu F^{0\nu} + \Gamma_{\nu\lambda}^0 F^{\lambda\nu} + \Gamma_{\nu\lambda}^\nu F^{0\lambda} \\ &= \frac{1}{c} \partial_i E^i + \frac{1}{c\sqrt{|g|}} \partial_i \left( \sqrt{|g|} \right) E^i,\end{aligned}$$

which only occurs for a time-independent metric. Combining both terms on the RHS using the product rule gives us the final result

$$\frac{1}{\sqrt{|g|}} \partial_i \left( \sqrt{|g|} g^{ij} E_j \right) = \frac{\rho}{\varepsilon_0}, \quad (2.25)$$

where  $\varepsilon_0$  as the vacuum permittivity. Note that the left-hand-side (LHS) of (2.25) is just the curvilinear form of the divergence in a coordinate basis, which only differs from its orthonormal analogue by its corresponding scale-factor (e.g. in spherical coordinates  $\mathbf{e}_\phi = r \sin(\theta) \hat{\phi}$ ). Thus, (2.25) is just the differential form of Gauss's law. The inverse metric is introduced simply to reproduce the same format of the divergence as found in most of physics literature. Following a similar procedure, the  $\mu = i$  component yields

$$\epsilon^{ijk} \partial_j B_k = \mu_0 J^i + \mu_0 \varepsilon_0 \partial_t E^i, \quad (2.26)$$

which is exactly the Maxwell-Ampere law.

An equivalent representation of (2.24) is given by

$$\epsilon^{\mu\sigma\nu\lambda} \partial_\sigma F_{\nu\lambda} = 0.$$

Note that the covariant derivative reduces to partial derivatives for the same reason shown to prove (2.11). The 4D Levi-Chevita tensor  $\epsilon^{\mu\sigma\nu\lambda}$  is analogous to (2.20) with the convention  $\epsilon^{0ijk} = \epsilon^{ijk}$  (some authors put a minus sign in front of the 3D version). The  $\mu = 0$  component becomes

$$\frac{1}{\sqrt{|g|}} \partial_i \left( \sqrt{|g|} g^{ij} B_j \right) = 0, \quad (2.27)$$

which is just  $\nabla \cdot \mathbf{B} = 0$ . For  $\mu = i$  we have

$$\begin{aligned} 0 &= \epsilon^{i0jk} \partial_0 F_{jk} + \epsilon^{ij0k} \partial_j F_{0k} + \epsilon^{ijk0} F_{k0} \\ &= -\frac{1}{c} \epsilon^{ijk} \partial_t (\epsilon_{jkl} B^l) - \frac{2}{c} \epsilon^{ijk} \partial_j E_k \\ &= -\partial_t B^i - \epsilon^{ijk} \partial_j E_k. \end{aligned}$$

Therefore, the  $\mu = i$  component of the Bianchi identity is

$$\epsilon^{ijk} \partial_j E_k = -\partial_t B^i, \quad (2.28)$$

or Faraday's law.

For curvilinear transformations, Maxwell's equations retain their non-relativistic form. It is important to note that restricting our transformations in this manner is only appropriate when sources of strong gravitational fields are absent. By this we mean that while we are always free to restrict our transformations in this way, strong gravitational fields introduce significant spacetime curvature, which would make it disadvantageous to restrict our transformations in such a way. However, since our intent here is to study relativistic electrons, which have incredibly small mass, in a local lab-frame environment on Earth, we can safely restrict our transformations in this manner.

## 2.2 Lorentz Boosts and Einstein's Velocity Addition

The last topic to be discussed in this section concerns the transformation laws in special relativity due to a change of reference frame. Specifically, we will derive the general Lorentz boost in order to determine the expression for the relative velocity. For the sake of simplicity we shall consider first a boost only in the  $x$ -direction and then generalize to a boost in an arbitrary direction. From the invariance of the  $dx^\mu dx_\mu$  in (2.1), in Cartesian coordinates:

$$-c^2 dt^2 + dx^2 + dy^2 + dz^2 = -c^2 (dt')^2 + (dx')^2 + (dy')^2 + (dz')^2.$$

At this point, we must ask ourselves what types of transformations we are willing to consider. A translation (i.e.  $x'^{\mu} = x^{\mu} + a^{\mu}$  where  $a^{\mu}$  is a four-vector of constant magnitude) clearly leaves the space-time interval invariant, but is not useful to consider for our purposes since the translation simply vanishes after taking the differential. If we take as an axiom Einstein's hypothesis of the homogeneity of space-time and the isotropy of space, then the transformation is linear and is independent of space-time. In this section, we shall only consider the impact of "boosts" in space-time (differences in measurements due to relative speed). One may also consider the impact of rotations, but since the ultimate goal of this section is to determine the form of the relative velocity, boosts are sufficient. Mathematically, such a transformation can be expressed as

$$dx'^{\mu} = \Lambda^{\mu}_{\nu} dx^{\nu}, \quad (2.29)$$

such that  $\Lambda^{\mu}_{\nu}$  satisfies

$$\eta_{\mu\nu} = \eta_{\lambda\rho} \Lambda^{\lambda}_{\mu} \Lambda^{\rho}_{\nu}, \quad (2.30)$$

or in vector notation  $\boldsymbol{\eta} = \mathbf{\Lambda}^T \boldsymbol{\eta} \mathbf{\Lambda}$ . Conceptually, what we have just done is reinforce the PGC.

If we denote the lab frame as  $K$  and the boosted frame as  $K'$ , and assume that  $dx = v_{Fx} dt$ , where  $v_{Fx}$  is the instantaneous relative speed between the two frames (where the  $F$  denotes that the velocity is that of the new frame), then (2.29) can be represented as

$$\begin{bmatrix} cdt' \\ dx' \\ dy' \\ dz' \end{bmatrix} = \begin{bmatrix} \Lambda^0_0 & \Lambda^0_1 & 0 & 0 \\ \Lambda^1_0 & \Lambda^1_1 & 0 & 0 \\ 0 & 0 & 1 & 0 \\ 0 & 0 & 0 & 1 \end{bmatrix} \begin{bmatrix} cdt \\ dx \\ dy \\ dz \end{bmatrix}. \quad (2.31)$$

Writing out  $\eta_{00}$ ,  $\eta_{11}$ , and  $\eta_{01}$  in (2.30), we get the following system of equations:

$$-(\Lambda^0_0)^2 + (\Lambda^1_0)^2 = -1 \quad (2.32)$$

$$-(\Lambda^0_1)^2 + (\Lambda^1_1)^2 = 1 \quad (2.33)$$

$$-(\Lambda^0_0)(\Lambda^0_1) + (\Lambda^1_0)(\Lambda^1_1) = 0. \quad (2.34)$$

Though (2.32)-(2.34) is an under-determined system of equations, a clever choice of parametrization, and (2.31), will help us find a solution. Letting  $\Lambda^0_1 = \sinh \phi$  and  $\Lambda^1_0 = \sinh \psi$ , where  $\phi$  and  $\psi$  are arbitrary functions, and plugging these new expressions into (2.32)-(2.34), we find that

$$\Lambda^0_0 = \sqrt{1 + \sinh^2 \phi} = \cosh \phi$$

$$\Lambda^1_1 = \sqrt{1 + \sinh^2 \psi} = \cosh \psi$$

$$\phi = \psi.$$

Defining this particular transformation matrix as  $(\Lambda_x)^\mu{}_\nu$ , we now have

$$(\Lambda_x)^\mu{}_\nu := \begin{bmatrix} \cosh \phi & \sinh \phi & 0 & 0 \\ \sinh \phi & \cosh \phi & 0 & 0 \\ 0 & 0 & 1 & 0 \\ 0 & 0 & 0 & 1 \end{bmatrix}.$$

Now, after taking the  $x$ -equation from (2.31) at the origin, and some algebra, we get the condition

$$\tanh \phi = -\frac{v_F x}{c},$$

or

$$\sinh \phi = -\frac{\gamma_F v_F x}{c}$$

$$\cosh \phi = \gamma_F,$$



where  $\gamma_F$  is just the Lorentz factor for  $\mathbf{v} \rightarrow \mathbf{v}_F$ . Therefore, the Lorentz boost matrix for a boost in the  $x$  direction from  $K$  to  $K'$  is given by

$$(\Lambda_x)^\mu{}_\nu := \begin{bmatrix} \gamma_F & -\gamma_F v_{Fx}/c & 0 & 0 \\ -\gamma_F v_{Fx}/c & \gamma_F & 0 & 0 \\ 0 & 0 & 1 & 0 \\ 0 & 0 & 0 & 1 \end{bmatrix}. \quad (2.35)$$

Note that plugging (2.35) into (2.31) yields the well known 1D Lorentz transformations:

$$dt' = \gamma_F \left( dt - \frac{v_{Fx}}{c^2} dx \right) \quad (2.36)$$

$$dx' = \gamma_F (dx - v_{Fx} dt) \quad (2.37)$$

$$dy' = dy \quad (2.38)$$

$$dz' = dz. \quad (2.39)$$

For (2.36)-(2.39), we can generalize to an arbitrary frame velocity pointing in an arbitrary direction. In general, we say that  $dx = v_x dt$ , where  $v_x$  is the  $x$ -component of the particle velocity. Furthermore, the expressions for time-dilation and relative velocity in this case can be derived by dividing (2.36) by  $dt$  and dividing (2.37) by  $dt'$ . Doing so yields

$$\frac{dt'}{dt} = \gamma_F \left( 1 - \frac{v_x v_{Fx}}{c^2} \right) \quad (2.40)$$

$$v'_x = \frac{v_x - v_{Fx}}{1 - \frac{v_x v_{Fx}}{c^2}}. \quad (2.41)$$

As we have just shown, finding the Lorentz boost in one direction, when the two frames are collinear, is relatively straight forward. However, what we desire is the general boost for an arbitrary  $\mathbf{v}$ . The rigorous way to do this involves the application of Lie theory, and requires a great deal of calculation. Alternatively, we could take the exact same approach as before, but now we would have a system of 16 equations to solve. Instead, we will make a rotational argument to get the general form of the Lorentz boost.

To generalize (2.35), we will effectively take the  $K'$  frame and rotate it to an arbitrary orientation relative to the  $K$  frame, thereby allowing for the frame velocity to point in any arbitrary direction. Under such a transformation, the time component should not transform, while space-time and spatial components will transform like 3-vectors and 3D dyadic tensors, respectively. Enforcing these transformation properties and ensuring that the general form reduces to (2.35) guarantees the correct general form. Hence, we will simply rewrite the components (2.35) in terms 3-vectors and 3D dyadic tensors.

In the 1D case,  $v_{Fx} = v_F$  and  $v_{Fy} = v_{Fz} = 0$ . Consider  $(\Lambda_x)^0_0$  for  $v_{Fy} \neq 0$  and  $v_{Fz} \neq 0$ . The Lorentz factor is a scalar under SL transformation. Ergo, we have  $\Lambda^0_0 = \gamma_F$ . For  $(\Lambda_x)^i_0$  and  $(\Lambda_x)^0_i$ , we can rewrite these components in 3-vector notation as

$$\Lambda^i_0 = -\frac{\gamma_F v_F^i}{c} \quad (2.42)$$

$$\Lambda^0_i = -\frac{\gamma_F v_{Fi}}{c}. \quad (2.43)$$

The tricky part of (2.35) to generalize is  $(\Lambda_x)^i_j$ . The trick is to decompose this part of the matrix into 3-covariant pieces, or

$$\begin{aligned} (\Lambda_x)^i_j &:= \begin{bmatrix} 1 & 0 & 0 \\ 0 & 1 & 0 \\ 0 & 0 & 1 \end{bmatrix} + \begin{bmatrix} \gamma_F - 1 & 0 & 0 \\ 0 & 0 & 0 \\ 0 & 0 & 0 \end{bmatrix} \\ &= \begin{bmatrix} 1 & 0 & 0 \\ 0 & 1 & 0 \\ 0 & 0 & 1 \end{bmatrix} + \frac{\gamma_F - 1}{v_F^2} \begin{bmatrix} v_{Fx}v_{Fx} & v_{Fx}v_{Fy} & v_{Fx}v_{Fz} \\ v_{Fy}v_{Fx} & v_{Fy}v_{Fy} & v_{Fy}v_{Fz} \\ v_{Fz}v_{Fx} & v_{Fz}v_{Fy} & v_{Fz}v_{Fz} \end{bmatrix} \end{aligned}$$

By inspection, the spatial components are given by

$$\Lambda^i_j = \delta^i_j + (\gamma_F - 1) \frac{v_F^i v_{Fj}}{v_F^2}. \quad (2.44)$$

Therefore, the general Lorentz boost is

$$\Lambda^\mu{}_\nu := \begin{bmatrix} \gamma_F & -\gamma_F \frac{v_{Fx}}{c} & -\gamma_F \frac{v_{Fy}}{c} & -\gamma_F \frac{v_{Fz}}{c} \\ -\gamma_F \frac{v_{Fx}}{c} & 1 + (\gamma_F - 1) \frac{v_{Fx}^2}{v_F^2} & (\gamma_F - 1) \frac{v_{Fx} v_{Fy}}{v_F^2} & (\gamma_F - 1) \frac{v_{Fx} v_{Fz}}{v_F^2} \\ -\gamma_F \frac{v_{Fy}}{c} & (\gamma_F - 1) \frac{v_{Fy} v_{Fx}}{v_F^2} & 1 + (\gamma_F - 1) \frac{v_{Fy}^2}{v_F^2} & (\gamma_F - 1) \frac{v_{Fy} v_{Fz}}{v_F^2} \\ -\gamma_F \frac{v_{Fz}}{c} & (\gamma_F - 1) \frac{v_{Fz} v_{Fx}}{v_F^2} & (\gamma_F - 1) \frac{v_{Fz} v_{Fy}}{v_F^2} & 1 + (\gamma_F - 1) \frac{v_{Fz}^2}{v_F^2} \end{bmatrix}. \quad (2.45)$$

Thanks to (2.45), we can now find the general form for the instantaneous relative velocity (henceforth we shall simply call this the relative velocity) Therefore, the logical choice would be to boost the four-velocity or

$$u'^\mu = \Lambda^\mu{}_\nu u^\nu. \quad (2.46)$$

Note that an equivalent representation of the transformed four-velocity is  $u'^\mu := (\gamma'c, \gamma'v'^n)$ . Ultimately, we wish to know what  $v'^n$  is. Unfortunately, we do not know how the Lorentz factor transforms in this frame yet. However, this information is stored in the time component of (2.45). Unpacking the  $\mu = 0$  component and using  $u'^0 = \gamma'c$  yields

$$\begin{aligned} u'^0 &= \Lambda^0{}_0 u^0 + \Lambda^0{}_i u^i \\ \gamma'c &= \gamma\gamma_F c - \gamma\gamma_F \left( \frac{v^n v_{Fn}}{c} \right) \\ \gamma' &= \gamma\gamma_F \left( 1 - \frac{v^n v_{Fn}}{c^2} \right). \end{aligned} \quad (2.47)$$

Now that we have  $\gamma'$ , taking the  $\mu = i$  component and dividing by this factor shows that the relative velocity is

$$\begin{aligned} v'^i &= \frac{u'^i}{\gamma'} \\ &= \frac{1}{\gamma'} \left[ -\gamma\gamma_F v_F^i + \gamma v^i + \gamma(\gamma_F - 1) \frac{1}{v_F^2} (v^n v_{Fn}) v_F^i \right] \\ &= \frac{1}{1 - \frac{v^n v_{Fn}}{c^2}} \left[ \frac{1}{\gamma_F} v^i - v_F^i + \frac{1}{v_F^2} \left( 1 - \frac{1}{\gamma_F} \right) (v^n v_{Fn}) v_F^i \right]. \end{aligned} \quad (2.48)$$

Though the above expression for the relative velocity is correct, the correction to the non-relativistic Galilean transformation  $\mathbf{v}' = \mathbf{v} - \mathbf{v}_F$  is not obvious from this form. The usual prescription to remedy this is to utilize the BAC-CAD vector identity, which in index notation, and Cartesian coordinates, takes the form

$$\varepsilon^{ijk}\varepsilon_{klm}v_F^jv_F^lv_F^m = (v^n v_{Fn})v_F^i - v_F^2v^i. \quad (2.49)$$

(2.49) lets us rewrite (2.48) in vector notation as

$$\mathbf{v}' = \frac{1}{1 - \frac{\mathbf{v} \cdot \mathbf{v}_F}{c^2}} \left[ \mathbf{v} - \mathbf{v}_F - \left( \frac{\gamma_F - 1}{\gamma_F} \right) \mathbf{v}_\perp \right], \quad (2.50)$$

where  $\mathbf{v}_\perp \equiv \mathbf{v}_F \times (\mathbf{v} \times \mathbf{v}_F)$  such that  $\mathbf{v} = \mathbf{v}_\parallel + \mathbf{v}_\perp$ .

The form given in (2.50) makes it much easier to see the relativistic corrections to the Galilean relative velocity. In particular, the denominator is simply a consequence of general expression for time-dilation

$$\frac{dt'}{dt} = \gamma_F \left( 1 - \frac{v^n v_{Fn}}{c^2} \right). \quad (2.51)$$

The previous equation is derived by applying the general boost to  $x^\mu$  and taking the  $\mu = 0$  component. The only other correction is the  $\mathbf{v}_\perp$  term, which shall be referred to as the non-collinear term. Note this disappears when the two frames *are* collinear. Moreover, for  $v \ll c$  and  $v_F \ll c$ ,  $\mathbf{v}' \approx \mathbf{v} - \mathbf{v}_F$ .

## CHAPTER 3

## RELATIVISTIC SINGLE-PARTICLE DESCRIPTION OF A PLASMA

**3.1 Relativistic Lagrangian of a Charged Particle**

In classical mechanics, Hamilton's principle of least action defines the Lagrangian  $L$  for a single particle as the time derivative of the action  $S$ , or

$$S = \int_{t_1}^{t_2} L dt, \quad (3.1)$$

such that  $\delta S = 0$ , where  $\delta S$  is the so called "variation" of  $S$ . Hence, Hamilton's principle requires that the action be a scalar. Non-relativistically, time is considered to be absolute and is therefore invariant, forcing  $\delta L = 0$ . To construct a relativistic analogue to Hamilton's principle, we will need to apply the same upgrade method that we did in the previous section. There are two different ways that we can accomplish this.

The first way would be to construct a fully covariant variational principle, with a covariant Lagrangian  $\mathcal{L}$  related to the action  $\mathcal{S}$  by

$$\mathcal{S} \equiv \int_{\tau_1}^{\tau_2} \mathcal{L} d\tau, \quad (3.2)$$

where  $\mathcal{L} = \mathcal{L}(x^\mu, u^\mu)$  and  $\mathcal{S}$  is not necessarily  $S$ . Note that this Lagrangian does not preserve the classical Euler-Lagrange equation. The covariant Euler-Lagrange equation can be derived in the same manner as the classical one, but with  $x^\mu$  and  $u^\mu$  as the parameters to be varied and  $\delta x^\mu$  vanishing at the endpoints. Varying (3.2), and utilizing integration by

parts on the term containing  $\delta u^\mu$ , we find that

$$\begin{aligned}\delta S &= \int_{\tau_1}^{\tau_2} \left( \frac{\partial \mathcal{L}}{\partial x^\mu} \delta x^\mu + \frac{\partial \mathcal{L}}{\partial u^\mu} \delta \left( \frac{dx^\mu}{d\tau} \right) \right) d\tau \\ &= \frac{\partial \mathcal{L}}{\partial u^\mu} \delta x^\mu \Big|_{\tau_1}^{\tau_2} + \int_{\tau_1}^{\tau_2} \left( \frac{\partial \mathcal{L}}{\partial x^\mu} \delta x^\mu - \frac{d}{d\tau} \left( \frac{\partial \mathcal{L}}{\partial u^\mu} \right) \delta x^\mu \right) d\tau \\ &= \int_{\tau_1}^{\tau_2} \left( \frac{\partial \mathcal{L}}{\partial x^\mu} - \frac{d}{d\tau} \left( \frac{\partial \mathcal{L}}{\partial u^\mu} \right) \right) \delta x^\mu d\tau.\end{aligned}$$

Enforcing  $\delta S = 0$  yields the relativistic Euler-Lagrange equation

$$\frac{\partial \mathcal{L}}{\partial x^\mu} - \frac{d}{d\tau} \left( \frac{\partial \mathcal{L}}{\partial u^\mu} \right) = 0. \quad (3.3)$$

Alternatively, we could simply make use of the relationship  $dt = \gamma d\tau$  to upgrade (3.1) to

$$S \equiv \int_{\tau_1}^{\tau_2} \gamma L_R d\tau, \quad (3.4)$$

where  $L_R = L_R(x^i, v^i, t)$  is the relativistic analogue to the classical Lagrangian. The subscript on the Lagrangian is simply a means of distinguishing the Lagrangian in the  $v \sim c$  regime. Note that the Lagrangian in (3.4) preserves the original Euler-Lagrange equation. We shall derive both relativistic forms of the Lagrangian.

While (3.4) looks fairly intuitive, the limitations of this form comes from the limited number of four-vectors we have to construct invariants with. If we wish for  $L_R \approx L$  when  $v \ll c$ , then we should choose our invariants such that the equations of motion reduce to the equations of motion generated by the non-relativistic Lagrangian for an ionized plasma:

$$L(\mathbf{x}, \mathbf{v}, t) = \frac{1}{2} m v^2 - q\Phi + q\mathbf{v} \cdot \mathbf{A}. \quad (3.5)$$

In other words, we will require that  $\delta L_R \approx \delta L$  in this limit. To imitate terms of (3.5) for a relativistic Lagrangian, we will further break up the action in (3.4) into  $S = S_F + S_{EM}$ , where  $S_F$  is the free-particle contribution and  $S_{EM}$  is the electromagnetic contribution. The Lagrangian is split up in the same manner.

First, we will consider the free-particle Lagrangian  $L_{RF}$ . The kinetic term in (3.5) suggests that the contraction  $u^\mu u_\mu = -c^2$  provides the correct analogue to  $v^2$ . To account for possible coefficients in front, we will pick  $\gamma L_{RF} = -ac^2$ , where  $a$  is an arbitrary constant. For  $v \ll c$ ,  $\delta L_{RF} \approx \delta (av^2/2)$ . Hence,  $a = m$  and the free-particle Lagrangian is given by

$$L_{RF} = -mc^2 \sqrt{1 - \frac{v^2}{c^2}}. \quad (3.6)$$

Analyzing the remaining terms in (3.5), the intuitive choice for  $L_{REM}$ 's invariant is  $u^\mu A_\mu = -\gamma\Phi + \gamma v^i A_i$ . Note that this invariant is identical to the last two terms in the non-relativistic Lagrangian for  $v \ll c$  save for the  $q$  out front. Therefore,  $L_{REM}$  is just

$$L_{REM} = -q\Phi + qv^i A_i, \quad (3.7)$$

which is exactly the same as the classical version. Finally, combining (3.6) and (3.7), the total relativistic Lagrangian for a single charged particle is then

$$L_R = -mc^2 \sqrt{1 - \frac{v^2}{c^2}} - q\Phi + qv^i A_i, \quad (3.8)$$

which produces the same equations of motion as (3.5) when  $v \ll c$ .

Having determined the invariants that describe the correct kinetic and electromagnetic behavior, they can again be used to determine the form of the covariant Lagrangian, albeit with a different coefficient on  $\mathcal{L}_F$ . Following the same procedure as the non-covariant formulation, it can be shown that the covariant version of (3.8) is

$$\mathcal{L} = \frac{1}{2} m u^\mu u_\mu + q u^\mu A_\mu. \quad (3.9)$$

The key difference between the covariant and non-covariant forms of the Lagrangian is the covariant version is a scalar, while the non-covariant one is only invariant under curvilinear transformations. As we will see, this choice has a significant effect on the construction of the relativistic Hamiltonian.

### 3.2 Conjugate Momenta and the Relativistic Hamiltonian

The construction of both relativistic Hamiltonians follows the same procedure as in classical mechanics, or

$$H_R \equiv P_i v^i - L_R \quad (3.10)$$

$$\mathcal{H} \equiv \mathcal{P}_\mu u^\mu - \mathcal{L}, \quad (3.11)$$

where  $P_i$  are the conjugate momenta corresponding to the non-covariant Hamiltonian  $H_R$  and  $\mathcal{P}_\mu$  are the conjugate momenta corresponding to the covariant Hamiltonian  $\mathcal{H}$ . The conjugate momenta for each are defined by the term inside the time/proper-time derivative in their respective Euler-Lagrange equations. These momenta are given by:

$$P_i \equiv \frac{\partial L_R}{\partial v^i} \quad (3.12)$$

$$\mathcal{P}_\mu \equiv \frac{\partial \mathcal{L}}{\partial u^\mu}. \quad (3.13)$$

For the time being, we shall assume that scalar and vector potentials are independent of the particle velocity. Therefore, under this assumption, the conjugate four-momentum is given by

$$\mathcal{P}_\mu = p_\mu + qA_\mu, \quad (3.14)$$

and the non-covariant conjugate momenta are given by

$$P_i = p_i + qA_i. \quad (3.15)$$

Upon inspection of (3.14) and (3.15), we can see that  $P_i = \mathcal{P}_i$ . Conceptually, this tells us that the choice to use the non-covariant Lagrangian formulation has effectively confined us to move along a surface in 8D phase-space, reducing the effective number of dimensions down to six. Additionally, we shall use  $\mathcal{P}_\mu \rightarrow P_\mu$  to represent the components of the conjugate momenta for the covariant formulation since the spatial components of the covariant case



overlap with the conjugate momenta in the non-covariant case.

With all conjugate momenta found, applying the transformations described by (3.10) and (3.11) yields the following covariant and non-covariant Hamiltonians

$$\mathcal{H} = \frac{g^{\mu\nu}}{2m} (P_\mu P_\nu - 2qP_\mu A_\nu + q^2 A_\mu A_\nu) \quad (3.16)$$

$$H_R = mc^2 \sqrt{1 + \frac{g^{ij}}{m^2 c^2} (P_i P_j - 2qP_i A_j + q^2 A_i A_j)} + q\Phi, \quad (3.17)$$

where both Hamiltonians are written in terms of their respective independent variables (i.e.  $(x^\mu, P^\mu)$  for the covariant case and  $(x^i, P^i)$  for the non-covariant case). Note that we can express (3.17) in the simpler form

$$H_R = \mathcal{E} + q\Phi, \quad (3.18)$$

with relativistic energy denoted by  $\mathcal{E} = \gamma mc^2$ . Note that  $p^0 c = \mathcal{E}$  and  $qA^0 c = q\Phi$ , which implies that  $P^0 = H_R/c$ . Therefore the covariant conjugate momentum can be expressed as  $P^\mu := (H_R/c, P^n)$ . Ergo, the covariant formulation implicitly stores the information gained from the non-covariant approach as components of the covariant approach's conjugate four-momentum. This suggests that the non-covariant approach contains the same relativistic mechanics as the covariant approach, but in a somewhat less organized manner. However, it should also be noted that (3.18) holds a much closer relationship to the non-relativistic limit than (3.16). Since a well-defined non-relativistic limit is ideal for numerical studies, we shall opt to use this form of the Hamiltonian.

Lastly, we now wish to know the equation of motion our particle obeys. In order to construct a 6D phase space with independent variables  $(\mathbf{x}, \mathbf{p}, t)$ , we will not be able to use Hamilton's equations to get said equation of motion, since  $\mathbf{p}$  is *not* the canonical momentum. However, we can address this complication by utilizing non-canonical Hamiltonian theory.

### 3.3 Non-Canonical Hamiltonian Theory for Single-Particle Motion

The ultimate goal of this section is to derive the equation of motion for a relativistic charged particle in an electromagnetic field, assuming a velocity independent four-vector potential. For this section, our derivation of non-canonical equations of motion follows almost the exact same procedure laid out by Cary (Cary & Brizard, 2009). Additionally, we will generalize the 3-position  $x^i$  such that  $x^i \rightarrow q^i$ , where  $q^i$  is the generalized position.

We first start with (3.10), which we rewrite in a slightly different form below for convenience:

$$L = P_i \dot{q}^i - H, \quad (3.19)$$

where the dot indicates the total time derivative with respect to the lab-frame time. Subscripts used in previous sections to distinguish between covariant and non-covariant formulations have been suppressed. Let the  $q^i = q(z^\alpha, t)^i$ , where  $z^\alpha \equiv (q^i, p^i)$  is a  $2N$  dimensional vector containing the new non-canonical position in the first  $N$  degrees of freedom, while the other  $N$  degrees of freedom contain the new non-canonical momentum, such that  $\alpha = 0, 1, \dots, 2N$ . The indices  $\beta$  and  $\gamma$  will also use the same range of values as  $\alpha$ . All other Greek indices will retain their original range from 0-3 from special relativity. We will leave these coordinates arbitrary for the sake of generality for now. Expanding  $\dot{q}^i$  yields:

$$\dot{q}^i = \frac{\partial q^i}{\partial t} + \dot{z}^\alpha \frac{\partial q^i}{\partial z^\alpha}. \quad (3.20)$$

Substitution of (3.20) into (3.10) gives the new transformation equation

$$L = \Lambda_\alpha \dot{z}^\alpha - \mathcal{H} \quad (3.21)$$

with  $\Lambda_\alpha$  and  $\mathcal{H}$  given by:

$$\Lambda_\alpha \equiv P_i \frac{\partial q^i}{\partial z^\alpha} \quad (3.22)$$

$$\mathcal{H} \equiv H - P_i \frac{\partial q^i}{\partial t}. \quad (3.23)$$

Here,  $\Lambda_\alpha \dot{z}^\alpha$  represents the symplectic part of the Lagrangian and  $\mathcal{H}$  the Hamiltonian part.

As mentioned in the previous section, the non-covariant formulation preserves the original form of Lagrange's equations, regardless of coordinate choice. Hence, Lagrange's equations in non-canonical coordinates are

$$\frac{d}{dt} \left( \frac{\partial L}{\partial \dot{z}^\alpha} \right) = \frac{\partial L}{\partial z^\alpha}. \quad (3.24)$$

Utilizing (3.21), (3.24) can be re-written as

$$\begin{aligned} \frac{\partial \Lambda_\alpha}{\partial t} + \frac{\partial \Lambda_\alpha}{\partial z^\beta} \dot{z}^\beta &= \frac{\partial \Lambda_\beta}{\partial z^\alpha} - \frac{\partial \mathcal{H}}{\partial z^\alpha} \\ \left( \frac{\partial \Lambda_\beta}{\partial z^\alpha} - \frac{\partial \Lambda_\alpha}{\partial z^\beta} \right) \frac{dz^\beta}{dt} &= \frac{\partial \Lambda_\alpha}{\partial t} + \frac{\partial \mathcal{H}}{\partial z^\alpha}. \end{aligned}$$

By defining the so called ‘‘Lagrange matrix’’ (or the symplectic form) as

$$\omega_{\alpha\beta} \equiv \frac{\partial \Lambda_\beta}{\partial z^\alpha} - \frac{\partial \Lambda_\alpha}{\partial z^\beta} \quad (3.25)$$

and the so called ‘‘Poisson matrix’’ (or the inverse symplectic form)  $\Pi^{\alpha\gamma}$  such that  $\Pi^{\alpha\gamma} \omega_{\gamma\beta} = \delta_\beta^\alpha$  (and doing a little algebra), (3.24) simplifies to the general form for Hamilton's non-canonical equations of motion:

$$\frac{dz^\alpha}{dt} = \Pi^{\alpha\beta} \left[ \frac{\partial H}{\partial z^\beta} + \frac{\partial P_i}{\partial t} \frac{\partial q^i}{\partial z^\beta} - \frac{\partial P_i}{\partial z^\beta} \frac{\partial q^i}{\partial t} \right]. \quad (3.26)$$

A useful way to check (3.26) is to let  $z^\alpha := (x^i, P^i)$ , i.e. canonical coordinates. If the coordinate choice is canonical, then the RHS of (3.26) should simply reduce to usual Poisson bracket form

$$\frac{dz^\alpha}{dt} = \sigma^{\alpha\beta} \frac{\partial H}{\partial z^\beta} \equiv \{z^\alpha, H\}, \quad (3.27)$$

where  $\sigma^{\alpha\beta}$  is the fundamental symplectic form given by:

$$\sigma_{\alpha\beta} := \begin{bmatrix} 0 & \eta^{mn} \\ -\eta^{mn} & 0 \end{bmatrix}. \quad (3.28)$$

To check this, we need to introduce some new notation. To make the calculation of  $\omega_{\alpha\beta}$ , and other  $2N$  dimensional tensors, more intuitive, we define un-primed roman indices to run from 1 to  $N$  and primed indices to run from  $N + 1$  to  $2N$ . For example, consider the case of  $N = 3$  (which is what we will be assuming most of the time). If  $i$  is the index in question, and  $i = 1, 2, 3$ , then this implies that  $i' = 4, 5, 6$ , or  $i' = i + 3$ . For arbitrary  $N$  we can simply relate primed indices to their un-primed counterpart by adding  $N$  to the un-primed index.

A more convenient form of (3.25) for calculating  $\omega_{\alpha\beta}$  is

$$\omega_{\alpha\beta} = \eta_{kl} \left( \frac{\partial P^k}{\partial z^\alpha} \frac{\partial q^l}{\partial z^\beta} - \frac{\partial P^k}{\partial z^\beta} \frac{\partial q^l}{\partial z^\alpha} \right). \quad (3.29)$$

Note that choosing  $z^\alpha := (x^i, P^i)$  yields the following components for  $\omega_{\alpha\beta}$ :

$$\omega_{ij} = \omega_{i'j'} = 0 \quad (3.30)$$

$$\omega_{i'j} = -\omega_{ij'} = \eta_{ij}, \quad (3.31)$$

or

$$\omega_{\alpha\beta} := \begin{bmatrix} 0 & -\eta_{mn} \\ \eta_{mn} & 0 \end{bmatrix}. \quad (3.32)$$

The inverse symplectic form  $\Pi^{\alpha\beta}$  is simply the inverse of the above expression, which implies that  $\Pi^{\alpha\beta} = \sigma^{\alpha\beta}$  for canonical coordinates. Moreover, the second and third terms in (3.26) vanish identically since  $x^i$  and  $P^i$  are independent of time given this choice of coordinates. Hence, (3.26) reduces to (3.27) when  $z^\alpha := (x^i, P^i)$ .

Now we turn our attention to finding the equation of motion for a charged particle moving in a velocity independent four-vector potential. Without loss of generality, we shall

let  $x^i$  replace  $q^i$  as the canonical position to avoid confusion with the particle's charge  $q$ . Letting  $z^\alpha := (x^i, p^i)$ , where  $p^i$  is the particle's momentum, from (3.15) and (3.29) we get

$$\omega_{ij} = q \left( \frac{\partial A_j}{\partial x^i} - \frac{\partial A_i}{\partial x^j} \right) = qF_{ij} \quad (3.33)$$

$$\omega_{i'j} = -\omega_{ij'} = \eta_{ij} \quad (3.34)$$

$$\omega_{i'j'} = 0, \quad (3.35)$$

or in the matrix representation:

$$\omega_{\alpha\beta} := \begin{bmatrix} qF_{mn} & -\eta_{mn} \\ \eta_{mn} & 0 \end{bmatrix}.$$

Therefore, the inverse symplectic form can be represented by

$$\Pi^{\alpha\beta} := \begin{bmatrix} 0 & \eta^{mn} \\ -\eta^{mn} & qF^{mn} \end{bmatrix}. \quad (3.36)$$

Note that the only difference between (3.36) and  $\sigma^{\alpha\beta}$  is the  $i'j'$  block. This change is a direct consequence of the four-vector potential's influence over the particle's trajectory in a non-conservative manner. Mathematically, this influence appears explicitly in (3.15). However, the velocity independence of the four-vector potential is another reason why  $\Pi^{\alpha\beta}$  deviates only slightly from  $\sigma^{\alpha\beta}$ . A velocity dependent four-vector potential would alter the  $i'j$  and  $ij'$  blocks as well.

Taking the  $i'$  component of (3.26) and substituting in (3.10) and (3.36), the equation of motion becomes:

$$\begin{aligned} \frac{dp^i}{dt} &= \Pi^{i'\beta} \left[ \frac{\partial H}{\partial z^\beta} + \eta_{kl} \frac{\partial A^k}{\partial t} \frac{\partial x^l}{\partial z^\beta} \right] \\ &= -q\eta^{ij} \left[ \frac{\partial \Phi}{\partial x^j} + \frac{\partial A_j}{\partial t} \right] \\ &= q \left[ E^i + \varepsilon^{ijk} v_j B_k \right]. \end{aligned} \quad (3.37)$$

Defining  $F^i \equiv \dot{p}^i$ , (3.37) simply tells us that our particle follows the trajectory dictated by the Lorentz force, the same as in non-relativistic mechanics. While this may seem odd at first, it should be noted special relativity time and time again has been shown to be easily derived from Maxwell's equations. The Lorentz force law does have a somewhat hidden caveat though; Newton's second law only holds for the rate of change of the momentum. This is easily seen from the spatial components of the four-momentum, or  $p^i = \gamma m v^i$ . Only when the particle's speed is constant will the  $F^i = m a^i$  form of Newton's Second Law hold.

While (3.37) contains almost all of the information we need, one might still wonder what would happen if instead of studying the non-canonical dynamics of  $H$ , what would happen if we had used  $\mathcal{H}$  instead? In short, there is very little difference between the two symplectic forms constructed using  $H$  and  $\mathcal{H}$ , respectively. However, as it will be shown, the covariant derivation will give us some additional information about our system.

Firstly, we would need to upgrade our number of degrees of freedom in position space to  $N = 4$ , and let  $P_i \rightarrow P_\mu$  and  $\dot{q}^i \rightarrow u^\mu$  in (3.19) so that

$$\mathcal{L} = P_\mu u^\mu - \mathcal{H}. \quad (3.38)$$

Following the exact same procedure as before, we would get the following definitions for the symplectic form and the equation of motion:

$$\omega_{\alpha\beta} = \eta_{\lambda\rho} \left( \frac{\partial P^\lambda}{\partial z^\alpha} \frac{\partial q^\rho}{\partial z^\beta} - \frac{\partial P^\lambda}{\partial z^\beta} \frac{\partial q^\rho}{\partial z^\alpha} \right) \quad (3.39)$$

$$\frac{dz^\alpha}{d\tau} = \Pi^{\alpha\beta} \left[ \frac{\partial \mathcal{H}}{\partial z^\beta} + \frac{\partial P_\mu}{\partial \tau} \frac{\partial q^\mu}{\partial z^\beta} - \frac{\partial P_\mu}{\partial z^\beta} \frac{\partial q^\mu}{\partial \tau} \right], \quad (3.40)$$

where  $\Pi^{\alpha\beta}$  is the inverse of the  $\omega_{\alpha\beta}$  defined by (3.39). Letting  $z^\alpha := (x^\mu, p^\mu)$  and taking the  $\mu'$  component of (3.40),  $\Pi^{\alpha\beta}$  becomes

$$\Pi^{\alpha\beta} := \begin{bmatrix} 0 & \eta^{\lambda\rho} \\ -\eta^{\lambda\rho} & q F^{\lambda\rho} \end{bmatrix} \quad (3.41)$$

and, after some algebra, the equation of motion reduces to

$$\frac{dp^\mu}{d\tau} = \frac{q}{m} F^{\mu\nu} p_\nu. \quad (3.42)$$

Note that the  $i$  component of (3.42) can be written as the following:

$$\begin{aligned} \frac{dp^i}{d\tau} &= \frac{q}{m} [F^{i0} p_0 + F^{ij} p_j] \\ &= \frac{q}{m} \left[ \left( -\frac{E^i}{c} \right) (-\gamma mc) + \left( \varepsilon^{ijk} B_k \right) (\gamma m v_j) \right] \\ &= q\gamma [E^i + \varepsilon^{ijk} v_j B_k]. \end{aligned}$$

Dividing the above expression by  $\gamma$ , and utilizing (2.4), the above expression is equivalent to (3.37). Therefore, the spatial components do not carry any new information. The  $\mu = 0$  equation can be expressed, after some manipulation, as

$$\frac{d\mathcal{E}}{dt} = qE^i v_i. \quad (3.43)$$

Hence, the time component gives us the condition for rate of change for the particle's kinetic energy, since the rest energy is a constant. Conceptually, this translates into the old adage: the magnetic field does no work. The only field capable of changing the particle's kinetic energy is the electric field. In other words, if the particle's velocity is perpendicular to the electric field, or if there is no electric field, then particle's velocity will remain constant and simply undergo circular motion about the magnetic field. This concept is consistent with non-relativistic dynamics of charged particles in electromagnetic fields.

While the condition for constant velocity, in the case of purely circular motion, may seem like new information, this information can also be obtained by simply contracting

both sides of (3.37) with  $p_i$ , which becomes:

$$p_i \frac{dp^i}{dt} = qE^i p_i$$

$$\frac{1}{2\gamma m} \frac{d}{dt} (p^2) = qE^i v_i.$$

Note that

$$\frac{d\mathcal{E}}{dt} = \frac{1}{2\gamma m} \frac{d}{dt} (p^2)$$

gives us back (3.43). Therefore, both the non-covariant and covariant Hamiltonians produced the exact same information. The covariant formulation simply produces this information in a neat and compact format.



## CHAPTER 4

### RELATIVISTIC KINETIC THEORY AND THERMODYNAMICS

In this chapter, we will initially be following along closely with Cercignani and Kremer's derivation of the relativistic Boltzmann equation, equilibrium distribution, and relativistic first law of thermodynamics (Cercignani & Kremer, 2002). However, we deviate slightly in regards to notation and definitions for various fluid tensors.

#### 4.1 Relativistic Boltzmann Equation

For the purpose of deriving the relativistic Boltzmann equation, we will first need to make the following assumptions:

1. Only binary collisions are considered. Since tokamak plasmas are dilute, this is a reasonable assumption.
2. Both particles are completely uncorrelated prior to the collision. This is the molecular chaos assumption.
3. We assume that the single-particle distribution function does not change much over a time-interval larger than the interaction time for a single collision. Additionally, this time-interval must be shorter than the time between collisions. This assumption also applies to the change in  $f_a$  over distances on the order of the interaction range.
4. We will work in 12D phase-space with independent variables  $(x_1^i, p_1^i, x_2^i, p_2^i, t)$ , where  $t$  is the lab-frame time shared by both particles. However, the final equation will be in terms of  $f_a$  as the  $x_2^i$  and  $p_2^i$  dependence will be integrated out due to collisions. Hence, we will ultimately only need to consider species  $a$ 's 6D phase space over the independent variables  $(x_1^i, p_1^i, t)$ .

The previous numbering system will be used to reference these assumptions through the derivation.

We begin by defining the phase space we will be working in by the same phase space volume element as is done non-relativistically,  $d^3x_1 d^3p_1$ . Note that for the purpose of this thesis, volume elements will implicitly store their corresponding scale factors as shown below

$$d^3x'_1 = \sqrt{|g|} dx_1^1 dx_1^2 dx_1^3 \quad (4.1)$$

$$d^3p'_1 = \sqrt{|g_p|} dp_1^1 dp_1^2 dp_1^3, \quad (4.2)$$

where  $g_p$  is the determinant of the the momentum space metric. Note that while, individually,  $d^3x_1$  and  $d^3p_1$  are not Lorentz invariant, the product of the two is.

To show this, we first consider the transformation to an arbitrary frame  $F$  moving at speed  $v_{Fx}$  along the x-axis. Note that (2.36)-(2.39) also hold in their non-differential forms. Consider a thin rod placed parallel to the x-axis with endpoints defined by  $x_{1a}$  and  $x_{1b}$  (Cercignani & Kremer, 2002). These endpoints as measured in  $F$  are then given by

$$x'_{1a} = \gamma_F (x_{1a} - v_{Fx} t) \quad (4.3)$$

$$x'_{1b} = \gamma_F (x_{1b} - v_{Fx} t). \quad (4.4)$$

Subtracting (4.4) from (4.3) we find that  $\Delta x'_1 = \gamma_F \Delta x_1$ , which is just the 1D concept of length contraction. Doing the same for the  $y$  and  $z$  direction, we find that the volume transforms as:

$$\Delta x'_1 \Delta y'_1 \Delta z'_1 = \gamma_F \Delta x_1 \Delta y_1 \Delta z_1. \quad (4.5)$$

Taking the infinitesimal limit thus gives us

$$d^3x'_1 = \gamma_F d^3x_1. \quad (4.6)$$

Now we turn our attention to  $d^3p_1$ . Fortunately, we can find  $d^3p'_1$  using a somewhat more straightforward method. In Cercignani & Kremer, 2002 it is proven that for any four-vector  $V^\mu$  such that  $V^\mu V_\mu$  is a constant, the corresponding 3D volume element  $d^3A'$  in a

Lorentz boosted frame  $F$  is related to the lab frame volume element by

$$\frac{d^3 A'}{A^{0'}} = \frac{d^3 A}{A^0}. \quad (4.7)$$

Moreover, (4.7) shows that the volume elements corresponding to four-vectors of this type can be made into "proper volumes" by simple dividing them by the time component of said four-vector. Therefore, we can find the boost momentum space volume element by simply finding the ration of  $p^{0'}/p^0$ . Boosting the four-momentum in the same manner as we did for  $d^3 x_1$ , and taking a ratio of the new and old time components, we find that

$$\frac{p^{0'}}{p^0} = \frac{1}{\gamma_F}. \quad (4.8)$$

Using (4.8), (4.7), and (4.6), we find that

$$d^3 x'_1 d^3 p'_1 = d^3 x_1 d^3 p_1. \quad (4.9)$$

Note that (4.9) is invariant under reorientation of the frame velocity and curvilinear transformations. Therefore, our phase-space volume area is Lorentz invariant in any curvilinear coordinates and orientation of the frame velocity.

Now that we have properly defined the nature of our phase-space, we can define the single-particle distribution function  $f_a$  for species  $a$  by

$$f_a \equiv \frac{dN_a}{d^3 x_1 d^3 p_1}. \quad (4.10)$$

Species  $b$ 's distribution function and four-position are defined in the same manner with subscripts of  $1 \rightarrow 2$ . Note that (4.10) implies by construction that the distribution function is Lorentz invariant since both the number of particles and the phase-space volume element are Lorentz invariant.

At a time  $t + \Delta t$ , measured in the lab-frame,  $f_a(x_1^i, p_1^i, t) \rightarrow f_a(x_1^i + v_1^i \Delta t, p_1^i + F_a^i \Delta t, t +$

$\Delta t$ ). The change in the number of particles in the volume element  $d^3x_1 d^3p_1$  in the time-interval  $\Delta t$  is then

$$\Delta dN_a = f_a(x_1^i + v_1^i \Delta t, p_1^i + F_1^i \Delta t, t + \Delta t) d\Gamma_1(t + \Delta t) - f_a(x_1^i, p_1^i, t) d\Gamma_1(t) \quad (4.11)$$

with  $d\Gamma_1 \equiv d^3x_1 d^3p_1$ .

Note that the relationship between  $d\Gamma_1(t + \Delta t)$  and  $d\Gamma_1(t)$  is given by

$$d\Gamma_1(t + \Delta t) = |J_1| d\Gamma_1(t), \quad (4.12)$$

where  $J$  is the Jacobian of transformation at time  $t + \Delta t$  given by

$$J_1 = \frac{\partial Z_1^\alpha}{\partial z_1^\beta} \quad (4.13)$$

such that  $Z_1^\alpha := (x_1^i(t + \Delta t), p_1^i(t + \Delta t))$  and  $z_1^\alpha := (x_1^i(t), p_1^i(t))$ . Assumption 3 is used here by keeping terms in (4.13) only up to order one in  $\Delta t$ , or

$$J_1 \approx 1 + \frac{\partial F_1^i}{\partial p_1^i} + \mathcal{O}(\Delta t^2). \quad (4.14)$$

While not explicitly shown here,  $\Delta t^2$  is a factor in every term in the  $\mathcal{O}(\Delta t^2)$  part of (4.14). This fact will become important later. Taylor expanding  $f_a(x_1^i + v_1^i \Delta t, p_1^i + F_1^i \Delta t, t + \Delta t)$  about  $\Delta t = 0$  and keeping only terms of order  $\Delta t$ , (4.11) simplifies to

$$\begin{aligned} \Delta dN_a &\approx \left[ \frac{\partial f_a}{\partial t} + v_1^i \frac{\partial f_a}{\partial x_1^i} + F_1^i \frac{\partial f_a}{\partial p_1^i} + \frac{\partial F_1^i}{\partial p_1^i} f_a \right] d^3x_1 d^3p_1 \Delta t + \mathcal{O}(\Delta t^2) \\ &= \left[ \frac{\partial f_a}{\partial t} + v_1^i \frac{\partial f_a}{\partial x_1^i} + \frac{\partial}{\partial p_1^i} (f_a F_1^i) \right] d^3x_1 d^3p_1 \Delta t + \mathcal{O}(\Delta t^2). \end{aligned} \quad (4.15)$$

The remainder of this derivation will focus on determining the form of the LHS of (4.15) by calculating the number of particles entering and leaving the volume element  $d^3x_1' d^3p_1'$  in the time interval  $\Delta t'$  or

$$\Delta dN_a = dN_a^+ - dN_a^-, \quad (4.16)$$

where  $dN_a^+$  is the number of particles entering the volume element and  $dN_a^-$  is the number of particles leaving the volume element. These two terms are often referred to as the gain and loss terms, respectively.

Consider a collision between two beams of particles that travel as speeds  $v'_1$  and  $v'_2$ , where the primes denote that the velocities are evaluated after the collision. In their own respective reference frames, the number of particles entering  $d^3x'_1d^3p'_1$  can be expressed as

$$dN_a^+ = \sum_b \left[ \int f_{ab}'^{(2)} d^3x'_{Rc} d^3p'_{R2} \right] d^3x'_1 d^3p'_1, \quad (4.17)$$

where  $f_{ab}'^{(2)}$  is the two-particle distribution function for species  $a$  and  $b$  before the collision. Note that the integration done in the bracketed term in (4.17) results in the fraction of the single particle distribution for species  $a$  that interacts with species  $b$  inside the collision cylinder  $d^3x'_{Rc} \equiv v'_{12} \Delta t'_2 d\sigma'_2$ , where  $v'_{12}$  is the relative velocity between particle one and two and  $d\sigma'_2$  is the differential cross-section prior to the collision in particle two's reference frame. This term is then summed over all potential species that can interact with species  $a$ . It is important to remember that the collisional cylinder volume in (4.17) is, by necessity, calculated in the second particle's reference frame, indicated by the subscript  $R$ . It is crucial that the term in brackets is calculated in particle two's rest frame so that (4.17) is Lorentz invariant. Unpacking (4.17), and utilizing the molecular chaos assumption  $f_{ab}'^{(2)} \equiv f'_a f'_b$ , we find that

$$dN_a^+ = \sum_b \left[ \int f'_a f'_b v'_{12} \Delta t'_2 d\sigma'_2 d^3p'_{R2} \right] d^3x'_1 d^3p'_1. \quad (4.18)$$

Now that we have determined the number of particles entering the volume element  $d^3x'_1d^3p'_1$ , determining the number leaving it can be done in exactly the same manner, except that parameters shall be evaluated after the collision (e.g.  $f'_a \rightarrow f_a$ ). Therefore, the number of particles leaving this volume element is given by

$$dN_a^- = \sum_b \left[ \int f_a f_b v_{12} \Delta t_2 d\sigma_2 d^3p_{R2} \right] d^3x_1 d^3p_1. \quad (4.19)$$

Liouville's theorem tells us that the volume element in phase-space is the same before and after the collision, which implies that

$$v_{12}\Delta t_2 d\sigma_2 d^3 p_{R2} d^3 x_1 d^3 p_1 = v'_{12}\Delta t'_2 d\sigma'_2 d^3 p'_{R2} d^3 x'_1 d^3 p'_1. \quad (4.20)$$

Therefore enforcing Liouville's theorem and plugging (4.18) and (4.19) into (4.16), (4.15) can now be written as

$$\frac{\partial f_a}{\partial t} + v_1^i \frac{\partial f_a}{\partial x_1^i} + \frac{\partial}{\partial p_1^i} (f_a F_a^i) + \mathcal{O}(\Delta t) = \sum_b \int (f'_a f'_b - f_a f_b) v_{12} \frac{\Delta t_2}{\Delta t} d\sigma_2 d^3 p_{R2}, \quad (4.21)$$

where the order in the error term was reduced by one due a division of  $\Delta t$  on both sides and  $d^3 x_1 d^3 p_1$  has also been divided out on every term. Since  $\Delta t$  represents an arbitrary time-interval, we can reduce the error term to zero by taking the limit of both sides of the equation as  $\Delta t \rightarrow 0$ , and utilizing (2.51). Doing so to (4.21) gives us the ‘‘relativistic Boltzmann equation’’ or:

$$\frac{\partial f_a}{\partial t} + v_1^i \frac{\partial f_a}{\partial x_1^i} + \frac{\partial}{\partial p_1^i} (f_a F_a^i) = \sum_b \int (f'_a f'_b - f_a f_b) \left(1 - \frac{v_1^k v_{2k}}{c^2}\right) v_{12} d\sigma_2 d^3 p_2. \quad (4.22)$$

## 4.2 The Maxwell-Jüttner Distribution and First Law of Thermodynamics

Since we are interested in solving for the RE distribution numerically, we will ultimately need a useful analytic initial condition for the distribution function. Moreover, we would like our initial condition to be the distribution when the plasma is in equilibrium, i.e. before the electrons have undergone significant acceleration. In non-relativistic plasma kinetic theory, the Maxwell-Boltzmann (MB) distribution is this distribution. Ergo, the purpose of this section is to derive the relativistic analogue to the MB distribution, as well as define new relativistic analogues to fluid variables and the first law of thermodynamics (FLOT).

First, we must establish the condition by which we define the equilibrium distribution. The condition for equilibrium is conceptually the same as the non-relativistic case: entropy production must vanish. To do this, it is convenient to first write (4.22) in the covariant

form:

$$p_1^\mu \frac{\partial f_a}{\partial x_1^\mu} + m_a \frac{\partial}{\partial p_1^\mu} (f_a K_a^\mu) = \sum_b \int (f'_a f'_b - f_a f_b) p_{12} d\sigma_2 \frac{d^3 p_2}{\gamma_2}, \quad (4.23)$$

where  $p_{12} \equiv \gamma_{12} m_a v_{12}$  is the relative momentum between the first and second particle and  $K_a^\mu$  is the Minkowski four-force for species  $a$  defined in (2.7). Additionally, we shall assume that  $\partial K_a^\mu / \partial p_1^\mu = 0$ , which is true for the case of the Lorentz force and, trivially, equilibrium.

To determine a form for the entropy production term, we define the entropy four-flow as

$$S_a^\mu \equiv -k \int u_1^\mu \ln (f_a h^3) f_a \frac{d^3 p_1}{\gamma_1}, \quad (4.24)$$

where  $h$  and  $k$  are the Planck and Boltzmann constants, respectively. Consider an arbitrary function  $\psi_1(x_1^\mu, p_1^\mu)$ . Multiplying both sides of (4.23) by  $\psi$  and integrating over  $d^3 p_1 / \gamma_1$ , and following the procedure in (Cercignani & Kremer, 2002), we can write a general equation of transfer given by

$$\frac{\partial}{\partial x_1^\mu} \int \psi_1 p_1^\mu f_a \frac{d^3 p_1}{\gamma_1} - \int \left[ p_1^\mu \frac{\partial \psi_1}{\partial x_1^\mu} + m_a K_a^\mu \frac{\partial \psi_1}{\partial p_1^\mu} \right] f_a \frac{d^3 p_1}{\gamma_1} = \mathcal{P}, \quad (4.25)$$

such that

$$\mathcal{P} \equiv \frac{1}{4} \int (\psi_1 + \psi_2 - \psi'_1 - \psi'_2) (f'_a f'_b - f_a f_b) p_{12} d\sigma_2 \frac{d^3 p_1}{\gamma_1} \frac{d^3 p_2}{\gamma_2}, \quad (4.26)$$

where  $\mathcal{P}$  is the production term for the quantity  $\psi$ . Thus, to find the entropy production term, we let  $\psi_1 = -k \ln (f_a h^3)$  and  $\psi_2 = -k \ln (f_b h^3)$ . Substituting this definition of  $\psi$  into (4.25), yields the final expression we need:

$$\frac{\partial S_a^\mu}{\partial x_1^\mu} = \zeta, \quad (4.27)$$

with the entropy production  $\zeta$  given by

$$\zeta \equiv \frac{1}{4} k \int f_a f_b \ln \left( \frac{f'_a f'_b}{f_a f_b} \right) \left( \frac{f'_a f'_b}{f_a f_b} - 1 \right) p_{12} d\sigma_2 \frac{d^3 p_1}{\gamma_1} \frac{d^3 p_2}{\gamma_2}. \quad (4.28)$$

Finally, we can begin determining the relativistic analogue to the MB distribution.

Upon inspection of (4.28), the condition by which entropy production is minimized is given by  $f'_a f'_b = f_a f_b$ . Note that under the molecular chaos assumption, where the two-particle distribution function for species  $a$  and  $b$  is given by  $f_{ab}^{(2)} = f_a f_b$ , this is equivalent to requiring that the two-particle distribution remain unchanged. This condition can also be written in the following form:

$$\ln(f_a h^3) + \ln(f_b h^3) = \ln(f'_a h^3) + \ln(f'_b h^3). \quad (4.29)$$

The form in (4.29) is what is known as a summational invariant form. In Cercignani & Kremer, 2002, it is proven that for any generalized function or distribution  $\psi(p^\mu)$ ,  $\psi$  is a summational invariant if and only if it takes the form

$$\psi(p^\mu) = A + B^\mu p_\mu, \quad (4.30)$$

such that  $A$  is an arbitrary scalar and  $B^\mu$  is an arbitrary four-vector that is independent of  $p^\mu$ . Therefore,  $\ln(f_a h^3)$  must have the form given in (4.30). Exponentiation of both sides of this expression yields

$$f_a = N_M e^{B^\mu p_\mu}, \quad (4.31)$$

where  $N_M$  is a constant Lorentz scalar that has absorbed all other constant coefficients.

Our task is now to determine the normalization constant  $N_M$  and the four-vector  $B^\mu$ . We do so by first defining the following moments of the distribution function

$$n_a = \int f_a d^3 p_1 \quad (4.32)$$

$$n_{Ra} U_a^\mu = \int u_1^\mu f_a \frac{d^3 p_1}{\gamma_1} \quad (4.33)$$

$$T_a^{\mu\nu} = m_a \int u_1^\mu u_1^\nu f_a \frac{d^3 p_1}{\gamma_1}, \quad (4.34)$$

where  $n_a$  is the lab-frame number density,  $n_{Ra}$  is the fluid-frame density,  $U_a^\mu$  is the four-flow, and  $T_a^{\mu\nu}$  is the stress-energy tensor for species  $a$ . Note that the relationship between the



lab-frame density and the fluid-frame density can be found by utilizing the invariance of  $U_a^\mu U_{a\mu}$ . Doing so yields the relationship:

$$n = \gamma_V n_R. \quad (4.35)$$

The factor  $\gamma_V$  is simply the Lorentz factor such that  $\mathbf{v} \rightarrow \mathbf{V}$ , where  $\mathbf{V}$  is the flow velocity. As previous mentioned, to complete our relativistic equilibrium description, we will also need to develop a relativistic analogue to the FLOT. It is important to note that the FLOT is defined in terms of the scalar pressure, which is a contraction of the pressure tensor, not the stress-energy tensor. Hence, we will need to rigorously define what we mean by relativistic pressure.

The pressure tensor, as in non-relativistic theory, is defined as the part of the stress-energy tensor (stress tensor non-relativistically) that is orthogonal to the flow. Consider the following projection operator

$$\Delta_\nu^\mu \equiv \delta_\nu^\mu + \frac{1}{c^2} U_a^\mu U_a^\nu, \quad (4.36)$$

with the properties:

$$\Delta_\lambda^\mu \Delta_\nu^\lambda = \Delta_\nu^\mu \quad (4.37)$$

$$\Delta_\mu^\mu = 3 \quad (4.38)$$

$$\Delta_\nu^\mu U_a^\nu = 0. \quad (4.39)$$

In the fluid-frame, (4.36) is completely diagonal with components  $\Delta_0^0 = 0$  and  $\Delta_j^i = \delta_j^i$ . The operator  $\Delta_\nu^\mu$  projects a given four-vector in a direction orthogonal to the four-flow. Therefore, applying (4.36) to both indices of (4.34), or  $P_a^{\mu\nu} \equiv \Delta_a^\mu \Delta_\beta^\nu T_a^{\alpha\beta}$  (de Groot et al., 1980), the pressure tensor can be written as

$$P_a^{\mu\nu} = m_a \int (u_1^\mu - \gamma_R U_a^\mu) (u_1^\nu - \gamma_R U_a^\nu) f_a \frac{d^3 p_1}{\gamma_1}. \quad (4.40)$$

In (4.40), only spatial components along the diagonal exist in the rest frame, hence we define the scalar pressure in the same way as is done non-relativistically, or  $p_{sa} \equiv P_{a\mu}^\mu/3$ . Therefore, after a fair amount of simplification, the scalar pressure is

$$p_{sa} = \frac{1}{3} \int p_R^2 f_a \frac{d^3 p_1}{\gamma_1}, \quad (4.41)$$

where  $p_R$  is the relative momentum in the fluid-frame. Note that in the non-relativistic limit, the spatial components of (4.40) and the scalar pressure become

$$P_a^{ij} \approx m_a \int v_R^i v_R^j f_a d^3 p_1 \quad (4.42)$$

$$p_{sa} \approx \frac{1}{3} m_a \int v_R^2 f_a d^3 p_1 \quad (4.43)$$

where  $v_R^i \approx v_1^i - V_a^i$ . Equations (4.42) and (4.43) are exactly the non-relativistic versions of the pressure tensor and scalar pressure. We have shown this non-relativistic limit to make a conceptual point. A common misconception regarding the pressure is that it is defined in terms of the relative velocity in the fluid-frame, and therefore in terms of the relative kinetic energy. As can be seen from (4.40), this is not the case. Hence the form in (4.42) and (4.43) are simply the result of a low-velocity projection operator and the scalar pressure is actually defined in terms of the *relative momentum* in the fluid frame.

Now that we have properly defined our fluid moments, we can begin to solve for our under-determined parameter/four-vector. Letting  $B_R^\mu = (z/m_a c, 0)$ , where  $z$  is an arbitrary scalar, and utilizing (4.32) and (4.33), it can be shown that

$$N_M = \frac{n_{Ra} z}{4\pi (m_a c)^3 K_2(z)} \quad (4.44)$$

$$B_a^\mu = \left( \frac{z}{m_a c^2} \right) U_a^\mu, \quad (4.45)$$

where  $K_2(z)$  is a Bessel function of the second kind. Our final task will be to determine the expression for the scalar  $z$ . By defining the relativistic FLOT, we can pin down this last

constraint. Defining the entropy per particle and energy density in the fluid-frame by

$$s_a \equiv \frac{1}{n_{Ra}c} S_a^\mu U_{a\mu} \quad (4.46)$$

$$n_{Ra}\varepsilon_{Ra} = \frac{1}{m_a} \int (p_R^0)^2 f_a \frac{d^3p_1}{\gamma_1} \quad (4.47)$$

and using (4.31) and (4.41), we can write the following relationship between the entropy, pressure, and energy per particle in the fluid-frame in equilibrium as

$$ds_{Ea} = \frac{kz}{m_a c^2} \left( d\varepsilon_{ERa} + \frac{1}{N_a} p_{Esa} dV_R \right), \quad (4.48)$$

Note that the subscript of  $E$  denotes that the parameter in question is measured in equilibrium. Moreover, (4.48) reduces exactly to the non-relativistic FLOT, save for the coefficient outside the parentheses. Therefore, to enforce the constraint that our new FLOT reduces to the non-relativistic regime, our parameter  $z$  must be

$$z_a = \frac{m_a c^2}{kT_{Ea}}, \quad (4.49)$$

where  $T_{Ea}$  is the species temperature in equilibrium. Substituting (5.1), (4.45), and (4.44) back into the (4.31), and unpacking the contraction in the exponent, gives us the final expression

$$f_a^{\text{MJ}} = \frac{n_{ERa}}{4\pi m_a^2 c k T_{Ea} K_2(m_a c^2 / k T_{Ea})} e^{-\gamma_R m_a c^2 / k T_{Ea}}, \quad (4.50)$$

which is exactly the Maxwell-Jüttner (MJ) distribution (Jüttner, 1911). Note that the MJ distribution is in fact a Lorentz scalar as implied by the Lorentz invariance of (4.10).

When working with the MJ distribution, it is often more useful to define it using a normalized momentum  $s_1 \equiv p_1/m_a c$  (not to be confused with the entropy per particle) and normalized "flow-momentum" defined by  $s_{Va} \equiv \gamma_V V_a/c$ , where  $V_a$  is the magnitude of the three-flow for species  $a$ . Additionally, the temperature dependence will be written in terms of  $z_a$  instead. Using this notation and defining the MJ distribution instead over normalized

momentum space, (4.50) becomes

$$f_a^{\text{MJ}}(\mathbf{s}_1) \equiv \frac{n_{ERa} z_a}{4\pi K_2(z_a)} e^{-z_a \gamma_R}, \quad (4.51)$$

where  $\gamma_R = \gamma_1 \gamma_V - \mathbf{s}_1 \cdot \mathbf{s}_V$ . The MJ distribution over normalized momentum space is both useful numerically and allows one to see the non-relativistic limit more clearly. Note that by substitution of (4.51) into (4.41), and switching to normalized fluid-frame momentum space coordinates, it can be show that

$$p_{Esa} = n_{ERa} k T_{Ea}, \quad (4.52)$$

which is analogous to the non-relativistic ideal-gas law. We can use the form of (4.52) to extend our definition of temperature outside of equilibrium to

$$n_{Ra} k T_a \equiv \frac{1}{3} \int p_R^2 f_a \frac{d^3 p_1}{\gamma_1}, \quad (4.53)$$

where we keep the integration and distribution over un-normalized momentum for consistency with other fluid moment definitions.

Unlike most of the non-relativistic limits we have taken thus far, simply taking a low velocity limit will not suffice to reproduce the MB distribution. In order for (4.51) to reduce to the MB distribution, we must also take a high  $z_a$  limit, or limit in which the thermal energy is much smaller than the rest energy for the species. Note that  $K_2(z_a)$  can be approximated as

$$K_2(z_a) \approx \sqrt{\frac{\pi}{2z_a}} \left( 1 + \frac{15}{8z_a} + O(z_a^{-2}) \right) \quad (4.54)$$

in the high  $z_a$  limit (Hazeltine & Waelbroeck, 2018). Additionally, since the MB distribution is generally defined over velocity space, which is only a factor of mass different from the momentum non-relativistically, we must divide (4.51) by a factor of  $c^3$  in order to put the distribution over the appropriate space. Doing so and taking the high  $z_a$  limit to first order

and the low velocity limit to second order, (4.51) reduces to

$$f_a^{\text{MJ}}(\mathbf{v}_1) \approx \frac{n_a}{\pi^{3/2} v_{T_a}^3} e^{-v_1^2/v_{T_a}^2}, \quad (4.55)$$

where the thermal velocity  $v_{T_a}$  is defined as the most probable velocity or

$$v_{T_a} \equiv \sqrt{\frac{2kT_a}{m_a}}. \quad (4.56)$$

Equation (4.55) is exactly the MB distribution.

### 4.3 The Beliaev-Budker Operator

While the relativistic Boltzmann collision operator is completely general for two particle collisions, it should be noted that the form of the integrand is intractable numerically. This is an issue for the non-relativistic Boltzmann operator as well, as it relates to the quantity  $f'_a f'_b$  in (4.22). The non-relativistic work around is to instead use an approximate form of the Boltzmann collision operator: the Landau collision operator (Ter Haar, 2013).

The Landau collision operator is given by

$$C(f_a, f_b) \equiv \frac{q_a^2 q_b^2 \ln \Lambda_{ab}}{8\pi\epsilon_0^2} \frac{\partial}{\partial p_1^i} \int U^{ij} \left( f_b \frac{\partial f_a}{\partial p_1^j} - f_a \frac{\partial f_b}{\partial p_2^j} \right) d^3 p_2, \quad (4.57)$$

where the kernel  $U^{ij}$  is given by

$$U^{ij} \equiv \frac{v_{12}^2 \eta^{ij} - v_{12}^i v_{12}^j}{v_{12}^3} \quad (4.58)$$

and  $\ln(\Lambda_{ab}) = \ln(\lambda_D/\rho_0)$  such that  $\lambda_D$  is the Debye length and the distance of closest approach  $\rho_0$  is given by

$$\rho_0 \equiv \frac{q_a q_b}{4\pi\epsilon_0 m_{ab} v_{12}^2}. \quad (4.59)$$

Here  $m_{ab}$  is the reduced mass between species  $a$  and  $b$ . We will not show the derivation of this operator here as we are concerned only with the relativistic variant. However, drawing

parallels between the assumptions of the Landau operator and the relativistic analogue will be invaluable. Equation (4.57) is derived from the following assumptions:

- The change in momentum due to a single, binary collision is small. The quantity  $f'_a f'_b$  is Taylor expanded to second order in  $\Delta \mathbf{p}_1$  and  $\Delta \mathbf{p}_2$ .
- The differential cross-section is determined by Rutherford scattering (i.e. Coulomb interaction), where we take the maximum distance for the interaction of both particles to be  $\lambda_D$ . Beyond this distance interactions are screened perfectly. This is often called cut-off Coulomb interaction.
- The Coulomb logarithm is large, or  $\ln \Lambda_{ab} \gg 1$ , and is independent of either particle's momentum. This is the case when there are a large number of charged particles participating in the screening process.

In relativistic kinetic theory, Beliaev and Budker's work is the main source for the so called "relativistic Landau operator" (Beliaev & Budker, 1956). The so called Beliaev-Budker collision operator is used as the basis for the vast majority of relativistic kinetic plasma physics related to runaway electrons in ITER-like tokamaks (Guo et al., 2017; Sandquist et al., 2006; Boozer, 2015; Papp et al., 2011; Stahl et al., 2017). The Beliaev-Budker Operator takes the exact same form as (4.57) with the exception of the kernel  $U^{ij}$ , which is now given by

$$U^{ij} \equiv \frac{\gamma_{12}}{\gamma_1 \gamma_2 c (\gamma_{12}^2 - 1)^{3/2}} \left[ (\gamma_{12}^2 - 1) \eta^{ij} - \frac{\gamma_1^2}{c^2} v_1^i v_1^j - \frac{\gamma_2^2}{c^2} v_2^i v_2^j + \frac{\gamma_{12}^2}{c^2} \left( \frac{v_1^i v_2^j + v_2^i v_1^j}{1 - \frac{v_1^k v_{2k}}{c^2}} \right) \right]. \quad (4.60)$$

Note that (4.60) does reduce to (4.58) for  $v_1 \ll c$  and  $v_2 \ll c$ . However, there is a fair amount of ambiguity surrounding this operator.

The Beliaev-Budker (BB) operator is not derived from (4.22). Rather, it is derived in 8D phase-space following the same procedure given in Landau's original derivation, but with all three dimensional parameters upgraded to their 4D versions (Beliaev & Budker, 1956; Ter Haar, 2013). In their derivation,  $\Delta p_1^\mu$  and  $\Delta p_2^\mu$  are considered to be small, which is

analogous to the assumptions of the Landau operator. It is also assumed that the Coulomb logarithm can be pulled out of the collision integral. Often this is done in non-relativistic mechanics by roughly approximating the kinetic energy due to random motion in a single collision as equal to the thermal energy. It should also be noted that this is a *very rough* approximation. Additionally, Beliaev and Budker never give an analogous approximation. We are then left to arbitrarily assume that this approximation has been made. Moreover, we are also left to assume that relativistic corrections to the Debye length and distance of closest approach have been made and that the largeness of the Coulomb logarithm holds. Lastly, there is no obvious connection between the BB operator and (4.22). With all of these factors taken into consideration, it is the view of this thesis to treat the utilization of the BB operator as simply a replication study with the goal of reproducing the work of the linearized version of the BB operator and the full version of the operator in the NIMROD code. Specifically, our goal ultimately is to reproduce the work of Stahl (Stahl et al., 2017).

## CHAPTER 5

### TEST PARTICLE OPERATOR IN NIMROD

#### 5.1 The Sandquist and Papp Operators

As mentioned at the end of the previous chapter, we first wish to implement in the NIMROD code a linear version of the BB operator. We do so as a means of simplifying the initial relativistic kinetic equation in NIMROD, as well as to test initial benchmarks for verifying simplified relativistic mechanics. This can be done by making the following assumptions. We begin by Taylor expanding the kernel in (4.60) about  $\mathbf{v}_2 = 0$  to second order, or

$$U^{ij} \approx U^{ij}|_{\mathbf{v}_b=0} + v_2^l \left[ \frac{\partial U^{ij}}{\partial v_2^l} \Big|_{\mathbf{v}_b=0} \right] + \frac{1}{2} v_2^k v_2^l \left[ \frac{\partial}{\partial v_2^k} \left( \frac{\partial U^{ij}}{\partial v_2^l} \right) \Big|_{\mathbf{v}_b=0} \right], \quad (5.1)$$

and assuming that the background is the non-relativistic Maxwell-Boltzmann distribution, with  $V_b = 0$ , in velocity-space

$$f_b^M = \frac{n_b}{\pi^{3/2} v_{Tb}^3} e^{-\frac{v_2^2}{v_{Tb}^2}}. \quad (5.2)$$

Here  $v_{Tb} \equiv \sqrt{2kT_b/m_b}$  is the bulk/thermal velocity for species  $b$  (Sandquist et al., 2006). Note that what we have just forced the background to be static and isotropic. This will have physical consequences later, namely, the background has in effect, infinite inertia and heat capacity compared to the relativistic, test-particle species.

Calculating each term in (5.1) is incredibly tedious. However, by exploiting the isotropy of  $f_b$ , we can greatly simplify the steps we need to get our approximate  $U^{ij}$ . First we define



the two integrals in (4.57) by the following:

$$I_1 \equiv \int U^{ij} f_b^M \frac{\partial f_a}{\partial p_1^j} d^3 v_2 \quad (5.3)$$

$$I_2 \equiv \int U^{ij} f_a \frac{\partial f_b^M}{\partial p_2^j} d^3 v_2. \quad (5.4)$$

Note that due to the isotropy of  $f_b$ , the first order term in (5.1) does not contribute to (5.3), while *only* the first order term contributes to (5.4). Simplifying  $I_1$  we find that

$$\begin{aligned} I_1 &= U^{ij} \Big|_{\mathbf{v}_2=0} \int f_b^M d^3 v_2 + \frac{1}{2} \left[ \frac{\partial}{\partial v_2^k} \left( \frac{\partial U^{ij}}{\partial v_2^l} \right) \Big|_{\mathbf{v}_2=0} \right] \int v_2^k v_2^l f_b^M d^3 v_2 \\ &= n_b U^{ij} \Big|_{\mathbf{v}_2=0} + \frac{1}{4} n_b v_{Tb}^2 \left[ \frac{\partial}{\partial v_{2k}} \left( \frac{\partial U^{ij}}{\partial v_2^k} \right) \Big|_{\mathbf{v}_2=0} \right] \end{aligned} \quad (5.5)$$

and  $I_2$  simplifies to

$$\begin{aligned} I_2 &= \left[ \frac{\partial U^{ij}}{\partial v_2^l} \Big|_{\mathbf{v}_2=0} \right] \eta_{jn} \int v_2^l v_2^n f_b^M d^3 v_2 \\ &= -\frac{n_b}{m_b} \left[ \frac{\partial U^{ij}}{\partial v_2^j} \Big|_{\mathbf{v}_2=0} \right]. \end{aligned} \quad (5.6)$$

Our goal now is to find the derivatives of  $U^{ij}$  denoted in brackets in (5.5) and (5.6). Firstly, the zeroth order term intuitively is just

$$U^{ij} \Big|_{\mathbf{v}_b=0} = \frac{v_1^2 \eta^{ij} - v_1^i v_1^j}{v_1^3}, \quad (5.7)$$

which takes the exact same form as the non-relativistic kernel. The fact that (5.7) retains the non-relativistic form is due to the form of the relative velocity when the boosted frame is stationary. In this case,  $\mathbf{v}_{12} \rightarrow \mathbf{v}_1$  as  $\mathbf{v}_2 \rightarrow 0$ . The other two terms, after a significant

amount of simplification, become

$$\left. \frac{\partial U^{ij}}{\partial v_2^j} \right|_{\mathbf{v}_b=0} = \frac{2v_1^i}{v_1^3} \quad (5.8)$$

$$\left. \frac{\partial}{\partial v_{2k}} \left( \frac{\partial U^{ij}}{\partial v_2^k} \right) \right|_{\mathbf{v}_b=0} = \frac{4}{v_1^5} v_1^i v_1^j - \frac{2}{v_1^2} \left( 1 - \frac{v_1^4}{c^4} \right) \left( \frac{v_1^2 \eta^{ij} - v_1^i v_1^j}{v_1^3} \right). \quad (5.9)$$

Using (5.7), (5.8), and (5.9), the following integrals may be found in advance to help simplify (4.57):

$$\int U^{ij} f_b^M d^3 v_2 \approx n_b \left[ \left( 1 - \frac{v_{Tb}^2}{2v_1^2} \left( 1 - \frac{v_1^4}{c^4} \right) \right) \left( \frac{v_1^2 \eta^{ij} - v_1^i v_1^j}{v_1^3} \right) + \frac{v_{Tb}^2}{v_1^5} v_1^i v_1^j \right] \quad (5.10)$$

$$\frac{\partial}{\partial p_1^i} \left( \int U^{ij} f_b^M d^3 v_2 \right) \approx -\frac{2n_b}{\gamma_a m_a c^2} \left[ \frac{1}{p_1} \left( 1 - \frac{v_{Tb}^2}{c^2} \right) + \frac{(m_a c)^2}{p_1^3} \left( 1 - \frac{3v_{Tb}^2}{2c^2} \right) \right] p_1^j \quad (5.11)$$

$$\int U^{ij} \frac{\partial f_b^M}{\partial p_2^j} d^3 v_2 \approx -\frac{2n_b \gamma_a^2 m_a^2}{m_b} \left( \frac{p_1^i}{p_1^3} \right) \quad (5.12)$$

$$\frac{\partial}{\partial p_1^i} \left( \int U^{ij} \frac{\partial f_b^M}{\partial p_2^j} d^3 v_2 \right) \approx -\frac{4n_b}{m_b c^2 p_1}. \quad (5.13)$$

Equation (4.57) can be written in the form

$$\begin{aligned} C(f_a, f_b) = \frac{\Gamma_{ab}}{2n_b} & \left[ \frac{\partial}{\partial p_1^i} \left( \int U^{ij} f_b^M d^3 v_2 \right) \frac{\partial f_a}{\partial p_1^j} + \left( \int U^{ij} f_b^M d^3 v_2 \right) \frac{\partial}{\partial p_1^i} \left( \frac{\partial f_a}{\partial p_1^j} \right) \right. \\ & \left. - \left( \int U^{ij} \frac{\partial f_b^M}{\partial p_2^j} d^3 v_2 \right) \frac{\partial f_a}{\partial p_1^i} - \frac{\partial}{\partial p_1^i} \left( \int U^{ij} \frac{\partial f_b^M}{\partial p_2^j} d^3 v_2 \right) f_a \right], \quad (5.14) \end{aligned}$$

where  $\Gamma_{ab}$  is defined by

$$\Gamma_{ab} \equiv \frac{n_b q_a^2 q_b^2 \ln \Lambda_{ab}}{4\pi \epsilon_0^2}. \quad (5.15)$$

By substituting (5.10)-(5.13) into (5.14), switching to spherical coordinates  $(p_1, \theta, \zeta)$ , and assuming there is no  $\zeta$  (gyroangle) dependence, the Sandquist operator can then be shown to be

$$C(f_a, f_b) \approx \Gamma_{ab} \left[ \frac{1}{p^2} \frac{\partial}{\partial p} \left( p^2 \left( A(p) \frac{\partial f_a}{\partial p} + F(p) f_a \right) \right) + \frac{B(p)}{p^2} \mathcal{L}(f_a) \right], \quad (5.16)$$

where the Lorentz operator  $\mathcal{L}(f_a)$  is given by

$$\mathcal{L}(f_a) \equiv \frac{\partial}{\partial \xi} \left( (1 - \xi^2) \frac{\partial f_a}{\partial \xi} \right) \quad (5.17)$$

where  $\xi \equiv \cos(\theta)$ . The subscript for the momentum is dropped to simplify notation. The coefficients  $A(p)$ ,  $F(p)$ , and  $B(p)$  in (5.16) are given by

$$A(p) = \frac{v_{Tb}^2}{2v^3} \quad (5.18)$$

$$F(p) = \frac{v}{kT_b} A(p) \quad (5.19)$$

$$B(p) = \frac{1}{v} \left( 1 - \frac{v_{Tb}^2}{2v^2} \left( 1 - \left( \frac{v}{c} \right)^4 \right) \right). \quad (5.20)$$

Unfortunately, the expansion in (5.1) only converges for ultra-relativistic test-particles. Since we wish to simulate the evolution of the RE distribution, limiting the domain of the momentum is not ideal. To the best of this author's knowledge, the only known relativistic test particle operator that encompasses both the ultra-relativistic and non-relativistic limit is the Papp operator which takes the form of (5.16), but with different coefficients (Papp et al., 2011). The coefficients in Papp's operator take the form:

$$A_p(p) = \frac{1}{v} G \left( \frac{v}{v_{Tb}} \right) \quad (5.21)$$

$$F_p(p) = \frac{v}{kT_b} A(p) \quad (5.22)$$

$$B_p(p) = \frac{1}{v} \left( \text{Erf} \left( \frac{v}{v_{Tb}} \right) - G \left( \frac{v}{v_{Tb}} \right) + \frac{1}{2} \left( \frac{v_{Tb}v}{c^2} \right)^2 \right), \quad (5.23)$$

where the function  $G(x)$  is given by:

$$G(x) \equiv \frac{1}{2x^2} \left( \text{Erf}(x) - \frac{d\text{Erf}(x)}{dx} \right). \quad (5.24)$$

Papp arrives at this form of the test-particle collision operator via what he refers to as "asymptotic matching" (Papp et al., 2011). Equations (5.21)-(5.23) do reduce to (5.18)-(5.20) in the ultra-relativistic limit and the appropriate coefficients in non-relativistic kinetic

theory (Helander & Sigmar, 2002). Thus, it appears that the only other condition that is enforced to construct these coefficients is to ensure continuity between these two limits. Since the exact meaning of "asymptotic matching" does not clearly define the constraints by which continuity is enforced, we shall treat the numerical implementation of the Papp operator as a replication study as well. For the purposes of our linear electron-electron test-particle operator, we shall employ the use of (5.16) with coefficients (5.21)-(5.23).

Note that the operator in (5.16) using (5.21)-(5.23) only refers to interactions between species  $a$  and species  $b$ . To get the total RHS to (4.22), we need to sum over all possible species  $b$  that particle  $a$  can interact with. If we assume that particle  $a$  is an electron and we assume that the plasma we are studying is a pure quasi-neutral plasma with only electrons and a single ion species, then the electron-electron collision operator,  $C_{ee}(f_e)$ , is simply just (5.16) for  $v_{Tb} \rightarrow v_{Te}$ , where  $v_{Te}$  is the electron thermal velocity.

To determine the form of the electron-ion collision operator,  $C_{ei}(f_e)$ , we will make one final assumption. If we assume that the ion mass  $m_i \rightarrow \infty$ , then the electron-ion collision operator is simply given by

$$C_{ei}(f_e) \approx \frac{\Gamma_{ee} Z_{\text{eff}}}{v p^2} \mathcal{L}(f_e), \quad (5.25)$$

where  $Z_{\text{eff}}$  is defined by

$$Z_{\text{eff}} \equiv -\frac{q_i \ln \Lambda_{ei}}{q_e \ln \Lambda_{ee}} \approx -\frac{q_i}{q_e} \quad (5.26)$$

and the quasi-neutrality assumption  $n_e q_e + n_i q_i = 0$  is utilized. Our final collision operator,  $C(f_e) = C_{ee}(f_e) + C_{ei}(f_e)$  is therefore

$$C(f_e) = \Gamma_{ee} \left[ \frac{1}{p^2} \frac{\partial}{\partial p} \left( p^2 \left( A_p(p) \frac{\partial f_e}{\partial p} + F_p(p) f_e \right) \right) + \frac{\tilde{B}_p(p)}{p^2} \mathcal{L}(f_e) \right], \quad (5.27)$$

where the new coefficient  $\tilde{B}_p(p)$  is just

$$\tilde{B}_p(p) \equiv \frac{1}{v} \left( Z_{\text{eff}} + \text{Erf} \left( \frac{v}{v_{Te}} \right) - G \left( \frac{v}{v_{Te}} \right) + \frac{1}{2} \left( \frac{v_{Te} v}{c^2} \right) \right). \quad (5.28)$$

Note that, given the assumption that the ion mass is effectively infinite, the only contribution the electron-ion operator makes is an additional constant term for pitch-angle scattering perpendicular to the magnetic field.

## 5.2 NIMROD Implementation

With (5.28) and the LHS of (4.22), we can now put together our final drift-kinetic equation. We first begin by establishing a 3D phase space similar to the one in the previous section, but in terms of the unit-less variables  $(s, \xi, \zeta)$ , where  $s \equiv p/m_e c$  and  $\xi \equiv p_{\parallel}/p$ . The subscript  $\parallel$  indicates that the parameter is the component of the corresponding vector that is parallel to the magnetic field. Likewise, a subscript  $\perp$  indicates that the parameter in question is the component of the corresponding vector that is perpendicular to the magnetic field. Additionally, for the sake of simplicity, we shall assume that both the electric and magnetic field terms are uniform and that the gyro-motion with gyro-frequency given by  $\omega_g = eB/m_e$  dominates.

In addition to (3.37), we incorporate into the force-per-particle  $F^i$  on the LHS of (4.22) the Abraham-Lorentz-Dirac force

$$F_{\text{ALD}}^i = \frac{e^2 \gamma^2}{6\pi \epsilon_0 c^3} \left[ \dot{a}^i + \frac{3\gamma^2}{c^2} (v^k a_k) a^i + \frac{\gamma^2}{c^2} \left( v^k \dot{a}_k + \frac{3\gamma^2}{c^2} (v^k a_k)^2 \right) v^i \right], \quad (5.29)$$

such that  $F^i = F_E^i + F_B^i + F_{\text{ALD}}^i$ , where  $F_E^i$  and  $F_B$  are the electric and magnetic forces, respectively (Decker et al., 2016). Equation (5.29) describes the radiation back-reaction force due to the acceleration of charged particles in electromagnetic fields. Using the assumptions that the frequency  $\omega_g$  dominates and the uniformity of the magnetic field (which will require that  $v^k a_k = 0$ ), we can rewrite the third term on the LHS of (4.22) using the variables  $(s, \xi)$  as the sum of an electric-field acceleration term and a synchrotron-radiation reaction force term (Stahl et al., 2017). Assuming that the electric field is purely along the direction of the magnetic field, or neglecting the small drift that arises when  $E_{\perp} \neq 0$ , our

drift-kinetic equation then becomes

$$\frac{\partial f_e}{\partial t} - \frac{eE_{\parallel}^i}{m_e c} \frac{\partial f_e}{\partial s^i} + \frac{\partial}{\partial s^i} (\mathcal{F}_S^i f_e) = C_s(f_e), \quad (5.30)$$

where the electric-field acceleration term can be written as

$$-\frac{eE_{\parallel}^i}{m_e c} \frac{\partial f_e}{\partial s^i} = -\frac{eE_{\parallel}}{m_e c} \left( \xi \frac{\partial f_e}{\partial s} + \frac{(1-\xi^2)}{s} \frac{\partial f_e}{\partial \xi} \right) \quad (5.31)$$

and the synchrotron-radiation reaction force term can be written as

$$\frac{\partial}{\partial s^i} (\mathcal{F}_S^i f_e) = -\frac{(1-\xi^2)}{\tau_r \gamma} \left[ \gamma^2 s \frac{\partial f_e}{\partial s} - \xi \frac{\partial f_e}{\partial \xi} + \left( 4s^2 + \frac{2}{1-\xi^2} \right) f_e \right]. \quad (5.32)$$

Here the parameter  $\tau_r$  is often referred to as the radiation time-scale and is given by

$$\tau_r \equiv \frac{6\pi\epsilon_0 (m_e c)^3}{e^4 B^2}. \quad (5.33)$$

The test-particle operator,  $C(f_e)$  in (5.27), as a function of normalized momentum is

$$C_s(f_e) = \frac{1}{\tau_{ee}} \left[ \frac{1}{s^2} \frac{\partial}{\partial s} \left( s^2 \left( A_s(s) \frac{\partial f_e}{\partial s} + F_s(s) f_e \right) \right) + \frac{\tilde{B}_s(s)}{s^2} \mathcal{L}(f_e) \right], \quad (5.34)$$

where the final forms for the operator coefficients are given by

$$A_s(s) = 2 \left( \frac{v}{v_{Te}} \right)^2 G \left( \frac{v}{v_{Te}} \right) \quad (5.35)$$

$$F_s(s) = \frac{\gamma}{s} G \left( \frac{v}{v_{Te}} \right) \quad (5.36)$$

$$\tilde{B}_s(s) = \frac{\gamma}{s} \left( Z_{\text{eff}} + \text{Erf} \left( \frac{v}{v_{Te}} \right) - G \left( \frac{v}{v_{Te}} \right) + \frac{1}{2} \left( \frac{v_{Te} v}{c^2} \right) \right). \quad (5.37)$$

Here the parameter  $\tau_{ee} \equiv \Gamma_{ee}/m_e^2 c^3$  is often referred to as the electron-electron collision time-scale. Our final step is to multiply both sides by  $\tau_{ee}$  so that we advance the distribution in time using a unit-less version of time,  $\tilde{t} \equiv t/\tau_{ee}$ . Doing so to (5.30) yields our final equation

for numerical implementation

$$\frac{\partial f_e}{\partial \tilde{t}} - \tilde{E}_{\parallel}^i \frac{\partial f_e}{\partial s^i} + \alpha \frac{\partial}{\partial s^i} \left( \tilde{\mathcal{F}}_S^i f_e \right) = \tilde{C}_s(f_e), \quad (5.38)$$

where  $\tilde{E}_{\parallel}^i \equiv E_{\parallel}^i/E_c$ ,  $E_c$  is the CH critical electric field, and  $\tilde{C}_s(f_e) = \tau_{ee}C_s(f_e)$ . Here the third term in (5.38) is simply (5.32) with  $\tau_r$  pulled outside of the  $s$  derivative. This is done to define  $\alpha \equiv \tau_{ee}/\tau_r$ , which is the parameter that will actually be implemented into NIMROD.

Note that the  $v^i \partial_i f_e$  term is missing from (5.30). Since we intend to always set our initial condition to (4.51), there will be no spatial dependence during the first time-step when solving for the  $f_e$ . Consequentially, the choice to keep the magnetic fields uniform through the evolution of the distribution function inherently restricts the distribution to be only dependent on the normalized momentum. Ergo, so long as we do not introduce spatial dependence into the force, it is safe to neglect this term.

Our goal is now to make (5.38) discrete. Since  $f_e = f_e(s, \xi, t)$  we need to first decouple the distribution's  $s$  and  $\xi$  dependence. We do so by expanding  $f_e$  in the following manner:

$$f_e(s, \xi, t) = \sum_{l=0}^{N_{\xi}} f_{e,l}(s, t) Q_l(\xi). \quad (5.39)$$

Here  $N_{\xi}$  is the maximum polynomial degree for the expansion in  $\xi$ . In NIMROD,  $Q_l(\xi)$  represents either 1D finite-element (FE) basis functions in  $\xi$  or Legendre polynomials (Held et al., 2015). Throughout this thesis, when we are utilizing the Legendre representation, we will switch notation from  $Q_l(\xi) \rightarrow P_l(\xi)$ . In the case of a 1D FE expansion,  $Q_l(\xi)$  can be represented as either Lagrange or Gauss-Lobatto-Legendre (GLL) polynomials. For the purpose of this thesis, we will only use GLL and Legendre expansions in  $\xi$ .

To handle  $s$  dependence, we opt to solve (5.38) at a set of  $N_s$  collocation points such that  $f_{e,l,i} \equiv f_{e,l}(s_i, t)$ , where  $s_i$  is the  $i$ th collocation point. Ultimately, what this boils down to is solving (5.38)  $N_s$  times. In order to complete this description, we must determine a form for  $s$  derivatives of the distribution function. We achieve this by providing an alternative

expansion for  $f_{e,l}$  in terms of the non-classical, orthogonal polynomials

$$f_{e,l}(s, t) = \sum_{k=0}^{N_s-1} \bar{f}_{e,l,k}(t) L_k(s) f_0(s), \quad (5.40)$$

which are defined by their orthogonality relationship

$$\int_0^\infty L_j(s) L_k(s) f_0(s) ds = \delta_{j,k}. \quad (5.41)$$

Here  $f_0(s)$  is the weight function by which we can define a non-classical quadrature scheme. In this thesis we will choose  $f_0(s) = e^{-z\sqrt{1+s^2}}$  to ensure that the expansion in (5.40) has the correct behavior at  $s = 0$  and  $s \rightarrow \infty$ . Note this weighting also coincides very closely with the  $V_e = 0$  case in (4.51). Additionally, we will choose the roots of  $L_{N_s}(s)$  to be our collocation points  $s_i$  and the quadrature nodes for integration over  $s$ .

Though the collocation points coincide with the indices in (5.40), we still need to relate the coefficients  $\bar{f}_{e,l,i}$  to  $f_{e,l,i}$  as they are not equivalent. By multiplying both sides of (5.40) by  $L_j(s)$  and integrating both sides, the coefficients of the non-classical expansion can be written in terms of the coefficients at the collocation points as

$$\bar{f}_{e,l,k} = \sum_{j=0}^{N_s-1} w_j L_k(s_j) f_{e,l,j}, \quad (5.42)$$

where  $w_j$  are the weights generated from the non-classical quadrature scheme. Therefore, using (5.40) and (5.42), we can write the  $n$ th derivative of  $f_{e,l}$  at the collocation points as

$$\left. \frac{\partial^n f_{e,l}}{\partial s^n} \right|_{s=s_i} = \sum_{j=0}^{N_s-1} \left[ \sum_{k=0}^{N_s-1} w_j L_k(s_j) \frac{\partial^n}{\partial s^n} (L_k(s) f_0(s)) \Big|_{s=s_i} \right] f_{e,l,j}. \quad (5.43)$$

Note the term in the brackets of (5.43) is completely independent of time. Ergo, this term can be pre-computed before even running the NIMROD relativistic, continuum kinetic



solver. We define an s-coupling matrix  $S_{i,j}^{(n)}$  such that

$$S_{i,j}^{(n)} \equiv \sum_{k=0}^{N_s-1} w_j L_k(s_j) \frac{\partial^n}{\partial s^n} (L_k(s) f_0(s)) \Big|_{s=s_i}, \quad (5.44)$$

which transforms (5.43) into

$$\frac{\partial^n f_{e,l}}{\partial s^n} \Big|_{s=s_i} = \sum_{j=0}^{N_s-1} S_{i,j}^{(n)} f_{e,l,j}. \quad (5.45)$$

Though (5.45) is general for any order derivative, only  $S_{i,j}^{(1)}$  and  $S_{i,j}^{(2)}$  have been implemented into NIMROD as there is no need for higher order derivatives at present.

Next, our time dependence is handled by using the limit definition of the derivative to approximate the time-derivative in (5.38) at the  $(k+1)$ th time-step

$$\frac{\partial f_e}{\partial \tilde{t}} \Big|_{\tilde{t}=\tilde{t}^{(k+1)}} \approx \frac{f_e^{(k+1)} - f_e^{(k)}}{\Delta \tilde{t}} \equiv \frac{\Delta f_e^{(k+1)}}{\Delta \tilde{t}}. \quad (5.46)$$

Note this implies that  $f_e^{(0)}$  refers to the initial condition (4.51). Using (5.46) we can re-write (5.38) in the  $\Theta$ -centered form

$$\begin{aligned} \Delta f_e^{(k+1)} + \Delta \tilde{t} & \left[ -\Theta_E \tilde{E}^i \frac{\partial \Delta f_e^{(k+1)}}{\partial s^i} + \Theta_S \alpha \frac{\partial}{\partial s^i} \left( \mathcal{F}_S^i \Delta f_e^{(k+1)} \right) - \Theta_c \tilde{C}_s \left( \Delta f_e^{(k+1)} \right) \right] \\ & = \Delta \tilde{t} \left[ \tilde{E}^i \frac{\partial f_e^{(k)}}{\partial s^i} - \alpha \frac{\partial}{\partial s^i} \left( \mathcal{F}_S^i f_e^{(k)} \right) + \tilde{C}_s \left( f_e^{(k)} \right) \right]. \end{aligned} \quad (5.47)$$

The  $\Theta$  parameters in (5.47) are centering parameters that determine the scheme used for the time-advance. Here  $\Theta_E = \Theta_S = \Theta_c = 1$  refers to an implicit advance whereas  $\Theta_E = \Theta_S = \Theta_c = 0$  is an explicit advance. Due to the high velocities REs can reach, it is possible for the distribution to change dramatically on even short time-scales. Since implicit solves remove this concern, for the purpose of this thesis, we shall always use  $\Theta_E = \Theta_S = \Theta_c = 1$ .

We can pick off the  $\xi$  dependence in (5.47) by multiplying both sides by the test-function  $Q_m(\xi)$  and integrating over the domain. This is often referred to as the Galerkin

approach for the finite-element method. This gives rise to the following  $\xi$ -coupling matrices:

$$M_{l,m}^{(t)} \equiv \int_{-1}^1 Q_l(\xi) Q_m(\xi) d\xi \quad (5.48)$$

$$M_{l,m}^{(s)} \equiv \int_{-1}^1 \xi Q_l(\xi) Q_m(\xi) d\xi \quad (5.49)$$

$$M_{l,m}^{(B)} \equiv -\frac{1}{2} \int_{-1}^1 (1 - \xi^2) \frac{\partial Q_l(\xi)}{\partial \xi} Q_m(\xi) d\xi \quad (5.50)$$

$$M_{l,m}^{(c)} \equiv \int_{-1}^1 \mathcal{L}(Q_l(\xi)) Q_m(\xi) d\xi \quad (5.51)$$

$$M_{l,m}^{(F1)} \equiv \int_{-1}^1 (1 - \xi^2) Q_l(\xi) Q_m(\xi) d\xi \quad (5.52)$$

$$M_{l,m}^{(F2)} \equiv \int_{-1}^1 \xi (1 - \xi^2) Q_l(\xi) Q_m(\xi) d\xi. \quad (5.53)$$

Like (5.44), (5.48)-(5.53) must be computed only once before the time-advance in (5.47).

This allows us to write (5.47) as

$$\sum_{l,j} I_{i,m,l,j}^{\text{LHS}} \Delta f_{e,l,j}^{(k+1)} = \sum_{l,j} I_{i,m,l,j}^{\text{RHS}} f_{e,l,j}^{(k)}, \quad (5.54)$$

where  $I_{i,m,l,j}^{\text{LHS}}$  and  $I_{i,m,l,j}^{\text{RHS}}$  are the total coupling matrices for the LHS and RHS, respectively.

The complete description of these matrices is given by (A.1)-(A.3). Note that the indices  $(l, j)$  in (5.54) can be consolidated into one index  $q = l + 1 + (j - 1)d_\xi$ , where  $d_\xi = N_\xi \mathcal{M}_\xi + 1$  is the number of degrees of freedom in  $\xi$  and  $\mathcal{M}_\xi$  is the number of subdivisions of the domain  $-1 \leq \xi \leq 1$ . Re-writing (5.54) in terms of  $q$  we now have the equation

$$\sum_q I_{i,m,q}^{\text{LHS}} \Delta f_{e,q}^{(k+1)} = \sum_q I_{i,m,q}^{\text{RHS}} f_{e,q}^{(k)} \quad (5.55)$$

Since the RHS of (5.55) is known for every  $k$ th time-step, letting  $i$  and  $m$  range over all possibilities leads to the algebraic system  $A\mathbf{x} = \mathbf{b}$ , which NIMROD solves using its native GMRES algorithm (Saad & Schultz, 1986). The distribution function at the  $(k + 1)$ th time-step is then calculated via  $f_{e,q}^{(k+1)} = f_{e,q}^{(k)} + \Delta f_{e,q}^{(k+1)}$ .

To set the time-advance in motion we must define some input parameters needed for

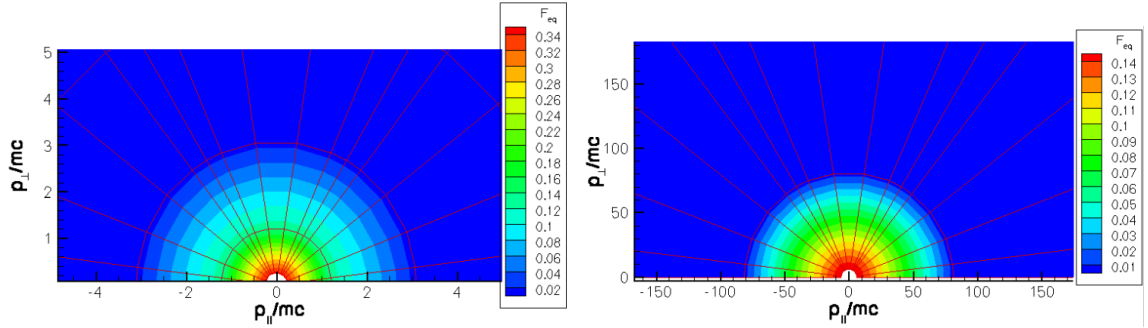


**Figure 5.1:** 2D phase-space representation of  $\tilde{f}_e^{\text{MJ}} \equiv f_e^{\text{MJ}}/N_M$  for  $z_e = 1$  (left) and  $z_e = 100$  (right). The parallel flow parameter  $s_{V\parallel} = 0$  for both cases. The normalization coefficient  $N_M$  is defined in (4.44). The 1D FE grid in  $\xi$  and the collocation grid in  $s$  is overlaid on the MJ distribution to give an indication of normalized momentum-space resolution.

$f_e^{(0)}$  given by (4.51). Arguably the most important input parameter is the  $z_e$  parameter. This parameter effectively determines how relativistic the initial distribution is. Moreover, as can be seen in Figure 5.1, it also can drastically affect its peak value and the rate at which the MJ distribution decays. The equilibrium number density for the electron population in the fluid rest-frame  $n_{REe}$  is assumed to be some fraction  $\beta$  of the bulk density  $n_B$ , or  $n_{REe} = \beta n_B$ . The bulk density is the same density as in (2.2). We write this density as  $n_B$  to distinguish it from the lab-frame density for the REs,  $n_e$ . In order for our assumption that the bulk electrons are unaffected by the RE population to hold true, it is important that  $\beta$  is quite small. Lastly, as indicated in Figure 5.1, we also incorporate into the initial condition a parallel flow parameter  $s_{V\parallel} \equiv \gamma_V V_{\parallel}/c$ . In other words, we pick our initial flow to lie purely along the direction of the magnetic field.

### 5.3 Results

For the purposes of this section we will discuss the following cases: collisional relaxation of the MJ distribution with flow, collisional relaxation of a double MJ distribution, and a full simulation of (5.30) with all parameters turned on. Unless stated otherwise, all parameters are calculated and shown in MKS units.

To properly benchmark our implementation in NIMROD, we start by considering the case of collisional relaxation of the MJ distribution given by (4.51). By collisional relaxation,

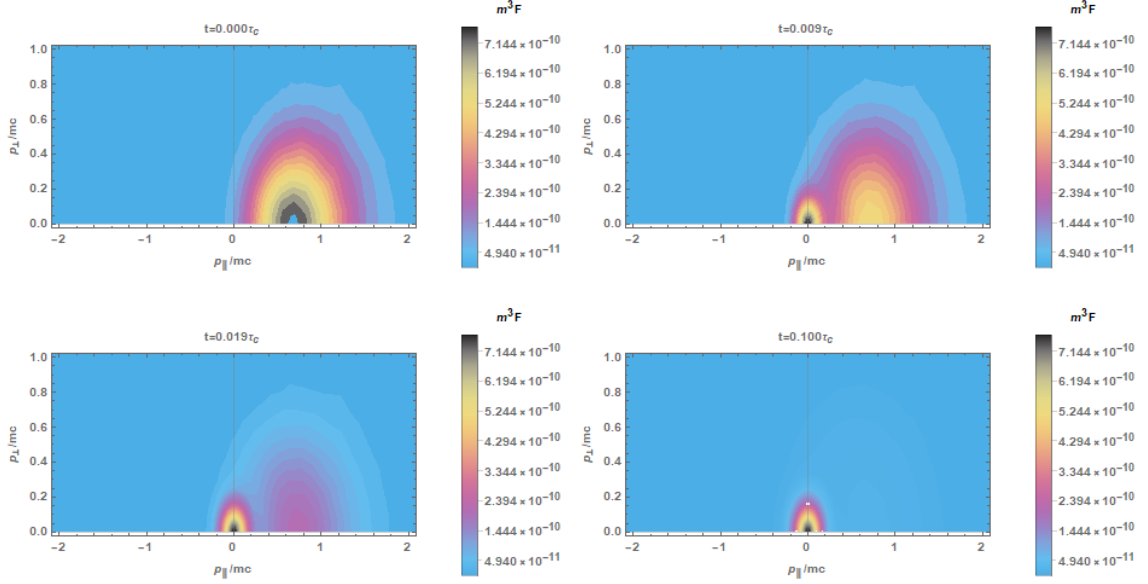


**Figure 5.2:** Collisional relaxation of  $m_e^3 f_e$  with 30 time-steps at  $\Delta\tilde{t} = 10^{-3}$  and 7 time-steps at  $\Delta\tilde{t} = 10^{-2}$ . The 2D normalized momentum space contour plots (read from left to right and top to bottom) show the distribution at four different times. Here  $N_s = 40$ ,  $N_\xi = 7$ ,  $\mathcal{M}_\xi = 3$ ,  $z_e = 10$ ,  $z_B = 100$ ,  $s_{V||} = 0.65$ ,  $\tilde{E}_{||} = 0$ ,  $\alpha = 0$ ,  $\beta = 10^{-4}$ , and  $n_B = 10^{19} \text{m}^{-3}$ .

we mean the process by which the test-particle distribution slowly evolves to the background distribution in the absence of external force. Note that since the assumptions of (5.38) require the potentially relativistic electron distribution to interact with the non-relativistic MB distribution, the collision operator does not trivially go to zero.

As can be seen in Figure 5.2, by turning off the parallel electric field and synchrotron radiation in NIMROD, the MJ distribution does indeed evolve to a MB distribution such that  $\mathbf{V}_e = 0$ . However, as Figure 5.2 suggests, the manner by which the MJ distribution relaxes into the MB distribution is somewhat un-physical. Instead of a smooth transformation from the initial condition into the background, the initial MJ distribution simply fades away while a MB distribution takes its place. While both the introduction of the background MB and the removal of the MJ distribution happen in a continuous manner, the two distributions are seemingly uncoupled. This is most likely due to the "asymptotic matching" assumption needed to transform the Sandquist's form of the test-particle operator, with coefficients (5.18)-(5.20) into the form given by Papp with coefficients instead

given by (5.21)-(5.23).

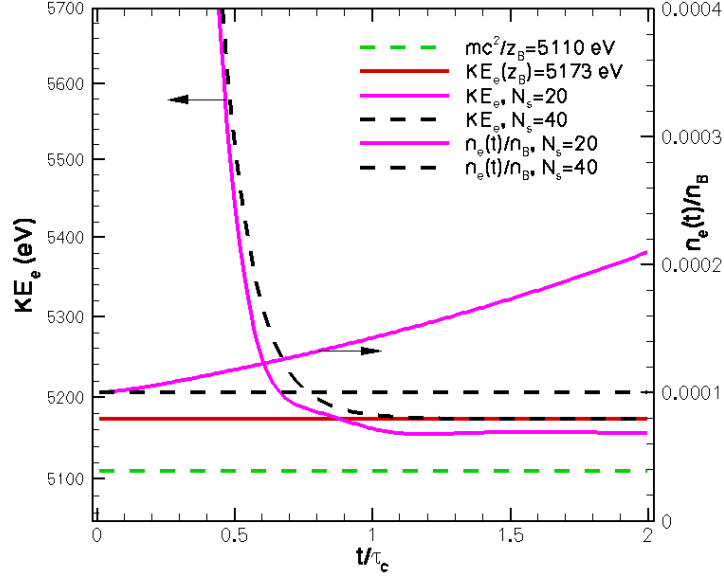


**Figure 5.3:** Convergence test for the case in Figure 5.2. This case is run for more time-steps in order to show fluid parameters evolving to the bulk population in equilibrium. Here (left-arrow) plots the average kinetic energy for different values of  $N_s$ , while (right-arrow) plots the RE number density normalized by the number density of the bulk population for the same  $N_s$  values.

We also wish to verify the behavior of several fluid parameters during the relaxation process. Additionally, we wish to ensure that our solution is independent of the resolution of our 2D normalized momentum space. Figure 5.3 shows the convergence of both the average kinetic energy and the number density as a function of time and  $N_s$ . The average kinetic energy is given by taking

$$KE_e = \frac{1}{n_e} \int (\gamma_1 - 1) m_e c^2 f_e d^3 p_1. \quad (5.56)$$

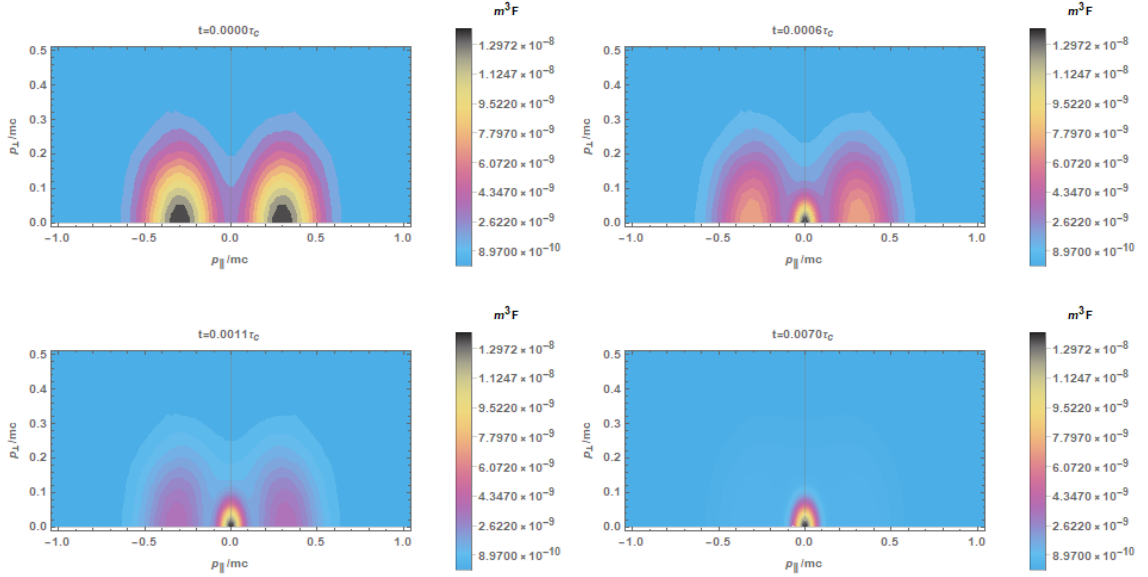


**Figure 5.4:** Collisional relaxation of a double MJ distribution with 20 time-steps at  $\Delta\tilde{t} = 10^{-4}$  and 5 time-steps at  $\Delta\tilde{t} = 10^{-3}$ . Here  $N_s = 40$ ,  $N_\xi = 7$ ,  $\mathcal{M}_\xi = 3$ ,  $z_e = 51$ ,  $z_B = 510$ ,  $s_{V\parallel} = 0.65$ ,  $\tilde{E}_\parallel = 0$ ,  $\alpha = 0$ ,  $\beta = 10^{-3}$ , and  $n_B = 10^{19}\text{m}^{-3}$ .

The parallel flow-velocity is found by taking the spatial component of (4.33), dividing by  $n_e$ , and taking the parallel component of the result. This can be written as

$$V_{e,\parallel} \equiv \frac{1}{n_e} \int v_\parallel f_e d^3 p_1. \quad (5.57)$$

In Figure 5.2,  $N_s = 40$  is sufficient to resolve our normalized momentum space. Upon inspection of the fully resolved versions of our fluid parameters in Figure 5.3, it can be seen that number density is conserved throughout this process. Although not shown explicitly, as expected, the flow velocity of the shifted relativistic test-particle distribution correctly, and continuously, goes to zero as the solution becomes an un-shifted MB distribution. However, the average kinetic energy is not conserved. This is due to the background distribution not being allowed to evolve in time. Constraining the simulation in this manner, that is, using a linearized test-particle collision operator that does not include “field” terms, makes it impossible for energy and momentum to be transferred from the RE population to the bulk population.

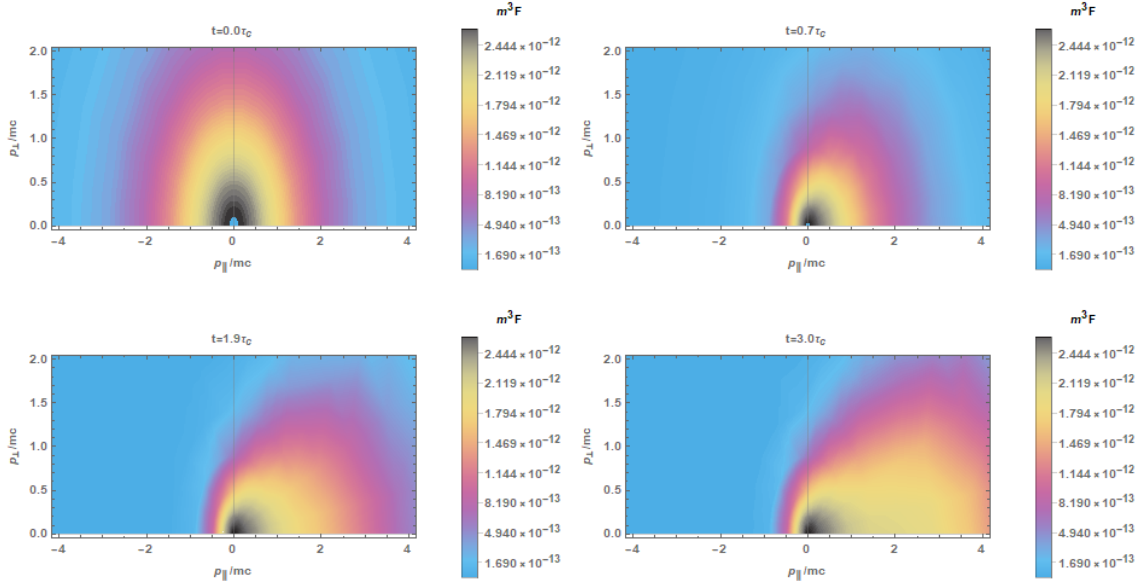


**Figure 5.5:** Evolution of unshifted ( $s_{V||} = 0$ ) MJ distribution over 30 time-steps at  $\Delta\tilde{t} = 10^{-1}$ . Here  $N_s = 40$ ,  $N_\xi = 7$ ,  $\mathcal{M}_\xi = 3$ ,  $z_e = 51$ ,  $z_B = 510$ ,  $s_{V||} = 0$ ,  $\tilde{E}_{||} = 2.25$ ,  $\alpha = 0.2$ ,  $\beta = 10^{-3}$ , and  $n_B = 10^{19}\text{m}^{-3}$ .

Our second benchmark is the collisional relaxation of a double MJ distribution, defined by

$$f_e^{2\text{MJ}} \equiv N_M \left( e^{-\gamma_R m_e c^2} + e^{-\gamma_{R-} m_e c^2} \right), \quad (5.58)$$

where  $\gamma_{R-}$  is simply  $\gamma_R$  such that  $s_{V||} \rightarrow -s_{V||}$ . Since (5.38) is symmetric in  $\xi$ , the same behavior that occurred in Figure 5.2 should occur in the same fashion, but on both sides symmetrically about  $\xi = 0$ . As shown in Figure 5.4, using the initial condition given by (5.58) does indeed yield exactly this behavior.

Given the results of these two benchmark cases, we consider the linearized test-particle operator given by the RHS of (5.38) to have been successfully implemented in the NIMROD code. We now turn our attention to testing the implementation of the electric-field acceleration and synchrotron radiation terms in (5.30). Here we set the electric-field to be higher than the CH critical electric-field, in order to observe the behavior of the RE distribution above this threshold. Additionally, we set  $\alpha$  in (5.38) to be fairly small so that the influence of the electron-electron interaction is somewhat more significant than the

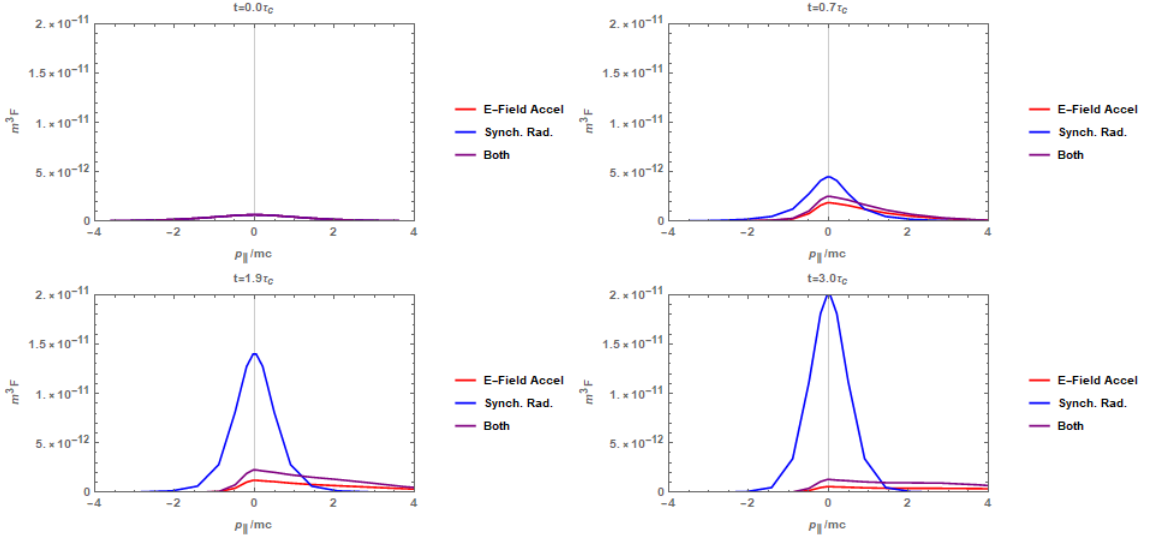


**Figure 5.6:** Three 1D ( $s_{\perp} = 0$ ) slices of the case from Figure 5.5 with two slightly modified and one un-modified. These cases are ( $\tilde{E}_{\parallel} = 2.25, \alpha = 0$ ) in red, ( $\tilde{E}_{\parallel} = 0, \alpha = 0.2$ ) in blue, and ( $\tilde{E}_{\parallel} = 2.25, \alpha = 0.2$ ) in purple.

influence of synchrotron radiation. In addition, we make our initial condition unshifted. We do this to ensure that our distribution stays closer to the center of the 2D normalized momentum-space grid. As the distribution accelerates to the right, it requires increasingly more grid points to properly resolve.

In Figure 5.5, it is clear that as time advances, increasingly more electrons are being accelerated in the direction along the magnetic field due to the parallel electric-field applied in the opposite direction. However, Figure 5.5 does not clearly show the influence of the synchrotron radiation reaction force. Additionally, despite the number density being conserved in this case, as it was in collisional relaxation cases, it seems as though the center of the distribution is locked in place. As a consequence, the number density does not appear to be conserved at first glance.

To clarify the role that each term on the LHS of (5.30) plays, we can look at 1D slices of our 2D normalized momentum-space distribution. Moreover, we run two additional simulations: one with just the electric-field acceleration term on and one with just the synchrotron radiation reaction force on. We then superimpose these two cases with the case in Figure 5.5. The time-advance of the purely synchrotron radiation and collisions run



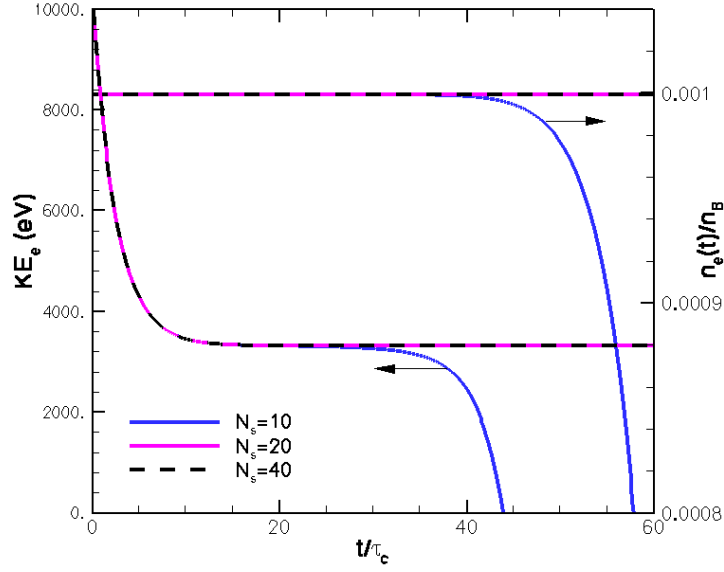


**Figure 5.7:** Convergence test for the purely synchrotron term in Figure 5.6. This case is run for more time-steps in order to show fluid parameters evolving to the bulk population in equilibrium. Here (left-arrow) plots the average kinetic energy for different values of  $N_s$  (shown as np), while (right-arrow) plots the RE number density normalized by the number density of the bulk population for the same  $N_s$  values.

in Figure 5.6 shows that without the push of the electric-field, the RE population appears to grow in an unbounded fashion. Obviously, such behavior would not be physical.

Nevertheless, plots of the density and kinetic energy (see Figure 5.7) reveal that conservation of density is obtained over several synchrotron radiation time-scales using  $N_s \geq 20$ . Furthermore, the expected decay of  $KE_e$  due to radiation shows a rapid decay early on followed by a slower decay later on. Taking into consideration the concerns raised regarding the linearized, test-particle operator, namely, "asymptotic matching" and a non-evolving background distribution, we turn now to implementation of the fully non-linear BB operator in the interest of obtaining the correct time-advance of the RE distribution and the conservation of energy and momentum.

## CHAPTER 6

### BRAAHMS-KARNY FORMULATION IN NIMROD

#### 6.1 Braams-Karney Differential Formulation

We now turn our attention to our final goal of reproducing some of the benchmarks in Stahl's work using the fully non-linear BB operator. As cited in the previous section, the (5.16) has a number of setbacks. To correct these issues, we again turn our attention to (4.57), which allows for the background distribution to evolve. Keep in mind that the electron-electron interaction term in (4.57)'s form is numerically challenging since it makes the kinetic equation a non-linear, integro-differential equation. One way to make progress is to express the collision operator in terms of potential functions that serve as relativistic analogues to Rosenbluth potentials (Braams & Karney, 1987). These potentials are given by

$$\Upsilon_{b,0} \equiv -\frac{1}{4\pi} \int (\gamma_{12}^2 - 1)^{-\frac{1}{2}} f_b(\mathbf{x}_2, \mathbf{s}_2, t) \frac{d^3 s_2}{\gamma_2} \quad (6.1)$$

$$\Upsilon_{b,1} \equiv -\frac{1}{8\pi} \int (\gamma_{12}^2 - 1)^{\frac{1}{2}} f_b(\mathbf{x}_2, \mathbf{s}_2, t) \frac{d^3 s_2}{\gamma_2} \quad (6.2)$$

$$\Upsilon_{b,2} \equiv -\frac{1}{32\pi} \int [\gamma_{12} \cosh^{-1}(\gamma_{12}) - (\gamma_{12}^2 - 1)] f_b(\mathbf{x}_2, \mathbf{s}_2, t) \frac{d^3 s_2}{\gamma_2} \quad (6.3)$$

$$\Pi_{b,0} \equiv -\frac{1}{4\pi} \int \gamma_{12} (\gamma_{12}^2 - 1)^{-\frac{1}{2}} f_b(\mathbf{x}_2, \mathbf{s}_2, t) \frac{d^3 s_2}{\gamma_2} \quad (6.4)$$

$$\Pi_{b,1} \equiv -\frac{1}{4\pi} \int \cosh^{-1}(\gamma_{12}) f_b(\mathbf{x}_2, \mathbf{s}_2, t) \frac{d^3 s_2}{\gamma_2}. \quad (6.5)$$

To begin, we first put the electron-electron interaction term in (4.57) into the Fokker-Planck form

$$C_{ee}(f_e) = \alpha_c \frac{\partial}{\partial s^i} \left( D_e^{ij} \frac{\partial f_e}{\partial s^j} - \mathcal{F}_e^i f_e \right), \quad (6.6)$$

where  $D_b^{ij}$  and  $\mathcal{F}_b^i$  are defined by

$$D_b^{ij} \equiv \frac{c}{8\pi} \int U^{ij} f_b(\mathbf{x}_2, \mathbf{s}_2, t) d^3 s_2 \quad (6.7)$$

$$\mathcal{F}_b^i \equiv -\frac{c}{8\pi} \int \frac{\partial U^{ij}}{\partial s_2^j} f_b(\mathbf{x}_2, \mathbf{s}_2, t) d^3 s_2, \quad (6.8)$$

$\alpha_c \equiv 4\pi/n\tau_c$ , and the subscript has been dropped from  $\mathbf{s}_1$  for simplicity. Here  $D_b^{ij}$  and  $\mathcal{F}_b^i$  are often referred to as the diffusion and drag terms, respectively. Additionally, we shall henceforth drop the  $b$  subscript on the potentials since the potential formulation will only be used for  $C_{ee}(f_e)$ . For  $C_{ei}(f_e)$ , we will use the same scattering operator used in Sec.(IV), which we write below for convenience:

$$C_{ei}(f_e) = \frac{\gamma}{\tau_c s^3} \mathcal{L}(f_e). \quad (6.9)$$

It is important to note that the variable  $n$  does not naturally come out of this formulation of the collision operator. It is artificially incorporated so that we may normalize our time coordinate in the same fashion as Sec.(IV). Therefore,  $n$  is a free parameter that has no connection to the RE number density and only influences the collisional time-scale that we are working with.

To connect (6.6) to (6.1)-(6.5), we introduce three new operators,  $L^{ij}$ ,  $K^i$ , and  $L_a$ . Additionally, for convenience, we have defined three new potentials  $\Upsilon_- \equiv 4\Upsilon_2 - \Upsilon_1$ ,  $\Upsilon_+ \equiv 4\Upsilon_2 + \Upsilon_1$ , and  $\Pi \equiv 2\Pi_1 - \Pi_0$ . By doing so, we can now rewrite (6.7) and (6.8) for the electron-electron interaction as

$$D_e^{ij} = \frac{1}{\gamma} [L^{ij}\Upsilon_- - (\eta^{ij} + s^i s^j) \Upsilon_+] \quad (6.10)$$

$$\mathcal{F}_e^i = \frac{1}{\gamma} K^i \Pi, \quad (6.11)$$

where  $L^{ij}$ ,  $K^i$ , and  $L_a$  are defined by

$$L^{ij}\Upsilon_- \equiv \left(\eta^{ik} + s^i s^k\right) \left(\eta^{lj} + s^l s^j\right) \frac{\partial^2 \Upsilon_-}{\partial s^k \partial s^l} + \left(\eta^{ij} + s^i s^j\right) \left(s^k \frac{\partial \Upsilon_-}{\partial s^k}\right) \quad (6.12)$$

$$K^i \Pi \equiv \left(\eta^{ij} + s^i s^j\right) \frac{\partial \Pi}{\partial s^j} \quad (6.13)$$

$$L_a \Psi \equiv \left(\eta^{ij} + s^i s^j\right) \frac{\partial^2 \Psi}{\partial s^i \partial s^j} + 3s^i \frac{\partial \Psi}{\partial s^i} + (1 - a^2) \Psi. \quad (6.14)$$

Through (6.14), it can also be shown that all five potentials are coupled to the kinetic equation via their own PDEs, which are given by:

$$L_0 \Upsilon_0 = f_e \quad (6.15)$$

$$L_2 \Upsilon_1 = \Upsilon_0 \quad (6.16)$$

$$L_2 \Upsilon_2 = \Upsilon_1 \quad (6.17)$$

$$L_1 \Pi_0 = f_e \quad (6.18)$$

$$L_1 \Pi_1 = \Pi_0. \quad (6.19)$$

With foundation of the five potential PDEs coupled to the collision operator, it is now possible to express the RHS of the kinetic equation as coefficients comprised of linear combinations of derivatives of potential functions onto linear derivatives of the distribution function. Once again we utilize our 3D momentum space coordinates  $(s, \xi, \zeta)$ , while assuming that there is no  $\zeta$  dependence, to write  $C_{ee}(f_e)$  (normalized by  $\alpha_c$ ) as

$$\frac{C_{ee}(f_e)}{\alpha_c} = C^{(s^2)} \frac{\partial^2 f_e}{\partial s^2} + C^{(s)} \frac{\partial f_e}{\partial s} + C^{(\xi^2)} \frac{\partial^2 f_e}{\partial \xi^2} + C^{(\xi)} \frac{\partial f_e}{\partial \xi} + C^{(s\xi)} \frac{\partial^2 f_e}{\partial s \partial \xi} + C^{(f)} f_e, \quad (6.20)$$

with the following coefficients:

$$C^{(s^2)} \equiv \gamma(8\Upsilon_2 - \Upsilon_0) - \frac{2\gamma^3}{s} \frac{\partial \Upsilon_-}{\partial s} - \frac{\gamma(1 - \xi^2)}{s^2} \frac{\partial^2 \Upsilon_-}{\partial \xi^2} + \frac{2\gamma\xi}{s^2} \frac{\partial \Upsilon_-}{\partial \xi} \quad (6.21)$$

$$\begin{aligned}
C^{(s)} \equiv & \frac{1}{\gamma s} (2 + 3s^2) (8\Upsilon_2 - \Upsilon_0) - 16\gamma \frac{\partial \Upsilon_2}{\partial s} + 6\gamma \frac{\partial \Upsilon_1}{\partial s} - \gamma \frac{\partial \Upsilon_0}{\partial s} \\
& - \frac{2\gamma^3}{s} \left( \frac{\partial^2 \Upsilon_-}{\partial s^2} + \frac{1}{s} \frac{\partial \Upsilon_-}{\partial s} \right) + \frac{1}{\gamma s} \left( 2 + \frac{1}{s^2} \right) \left( 2\xi \frac{\partial \Upsilon_-}{\partial \xi} - (1 - \xi^2) \frac{\partial^2 \Upsilon_-}{\partial \xi^2} \right) \\
& - \gamma \frac{\partial \Pi}{\partial s}
\end{aligned} \tag{6.22}$$

$$C^{(\xi^2)} \equiv \frac{1 - \xi^2}{\gamma s^2} \left[ \frac{\gamma^2}{s} \frac{\partial \Upsilon_-}{\partial s} + \frac{1}{s^2} \left( (1 - \xi^2) \frac{\partial^2 \Upsilon_-}{\partial \xi^2} - \xi \frac{\partial \Upsilon_-}{\partial \xi} \right) - \Upsilon_+ \right] \tag{6.23}$$

$$\begin{aligned}
C^{(\xi)} \equiv & - \frac{\xi (1 - \xi^2)}{\gamma s^4} \frac{\partial^2 \Upsilon_-}{\partial \xi^2} - \frac{2\gamma (1 - \xi^2)}{s^3} \frac{\partial^2 \Upsilon_-}{\partial s \partial \xi} - \frac{2\gamma \xi}{s^3} \frac{\partial \Upsilon_-}{\partial s} \\
& + \left( \frac{2}{\gamma s^4} + \frac{3(1 - \xi^2)}{\gamma s^2} \right) \frac{\partial \Upsilon_-}{\partial \xi} - \frac{(1 - \xi^2)}{\gamma s^2} \left( 4 \frac{\partial \Upsilon_2}{\partial \xi} - 3 \frac{\partial \Upsilon_1}{\partial \xi} + \frac{\partial \Upsilon_0}{\partial \xi} + \frac{\partial \Pi}{\partial \xi} \right) \\
& + \frac{2\xi}{\gamma s^2} \Upsilon_+
\end{aligned} \tag{6.24}$$

$$C^{(s\xi)} \equiv \frac{2\gamma (1 - \xi^2)}{s^3} \left( s \frac{\partial^2 \Upsilon_-}{\partial s \partial \xi} - \frac{\partial \Upsilon_-}{\partial \xi} \right) \tag{6.25}$$

$$C^{(f)} \equiv -\gamma \frac{\partial^2 \Pi}{\partial s^2} - \frac{1}{\gamma s} (2 + 3s^2) \frac{\partial \Pi}{\partial s} - \frac{(1 - \xi^2)}{\gamma s^2} \frac{\partial^2 \Pi}{\partial \xi^2} + \frac{2\xi}{\gamma s^2} \frac{\partial \Pi}{\partial \xi}. \tag{6.26}$$

With the above differential formulation of the RHS of the BB operator, the last step is to find a way to solve for the five potentials. Specifically, we will be solving for their Legendre coefficients. First, for any function  $\chi$  that can be expanded in terms of Legendre polynomials, or  $\chi(s, \xi, t) = \sum_l \chi_l(s, t) P_l(\xi)$ , we can define a new operator  $L_{l,a}$  on  $\chi_l$  by

$$L_{l,a} \chi_l \equiv \gamma^2 \frac{\partial^2 \chi_l}{\partial s^2} + \left( \frac{2}{s} + 3s \right) \frac{\partial \chi_l}{\partial s} + \left( 1 - a^2 - \frac{l(l+1)}{s^2} \right) \chi_l. \tag{6.27}$$

Note that  $L_{l,a}$  is simply  $L_a$  when the function it is operating on is expanded in terms of Legendre polynomials and has no  $\zeta$  dependence. Additionally, if we do a Legendre expansion for  $f_e$  as well, then (6.15)-(6.18) effectively become ODEs in terms of the normalized

momentum variable  $s$ .

To proceed any further, we will need to invent some new notation (Braams & Karney, 1989). We write (6.15)-(6.18) in the more concise notation

$$L_{l,a}\psi_{l,a} = f_{e,l} \quad (6.28)$$

$$L_{l,a'}\psi_{l,aa'} = \psi_{l,a} \quad (6.29)$$

$$L_{l,a''}\psi_{l,aa'a''} = \psi_{l,aa'}. \quad (6.30)$$

One can quickly verify that all five potential equations are stored in these three equations by simply plugging in values for  $a$ ,  $a'$  and  $a''$  where appropriate. For example, for  $a = 0$ ,  $a' = 2$ , and  $a'' = 2$ , the above equations simply become  $L_{l,0}\psi_{l,0} = f_{e,l}$ ,  $L_{l,2}\psi_{l,02} = \psi_{l,0}$ , and  $L_{l,2}\psi_{l,022} = \psi_{l,02}$ . Comparing these equations with (6.15)-(6.17) allows us to identify  $\psi_{l,0} = \Upsilon_{0,l}$ ,  $\psi_{l,02} = \Upsilon_{1,l}$ , and  $\psi_{l,022} = \Upsilon_{2,l}$ . Keep in mind that the first subscript on the  $\Upsilon$  and  $\Pi$  potentials is just a label. A similar comparison can be done for the  $\Pi$  potentials. In our case, although (6.30) only applies for  $\psi_{l,022}$ , we leave the labels arbitrary for the sake of generality.

What we have done is change the way we label each potential. Instead of having three  $\Upsilon$  potentials and two  $\Pi$  potentials, we label them all as  $\psi$  potentials. The labels  $a$ ,  $a'$ , and  $a''$  below  $\psi$  refer to the corresponding labels of the list of operators, in order from left to right, required to make the RHS of the potential equation equal to  $f_{e,l}$ . For (6.28) this is self-explanatory as the RHS is already  $f_{e,l}$ . However, applying  $L_{l,a}$  to both sides of (6.29) and  $L_{l,a}L_{l,a'}$  to both sides of (6.30), and utilizing (6.28) we have the following equations:

$$L_{l,a}L_{l,a'}\psi_{l,aa'} = f_{e,l} \quad (6.31)$$

$$L_{l,a}L_{l,a'}L_{l,a''}\psi_{l,aa'a''} = f_{e,l}. \quad (6.32)$$

Closer inspection of (6.31) and (6.32) shows that the second label on each of the operators in their respective equations spells out, in order, the label for the corresponding  $\psi$  potential. Assuming that  $f_{e,l}$  is known, (6.28), (6.31), and (6.32) are effectively (ignoring time which is

un-coupled to  $s$  in each equation) linear inhomogeneous ODEs that can be solved by using the Green's function approach.

To start, let us consider the two homogeneous solutions to (6.28) defined by

$$j_{l,a}(s) \equiv \sqrt{\frac{\pi}{2s}} P_{a-1/2}^{-(l+1/2)}(\gamma) \quad (6.33)$$

$$y_{l,a}(s) \equiv (-1)^{l+1} \sqrt{\frac{\pi}{2s}} P_{a-1/2}^{l+1/2}(\gamma), \quad (6.34)$$

where  $P_\nu^\mu(x)$  is the extension of the associated Legendre polynomials of the first kind for real-valued indices  $\mu$  and  $\nu$ . Using (6.33) and (6.34), we can construct a Green's function  $N_{l,a}(s_>, s_<)$  for (6.28), with  $N_{l,a}(s, s')$  given by

$$N_{l,a}(s, s') \equiv y_{l,a}(s) j_{l,a}(s'). \quad (6.35)$$

Here  $s_> \equiv \max(s, s')$  and  $s_< \equiv \min(s, s')$ . Note that  $N_{l,a}(s_>, s_<)$  satisfies the equation

$$L_{l,a} N_{l,a}(s_>, s_<) = \frac{\gamma^2}{s^2} \delta(s - s'), \quad (6.36)$$

where we make use of the jump condition

$$\left( \frac{\partial N_{l,a}(s, s')}{\partial s} - \frac{\partial N_{l,a}(s', s)}{\partial s} \right) \Big|_{s=s'} = \frac{1}{\gamma' s'^2}. \quad (6.37)$$

For a more detailed proof of (6.36), see the Appendix. Using (6.36), it can be shown that a particular solution to (6.28) is

$$\psi_{l,a}^{\text{PS}}(s) = \int_0^\infty N_{l,a}(s_>, s_<) \frac{s'^2}{\gamma'} f_{e,l}(s') ds'. \quad (6.38)$$

In order to construct Green's functions for  $\psi_{l,aa'}$  and  $\psi_{l,aa'a''}$ , we will use the formulation for  $\psi_{l,a}$ 's Green's function as a basis.

It is important to note that we do not have as much freedom to pick the particular solution for  $\psi_{l,aa'}$  and  $\psi_{l,aa'a''}$  as we did when picking it for  $\psi_{l,a}$ . This is due to the fact that

$\psi_{l,a}$ ,  $\psi_{l,aa'}$ , and  $\psi_{l,aa'a''}$  must satisfy the system of equations (6.28)-(6.30). In other words we need to construct  $N_{l,aa'}(s_>, s_<)$  and  $N_{l,aa'a''}(s_>, s_<)$  such that

$$L_{l,a}N_{l,*a}(s_>, s_<) = N_{l,*}(s_>, s_<), \quad (6.39)$$

where

$$N_l(s_>, s_<) \equiv \frac{\gamma}{s^2} \delta(s - s'). \quad (6.40)$$

The \* in (6.39) refers to any arbitrary list of indices. From this equation we see that the last index on the LHS must match the index for the operator of the corresponding equation, while the RHS must have all the same indices as the LHS (notated by \*) except for the last one. We will make use of this \* notation often as it will help generalize statements that would be cumbersome otherwise.

Adhering to the constraints set forth by (6.39), we can construct the Green's functions  $N_{l,aa'}(s_>, s_<)$  and  $N_{l,aa'a''}(s_>, s_<)$  such that

$$N_{l,aa'}(s, s') \equiv y_{l,a}(s)j_{l,aa'}(s') + y_{l,aa'}(s)j_{l,a'}(s') \quad (6.41)$$

$$N_{l,aa'a''}(s, s') \equiv y_{l,a}(s)j_{l,aa'a''}(s') + y_{l,aa'}(s)j_{l,a'a''}(s') + y_{l,aa'a''}(s)j_{l,a''}(s'), \quad (6.42)$$

where  $j_{l,*}$  is defined for multi-indexed polynomials by

$$j_{l,*aa'} \equiv \frac{\dot{j}_{l,*a} - \dot{j}_{l,*a'}}{a^2 - a'^2}, \quad (6.43)$$

which also satisfy their own system of equations

$$L_{l,a}j_{l,*a} = j_{l,*}. \quad (6.44)$$

The relationships for multi-indexed  $y_{l,*}$  are analogous to that in (6.43) and (6.44). Note that for  $a = a'$ , a limit must be taken. Following the same process as before, it can be



shown that the particular solution for  $\psi_{l,*}$  is given by

$$\psi_{l,*}^{\text{PS}}(s) = \int_0^\infty N_{l,*}(s_>, s_<) \frac{s'^2}{\gamma'} f_{e,l}(s') ds'. \quad (6.45)$$

To find the full solution for  $\psi_{l,*}$  we must also account for the corresponding homogeneous solutions to (6.28), (6.31), and (6.32), such that  $\psi_{l,*} = \psi_{l,*}^{\text{HS}} + \psi_{l,*}^{\text{PS}}$ . The expressions for  $\psi_{l,*}^{\text{HS}}$  are

$$\psi_{l,a}^{\text{HS}} = A_{l,a} y_{l,a} + B_{l,a} j_{l,a} \quad (6.46)$$

$$\psi_{l,aa'}^{\text{HS}} = A_{l,aa'} y_{l,a'} + B_{l,aa'} j_{l,a'} + A_{l,a} y_{l,aa'} + B_{l,a} j_{l,aa'} \quad (6.47)$$

$$\psi_{l,aa'a''}^{\text{HS}} = A_{l,aa'a''} y_{l,a''} + B_{l,aa'a''} j_{l,a''} + A_{l,aa'} y_{l,a'a''} + B_{l,aa'} j_{l,a'a''} + A_{l,a} y_{l,aa'a''} + B_{l,a} j_{l,aa'a''}. \quad (6.48)$$

Note that several coefficients repeat throughout (6.46)-(6.48). Due to the system of equations (6.28)-(6.30), many solutions are constrained to have the same coefficients as the ones from the previous equations in the system. Hence, our goal is now to determine  $A_{l,*}$  and  $B_{l,*}$  by imposing further constraints on our solution.

The coefficients  $A_{l,*}$  can be determined by noting the behavior of  $y_{l,*}$  and  $j_{l,*}$  near  $s = 0$ . For low  $s$ ,

$$j_{l[k]*}(s) = \frac{s^{l+2k-2}}{(2k-2)!!(2l+2k-1)!!} + O(s^{l+2k}) \quad (6.49)$$

$$y_{l[k]*}(s) = \frac{(-1)^k (2l-2k+1)!!}{(2k-2)!! s^{l-2k+3}} + O(s^{-(l-2k+1)}), \quad (6.50)$$

where the new  $k$  index just indicates the the number of indices in  $*$ . This new notation is helpful for determining low  $s$  behavior in an index independent way, but will be suppressed from here on out as it is ultimately redundant. Upon inspecting (6.50), it can be seen that  $y_{l[k]*}$  diverges as  $s \rightarrow 0$ . Requiring the potentials to be regular at  $s = 0$ , this implies that  $A_{l,*} = 0$ .

To find the coefficients  $B_{l,*}$ , we will have to put in a little more legwork. Namely, we

will need to match our general solution and the Legendre coefficients for (6.1)-(6.5) in the non-relativistic limit. We first start by taking our general solution and truncate it to lowest order in  $s$ , or

$$\psi_{l,*}^{\text{sol}}(s) \approx \frac{s^l}{(2l+1)!!} \left[ B_{l,*} + \int_0^\infty y_{l,*}(s') \frac{s'^2}{\gamma'} ds' \right], \quad (6.51)$$

where the superscript is to distinguish the Green's function solution from the definition form. We can then condense (6.1)-(6.5) into the single equation:

$$\psi_*(\mathbf{s}) = \frac{1}{4\pi} \int y_{0,*} \left( \frac{w}{c} \right) f(\mathbf{s}') \frac{d^3 \mathbf{s}'}{\gamma'}, \quad (6.52)$$

where  $w = c\sqrt{\gamma_{\text{rel}}^2 - 1}$  and  $\gamma_{\text{rel}} = \gamma\gamma' - \mathbf{s} \cdot \mathbf{s}'$ . Note that  $\gamma_{\text{rel}}$  and  $\gamma_{12}$  represent the same quantity, but in different notation.

Since (6.52) is written with  $\zeta$  and  $\zeta'$  dependence, we will need to expand  $\psi_*(\mathbf{s})$  in terms of spherical harmonics and then convert these coefficients to those for our solution's Legendre expansion. Doing said expansion, for both the potentials and the distribution function, and solving for the the coefficients gives us

$$\psi_{lm,*}(s) = \frac{1}{4\pi} \sum_{n=0}^{\infty} \sum_{k=-n}^n \int_0^\infty \int_{\Omega'} \int_{\Omega} y_{0,*} \left( \frac{w}{c} \right) f_{e,nk}(s') \frac{s'^2}{\gamma'} Y_{lm}^*(\theta, \zeta) Y_{nk}(\theta', \zeta') d\Omega d\Omega' ds', \quad (6.53)$$

where we have utilized (6.52) for  $\psi_*(\mathbf{s})$  above.

From here we need to write  $y_{0,*}(s')$  in a more tractable form that allows us to integrate over the solid angles and compare these coefficients to (6.51). Namely, as shown in the Braams & Karney, 1989,

$$y_{0,*} \left( \frac{w}{c} \right) = \sum_{j=0}^{\infty} y_{j,*}(s') \frac{\epsilon^j}{j!}, \quad (6.54)$$

such that

$$\epsilon \equiv s \cos \alpha - \frac{(\gamma - 1)\gamma'}{s'} \quad (6.55)$$

and

$$\alpha \equiv \cos^{-1} \left( \frac{\mathbf{s} \cdot \mathbf{s}'}{ss'} \right). \quad (6.56)$$

Note that, to lowest order in  $s$ ,  $\epsilon \approx s \cos \alpha$ . Finally, we can use the following identity from Gradshteyn and Ryzhik

$$\cos^j \alpha = \sum_{i=0}^{\lfloor j/2 \rfloor} \frac{j!}{2^i i!} \frac{2j - 4i + 1}{(2j - 2i + 1)!!} P_{j-2i}(\cos \alpha) \quad (6.57)$$

and an expansion for  $P_{j-2i}(\cos \alpha)$  given by (3.62) in Jackson, or

$$P_{j-2i}(\cos \alpha) = \frac{4\pi}{2j - 4i + 1} \sum_{r=-(j-2i)}^{j-2i} Y_{j-2i,r}^*(\theta', \zeta') Y_{j-2i,r}(\theta, \zeta), \quad (6.58)$$

to obtain the form for the solid angle integration we need in (6.53) (Gradshteyn et al., 2007; Jackson, 1975). Using (6.57) and (6.58), (6.53) can be integrated over the solid angles, which to lowest order in  $s$  is given by

$$\psi_{lm,*}(s) \approx \frac{s^l}{(2l+1)!!} \int_0^\infty y_{l,*}(s') f_{lm}(s') \frac{s'^2}{\gamma'} ds'. \quad (6.59)$$

Letting  $m = 0$  and noting that  $\psi_{l0}/f_{l0} = \psi_l/f_l$ , we have our final expression for the Legendre coefficients for the gyro-angle independent potential case, or

$$\psi_{l,*}(s) \approx \frac{s^l}{(2l+1)!!} \int_0^\infty y_{l,*}(s') f_l(s') \frac{s'^2}{\gamma'} ds'. \quad (6.60)$$

Upon inspection of (6.51), we can see that this means that  $B_{l,*} = 0$ , thereby making  $\psi_{l,*}^{\text{HS}} = 0$ . Therefore, the overall solution, given in a slightly more numerically tractable form, is given purely by the particular solution or

$$\psi_{l,*}(s) = \int_0^s N_{l,*}(s, s') f_l(s') \frac{s'^2}{\gamma'} ds' + \int_s^\infty N_{l,*}(s', s) f_l(s') \frac{s'^2}{\gamma'} ds'. \quad (6.61)$$

## 6.2 NIMROD Implementation

The only change that needs to be made to (5.55) to implement the BB operator into NIMROD is the adjustment of the collisional coupling term  $I_{i,m,l,j}^{\text{COLL}}$  in (A.1). There are ten new pitch-angle coupling matrices that can be pre-computed before the first time step.

These are given by the following definitions:

$$M_{l,m,n}^{(aa)} \equiv \int_{-1}^1 Q_l(\xi) Q_m(\xi) P_n(\xi) d\xi \quad (6.62)$$

$$M_{l,m,n}^{(ab)} \equiv \int_{-1}^1 \xi Q_l(\xi) Q_m(\xi) \frac{\partial P_n(\xi)}{\partial \xi} d\xi \quad (6.63)$$

$$M_{l,m,n}^{(ac)} \equiv \int_{-1}^1 (1 - \xi^2) Q_l(\xi) Q_m(\xi) \frac{\partial^2 P_n(\xi)}{\partial \xi^2} d\xi \quad (6.64)$$

$$M_{l,m,n}^{(ba)} \equiv \int_{-1}^1 \xi \frac{\partial Q_l(\xi)}{\partial \xi} Q_m(\xi) P_n(\xi) d\xi \quad (6.65)$$

$$M_{l,m,n}^{(bb1)} \equiv \int_{-1}^1 \frac{\partial Q_l(\xi)}{\partial \xi} Q_m(\xi) \frac{\partial P_n(\xi)}{\partial \xi} d\xi \quad (6.66)$$

$$M_{l,m,n}^{(bb2)} \equiv \int_{-1}^1 (1 - \xi^2) \frac{\partial Q_l(\xi)}{\partial \xi} Q_m(\xi) \frac{\partial P_n(\xi)}{\partial \xi} d\xi \quad (6.67)$$

$$M_{l,m,n}^{(bc)} \equiv \int_{-1}^1 \xi (1 - \xi^2) \frac{\partial Q_l(\xi)}{\partial \xi} Q_m(\xi) \frac{\partial^2 P_n(\xi)}{\partial \xi^2} d\xi \quad (6.68)$$

$$M_{l,m,n}^{(ca)} \equiv \int_{-1}^1 (1 - \xi^2) \frac{\partial^2 Q_l(\xi)}{\partial \xi^2} Q_m(\xi) P_n(\xi) d\xi \quad (6.69)$$

$$M_{l,m,n}^{(cb)} \equiv \int_{-1}^1 \xi (1 - \xi^2) \frac{\partial^2 Q_l(\xi)}{\partial \xi^2} Q_m(\xi) \frac{\partial P_n(\xi)}{\partial \xi} d\xi \quad (6.70)$$

$$M_{l,m,n}^{(cc)} \equiv \int_{-1}^1 (1 - \xi^2)^2 \frac{\partial^2 Q_l(\xi)}{\partial \xi^2} Q_m(\xi) \frac{\partial^2 P_n(\xi)}{\partial \xi^2} d\xi \quad (6.71)$$

The notation for the superscript of each coupling matrix denotes the order of derivative taken on the the distribution's  $\xi$  basis,  $Q_l(\xi)$ , and the potential's Legendre basis in  $\xi$ ,  $P_n(\xi)$ . The letter  $a$  represents no derivative,  $b$  the first derivative, and  $c$  the second derivative. Note that in the case of  $M_{l,m,n}^{(bb)}$  there are two such integrals, which have been denoted with  $(bb1)$  and  $(bb2)$ , respectively. The complete breakdown of the construction of  $I_{i,m,l,j}^{\text{COLL}}$  is given in (A.4)-(A.9) and (A.10).

The most noticeable difference between the construction of the Papp operator and the BB operator is the need to solve for  $\Upsilon$  and  $\Pi$  potentials at the  $k$ th time-step, regardless of whether it is a part of the LHS or RHS total coupling matrices. Doing so allows us to preserve the form given by (5.55).

In order to construct these potentials, we must first build the polynomials  $j_{l,*}(s)$  and  $y_{l,*}(s)$  in (6.35), (6.41), and (6.42). We do this by first establishing the recursion relation

for the single-index polynomials by

$$\tilde{j}_{l-2,a}(s) = \gamma \tilde{j}_{l-1,a}(s) - \frac{(l-a)(l+a)}{(2l-1)(2l+1)} s^2 \tilde{j}_{l,a}(s), \quad (6.72)$$

where we use

$$\tilde{j}_{l,a}(s) \equiv \frac{(2l+1)!!}{s^l} j_{l,a}(s) \quad (6.73)$$

instead of  $j_{l,a}$ . Note that what we have done is divide out the leading order dependence ( $k = 0$ ) for  $j_{l,a}$  in (6.49). Solving for this normalized version of  $j_{l,a}$  helps us to avoid potential issues related to numerical underflow and overflow (Braams & Karney, 1989). To determine an initial condition to the backward recursion relation, we first must take the limit of (6.72) for high  $l$ . Doing so gives the relationship for a particular index  $L$ :

$$\frac{\tilde{j}_{L,a}(s)}{\tilde{j}_{L-1,a}(s)} \approx \frac{2}{\gamma + 1}. \quad (6.74)$$

Therefore, if we simply pick a new version of  $\tilde{j}'_{L-1,a} = 1$  and  $\tilde{j}'_{L,a} = 2/(\gamma + 1)$ , we can use (6.72) to generate  $\tilde{j}'_{l,a}$  from  $0 \leq l \leq L$ . Note that  $\tilde{j}'_{l,a}$  is only a multiplicative factor away from our desired polynomials  $\tilde{j}_{l,a}$ . Utilizing the fact that  $\tilde{j}_{a-1,a} = 1$ , and enforcing that like ratios of both types of polynomials are equal, we have the following relationship:

$$\tilde{j}_{l,a} = \frac{\tilde{j}'_{l,a}}{\tilde{j}'_{a-1,a}}. \quad (6.75)$$

Though this scheme works very well for small  $s$ , the presence of the  $s^2$  in (6.72) will lead to compounding error for each iteration in the recursion for large values of  $s$ . Hence, it is useful to also implement a forward-recursion version of (6.72). This is given by

$$\tilde{j}_{l,a}(s) = \frac{(2l-1)(2l+1)}{(l-a)(l+a)s^2} (\gamma \tilde{j}_{l-1,a}(s) - \tilde{j}_{l-2,a}(s)). \quad (6.76)$$

To avoid the singularity at  $l = a$ , one must first define all  $\tilde{j}_{l,a}$  for  $0 \leq l \leq 2$  and  $0 \leq a \leq 2$ . The  $\tilde{j}_{l,a}$  corresponding to these values of  $l$  and  $a$  can be quickly computed in

Mathematica, or other computational software, and then hard-coded. A splitting parameter  $s_{sp}$  is implemented in NIMROD that can then be used to enforce the use of the scheme set forth by (6.72) for  $s \leq s_{sp}$ . All other values of  $s$  will utilize (6.76). From here,  $j_{l,a}$  can be calculated using (6.73). For the purposes of this thesis, we will always have  $s_{sp} = 2$ . The multiple-index  $j_{l,*}$  present in (6.41) and (6.42) can be calculated in terms of the single-index  $j_{l,a}$  using

$$j_{l,02}(s) = \frac{s}{2} j_{l+1,1}(s) \quad (6.77)$$

$$j_{l,11}(s) = \frac{s}{2} j_{l+1,0}(s) \quad (6.78)$$

$$j_{l,22}(s) = \frac{s}{2} j_{l+1,1}(s) + \frac{s^2}{2} j_{l+2,0}(s) \quad (6.79)$$

$$j_{l,022}(s) = \frac{s^2}{8} j_{l+2,0}(s). \quad (6.80)$$

Once all  $j_{l,*}$  have been calculated,  $y_{l,*}$  can then be calculated by using

$$y_{l,*} = (-1)^{l+1} j_{-(l+1),*}. \quad (6.81)$$

Note that the values of  $f_{e,l}$  that are fed into (6.61) are by necessity expanded in terms of Legendre polynomials. In general, we could map the coefficients of the distribution on an arbitrary  $Q_l(\xi)$  basis onto a Legendre one. However, this has not yet been implemented into NIMROD. Hence, we shall assume that the distribution is also expanded in terms of Legendre polynomials for now, or  $Q_l(\xi) \rightarrow P_l(\xi)$ . The integrals in (6.61) are then calculated using an optimized Romberg integration scheme that was implemented into NIMROD explicitly for the calculation of these potentials. For the explicit representations of these integrals see (B.1)-(B.5). Consequentially, this requires us to know the value of the distribution at the limits of integration, which are not a part of our collocation points. However, these can be easily calculated by direct evaluation of (5.40) and using (5.42).

It is important to note that the manner in which we handled derivatives of  $f_{e,l}$  at the collocation points cannot be used to evaluate derivatives of the potentials. This problem

arises due to the fact that our potentials cannot be expanded using the same weight function as is used for the distribution in (5.40). However, since we have an analytic form for the potentials, we can get around this by directly taking first and second derivatives. As a result, we must also find a way to calculate the first and second derivatives of  $j_{l,*}$  and  $y_{l,*}$ . This can be achieved using the following relationships:

$$\frac{\partial j_{l,*}(s)}{\partial s} = \frac{1}{\gamma} j_{l-1,*}(s) - \frac{(l+1)}{s} j_{l,*}(s) \quad (6.82)$$

$$\frac{\partial^2 j_{l,*}(s)}{\partial s^2} = \frac{1}{\gamma^2} j_{l-2,*}(s) - \left( \frac{s}{\gamma^3} + \frac{(2l+1)}{\gamma s} \right) j_{l-1,*} + \frac{(l+1)(l+2)}{s^2} j_{l,*}(s) \quad (6.83)$$

$$\frac{\partial y_{l,*}(s)}{\partial s} = -\frac{1}{\gamma} y_{l+1,*}(s) + \frac{l}{s} y_{l,*}(s) \quad (6.84)$$

$$\frac{\partial^2 y_{l,*}(s)}{\partial s^2} = \frac{1}{\gamma^2} y_{l+2,*}(s) + \left( \frac{s}{\gamma^3} - \frac{(2l+1)}{\gamma s} \right) y_{l+1,*} + \frac{l(l-1)}{s^2} y_{l,*}(s) \quad (6.85)$$

The first and second derivatives of all five potentials in terms of (6.82)-(6.85) are shown in (B.24)-(B.33).

### 6.3 Results

The process by which the LHS and RHS of (5.55) is constructed in the case of the BB collision operator is very involved. At multiple steps throughout its construction there is a very high chance for coding and round-off errors long before GMRES iterations even begin. Due to the high chance of error in calculating the  $\Upsilon$  and  $\Pi$  potentials, we benchmark our solutions for these potentials, as well as their first and second derivatives, with Mathematica. Specifically, we use Mathematica's built in NIntegrate feature to calculate the integrals in (B.6)-(B.23) for comparison with the Romberg integration scheme that we implemented in NIMROD. Values for  $P_\nu^\mu(\gamma)$  can also be explicitly evaluated in Mathematica. This allows analytic construction of  $j_{l,*}$  and  $y_{l,*}$  instead of generating them recursively.

As seen in the previous chapter, the parameter  $z_e$  can wildly change the behavior of the distribution. Ergo, for this section we have decided to normalize our initial condition by its peak value in (4.51), or

$$\tilde{f}_e^{(0)} = \frac{f_e^{\text{MJ}}}{N_M e^{-z}}. \quad (6.86)$$

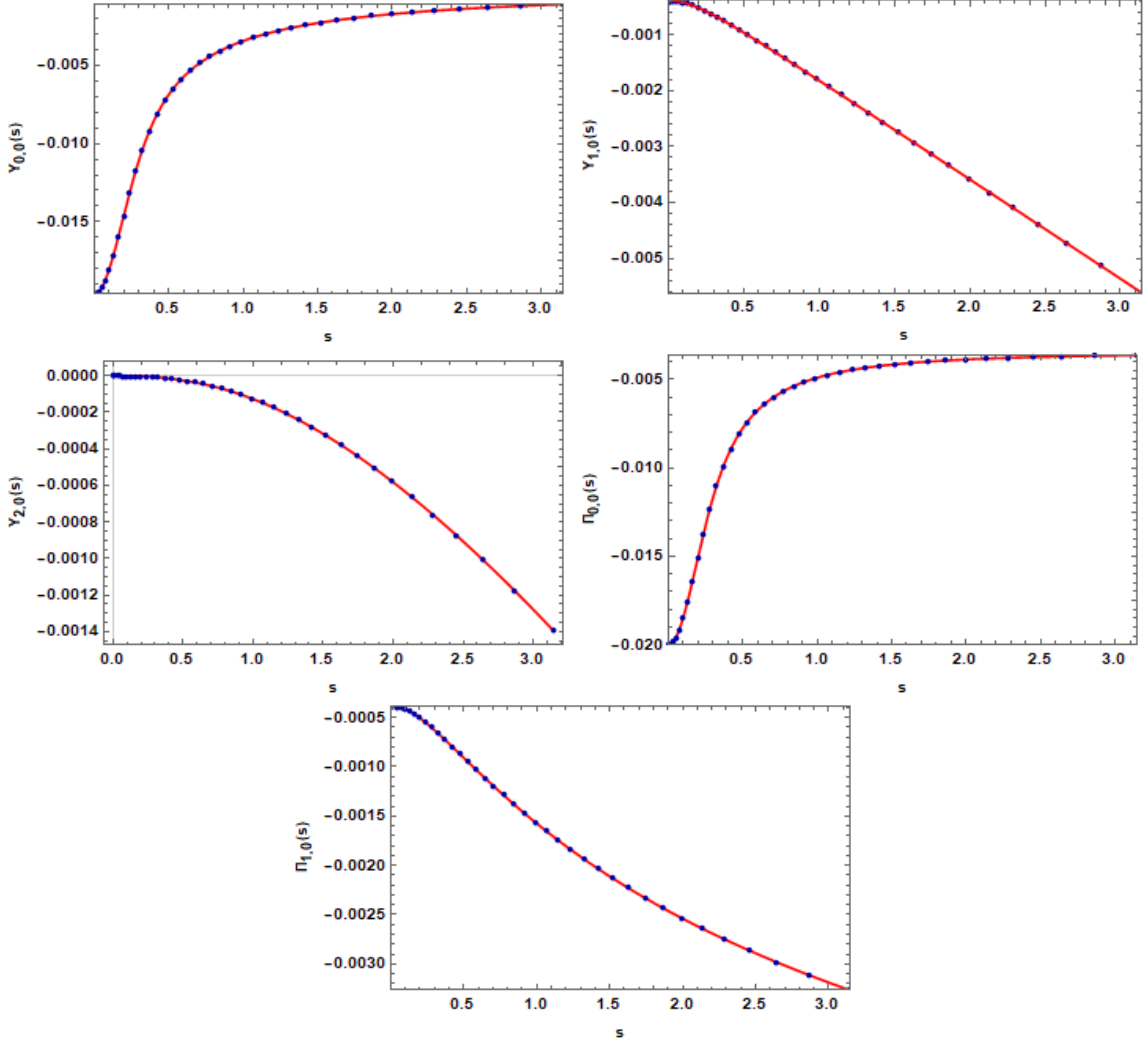


**Figure 6.1:**  $\Upsilon$  and  $\Pi$  potentials calculated using  $\tilde{f}_e^{(0)}$  for  $l = 0$  such that  $s_{V\parallel} = 0$  and  $z_e = 51$ . Blue dots are values of the potential calculated using NIMROD and red lines are the potentials using Mathematica’s capabilities. Here  $N_s = 40$ ,  $N_\xi = 7$ , and  $\mathcal{M}_\xi = 1$ .

This normalization restricts the range of the distribution to  $[0, 1]$ . Note that due to the bilinear nature of the BB operator, this normalization will also introduce an additional factor of  $N_M e^{-z}$  in front of the collision operator. Figure 6.1 shows that the potentials calculated by NIMROD are in good agreement with those calculated using NIntegrate and analytic versions of the  $j_{l,*}$  and  $y_{l,*}$  polynomials. Moreover, careful inspection of these



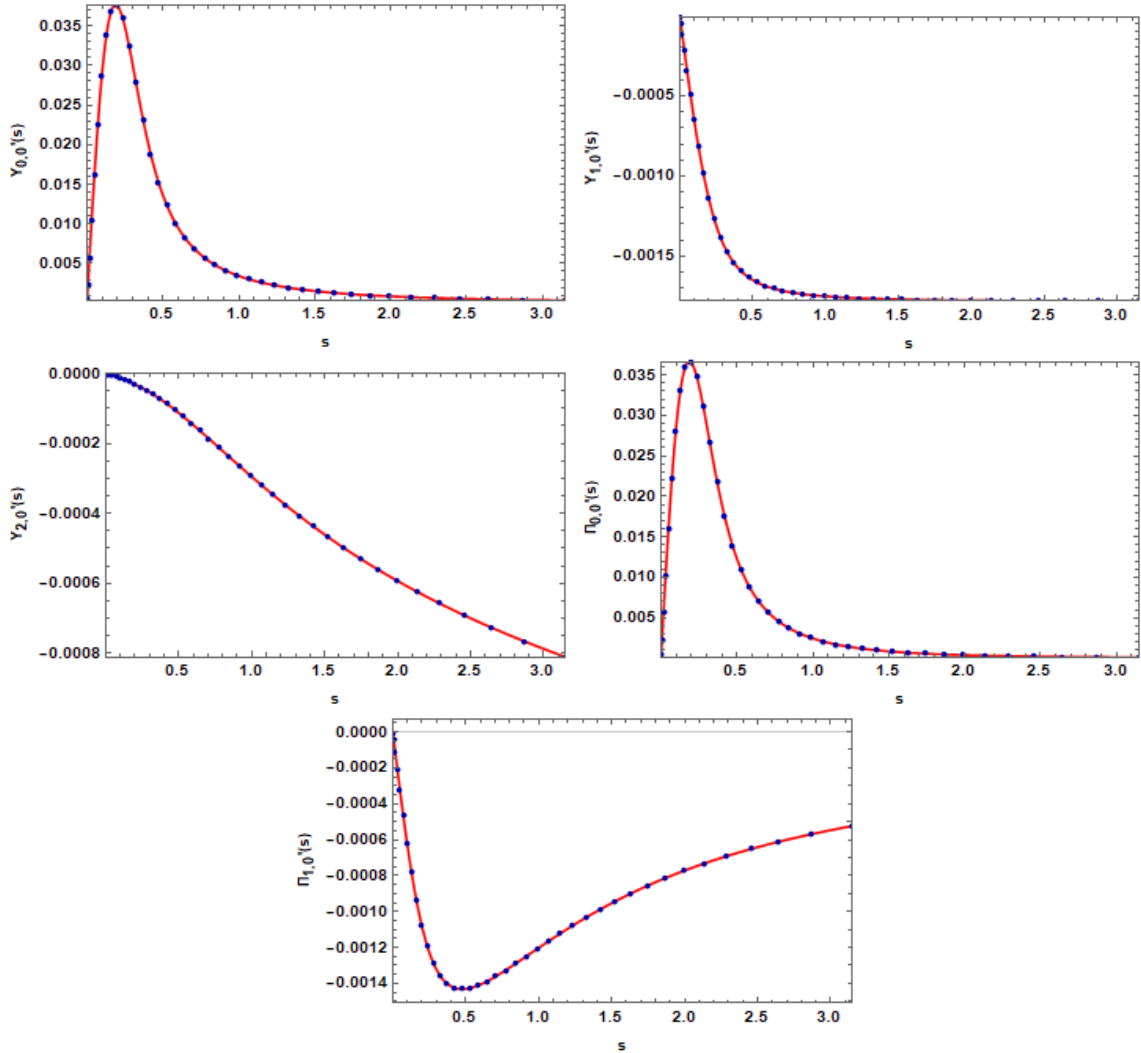


**Figure 6.2:** First derivatives of potentials from Figure 6.1.

plots verifies that the majority of the potentials presented do not share the same limiting behavior as the distribution. Ergo, the choice to avoid the non-classical quadrature scheme as an expansion for the potentials was a wise one.

To benchmark the first and second derivatives, it is not enough for the potentials from both methods to agree with each other. They must also behave like first and second derivatives. Comparing each plot in Figure 6.1 to their counterpart in Figure 6.2, it is clear that taking the tangent line to each point in a particular potential plot does indeed yield the behavior seen in Figure 6.2. Performing the same analysis on Figure 6.2, it can be seen that

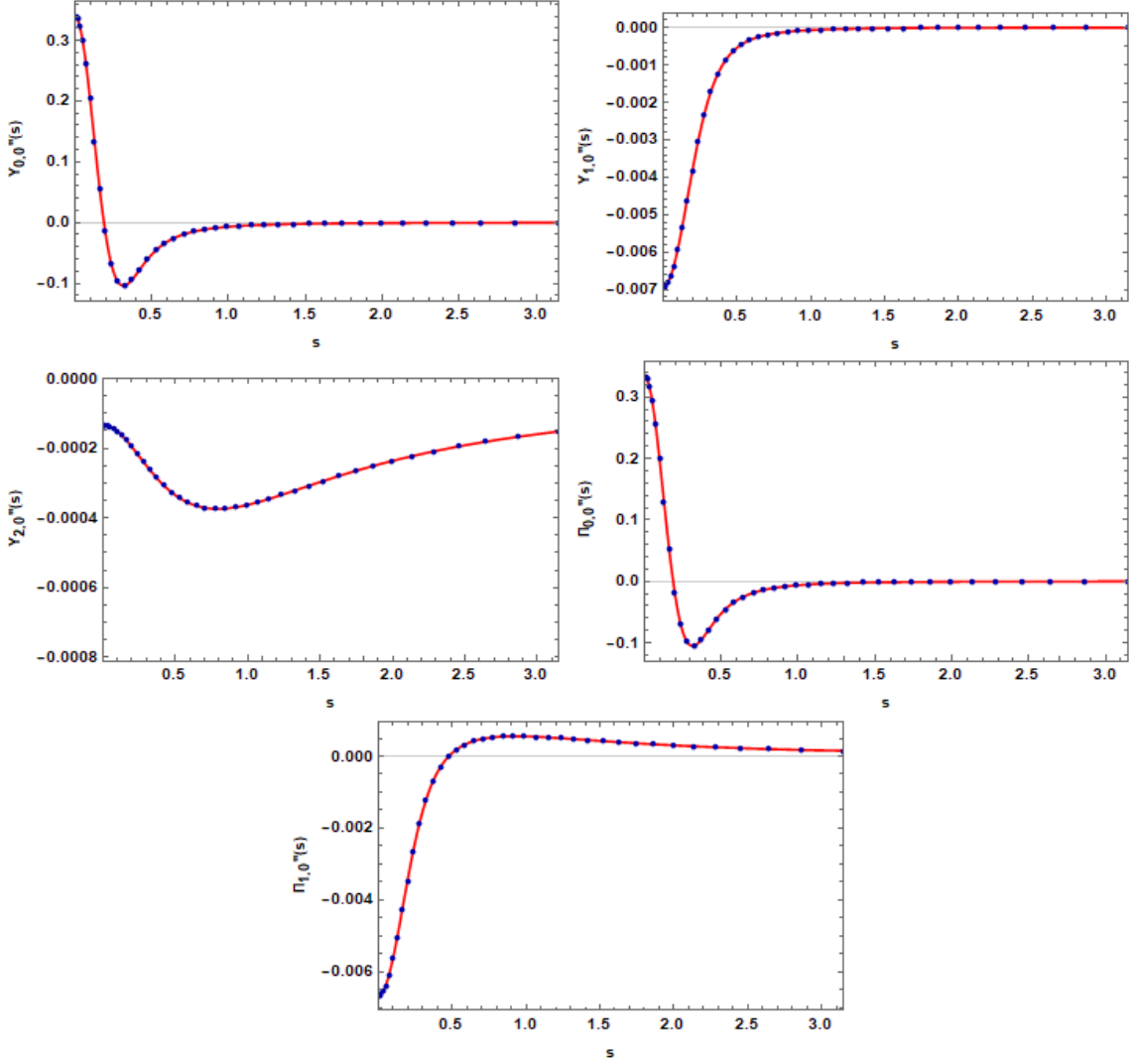


**Figure 6.3:** Second derivatives of potentials from Figure 6.1.

both the behavior of the tangent line of the first derivative plots, as well as the concavity of the potentials themselves, are in agreement with Figure 6.3. Therefore we deem that we have successfully implemented a solver for the BK potentials into NIMROD.

With the potentials successfully benchmarked, we now turn our attention to benchmarking the the new form of  $I_{i,m,l,j}^{(\text{COLL})}$ . To verify that this coupling matrix has been successfully updated in NIMROD, we simulate the evolution of an unshifted MJ distribution in the absence of electric-field acceleration and synchrotron radiation. From the derivation of (4.50), we know that the MJ distribution represents the equilibrium solution to the rel-

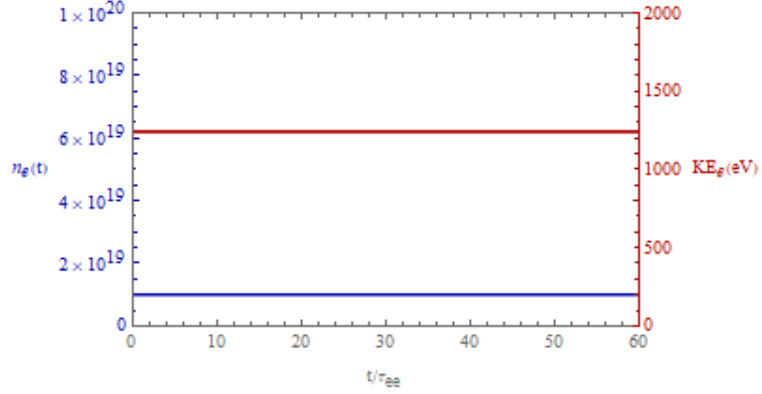


**Figure 6.4:** Equilibrium benchmark for case in Figure 6.1 with  $\Delta\tilde{t} = 1$  over 60 time-steps. Here  $\tilde{E}_{\parallel} = 0$ ,  $\alpha = 0$ , and  $n_{ERe} = 10^{19}m^{-3}$ . Number density is shown in blue, while the kinetic energy is shown in red.

ativistic Boltzmann equation. Moreover, this should also be the case when the collision operator is given by the BB collision operator. Ergo, we expect that the resulting distribution and fluid parameters will remain unchanged. In Figure 6.4, we can see that is indeed the case. Note, that unlike the collisional relaxation cases for the Papp operator, we do not include similar plots for lower  $N_s$ . This is due to the fact that in this specific case the result is independent of our normalized momentum-space resolution. Note that this is only true due to the fact that the distribution does not evolve in time. If the distribution evolves away from the initial condition at all, then its projection onto the 2D normalized momentum-space grid would change as well. However, it should be noted that the choice to run this simulation with only the unshifted MJ distribution serves only as a benchmark for the  $l = 0$  terms in  $I_{i,m,l,j}^{(\text{COLL})}$ . To test the  $l \neq 0$  terms, we could need to run a simulation with an initial condition that has  $\xi$  dependence.

## CHAPTER 7

### CONCLUSION

In this thesis, we have shown the successful implementation of many RE features in the NIMROD code, with the goal of self-consistently advancing the RE distribution in mind. Firstly, we have shown the successful implementation of the relativistic drift kinetic equation in 2D normalized momentum space with the Papp collision operator acting as our RHS. This linear implementation was benchmarked with both MJ and double MJ distribution collisional relaxation simulations. In both cases, the distribution evolved to the stationary background MB distribution. The simulation of the relativistic drift kinetic equation using the Papp operator revealed that there were issues with the method of “asymptotic matching” used to derive the operator. Though the MJ distribution evolved to the background MB distribution continuously, it evolved in a manner that was inconsistent with normal diffusive behavior. Additionally, we showed that neither energy, nor momentum were conserved. Consequentially, these concerns were used to motivate the implementation of the fully non-linear BB operator, which contains a proper diffusion tensor in its definition. Moreover, it allows for interaction of REs with background electrons and avoids the “asymptotic matching” assumption.

A scheme for solving the relativistic drift kinetic equation with the BB collision operator was then implemented into NIMROD utilizing the BK differential formulation. This scheme removes the “integro” portion of the non-linear relativistic drift kinetic equation by coupling to five ODEs for the Legendre coefficients of five corresponding potentials. By using the solution for the distribution function at the previous time-step to construct these potentials, we are able to turn the nonlinear BB operator into a pseudo-linearized form.

Green’s function solutions for these potentials are presented in integral form and implemented numerically in NIMROD via the combination of a  $j_{l,*}$  recursion scheme and an optimized Romberg integration scheme. This same scheme was then also used to calculate

the respective first and second derivatives of these potentials, and were bench-marked to Mathematica’s NIntegrate functionality and it’s analytic forms for  $j_{l,*}$  and  $y_{l,*}$ . Finally, the NIMROD implementation of the BB operator was benchmarked by simulating the evolution, or lack there of, of the RE distribution in equilibrium. It was show that number density and kinetic energy were conserved for a large number of collision times for the case of an unshifted MJ distribution.

Further benchmarking of the implementation of the BB operator in NIMROD is required. The equilibrium simulation for the case of an unshifted MJ distribution only tests the  $l = 0$  terms in  $I_{i,m,l,j}^{\text{COLL}}$ . Since (4.50), with nonzero flow-velocity, is also an equilibrium solution, simulation of this case in equilibrium can also be used to benchmark the  $l \neq 0$  terms. Additionally, running an analogous double MJ distribution simulation can be used to confirm the symmetry of the BB operator. Upon completion of these benchmarks, we would seek to reproduce the “electron slide-away” case in Stahl’s work (Stahl et al., 2017). The final goal would then be to simulate the non-linear analogue to the case in Figure 5.5.

## References

- Beliaev, S., & Budker, G. (1956). The relativistic kinetic equation. In *Soviet physics doklady* (Vol. 1, p. 218).
- Boozer, A. H. (2015). Theory of runaway electrons in iter: Equations, important parameters, and implications for mitigation. *Physics of Plasmas*, *22*(3), 032504.
- Braams, B. J., & Karney, C. F. (1987). Differential form of the collision integral for a relativistic plasma. *Physical review letters*, *59*(16), 1817.
- Braams, B. J., & Karney, C. F. (1989). Conductivity of a relativistic plasma. *Physics of Fluids B: Plasma Physics*, *1*(7), 1355–1368.
- Carroll, S. M. (1997). Lecture notes on general relativity. *arXiv preprint gr-qc/9712019*.
- Cary, J. R., & Brizard, A. J. (2009). Hamiltonian theory of guiding-center motion. *Reviews of modern physics*, *81*(2), 693.
- Cercignani, C., & Kremer, G. M. (2002). Relativistic boltzmann equation. In *The relativistic boltzmann equation: Theory and applications* (pp. 31–63). Springer.
- Connor, J., & Hastie, R. (1975). Relativistic limitations on runaway electrons. *Nuclear fusion*, *15*(3), 415.
- Decker, J., Hirvijoki, E., Embreus, O., Peysson, Y., Stahl, A., Pusztai, I., & Fülöp, T. (2016). Numerical characterization of bump formation in the runaway electron tail. *Plasma Physics and Controlled Fusion*, *58*(2), 025016.
- de Groot, S., van Leeuwen, W., & van Weert, C. G. (1980). *Relativistic kinetic theory: principles and applications*. North-Holland.
- Dreicer, H. (1959). Electron and ion runaway in a fully ionized gas. i. *Physical Review*, *115*(2), 238.
- Gradshteyn, I., Ryzhik, I., Jeffrey, A., & Zwillinger, D. (2007). Table of integrals, series, and products. *Table of Integrals*.
- Guo, Z., McDevitt, C. J., & Tang, X.-Z. (2017). Phase-space dynamics of runaway electrons in magnetic fields. *Plasma Physics and Controlled Fusion*, *59*(4), 044003.

- Hazeltine, R. D., & Waelbroeck, F. L. (2018). *The framework of plasma physics*. CRC Press.
- Helander, P., & Sigmar, D. (2002). *Collisional transport in magnetized plasmas cambridge university press*. Cambridge.
- Held, E., Kruger, S., Ji, J.-Y., Belli, E., & Lyons, B. (2015). Verification of continuum drift kinetic equation solvers in nimrod. *Physics of Plasmas*, *22*(3), 032511.
- Iter*. (n.d.). <https://www.iter.org/>. (Accessed: November 30, 2022)
- Izzo, V., Hollmann, E., James, A., Yu, J., Humphreys, D., Lao, L., . . . others (2011). Runaway electron confinement modelling for rapid shutdown scenarios in diiii-d, alcator c-mod and iter. *Nuclear Fusion*, *51*(6), 063032.
- Jackson, J. D. (1975). *Classical electrodynamics.(2d ed.)*. Wiley.
- Jüttner, F. (1911). Das maxwellsche gesetz der geschwindigkeitsverteilung in der relativtheorie. *Annalen der Physik*, *339*(5), 856–882.
- Papp, G., Drevlak, M., Fülöp, T., & Helander, P. (2011). Runaway electron drift orbits in magnetostatic perturbed fields. *Nuclear Fusion*, *51*(4), 043004.
- Rosenbluth, M., & Putvinski, S. (1997). Theory for avalanche of runaway electrons in tokamaks. *Nuclear fusion*, *37*(10), 1355.
- Saad, Y., & Schultz, M. H. (1986). Gmres: A generalized minimal residual algorithm for solving nonsymmetric linear systems. *SIAM Journal on scientific and statistical computing*, *7*(3), 856–869.
- Sandquist, P., Sharapov, S., Helander, P., & Lisak, M. (2006). Relativistic electron distribution function of a plasma in a near-critical electric field. *Physics of plasmas*, *13*(7), 072108.
- Sovinec, C., Glasser, A., Gianakon, T., Barnes, D., Nebel, R., Kruger, S., . . . others (2004). Nonlinear magnetohydrodynamics simulation using high-order finite elements. *Journal of Computational Physics*, *195*(1), 355–386.
- Stahl, A., Landreman, M., Embréus, O., & Fülöp, T. (2017). Norse: A solver for the relativistic non-linear fokker–planck equation for electrons in a homogeneous plasma.

*Computer Physics Communications*, 212, 269–279.

Ter Haar, D. (2013). *Collected papers of ld landau*. Elsevier.



APPENDICES

APPENDIX A  
DISCRETIZATION OF COUPLING MATRICES

**A.1 Linear DKE and Papp Operator Coupling**

The total coupling matrix for the LHS of (5.47)  $I_{i,m,l,j}^{\text{LHS}}$  is the sum of a streaming coupling matrix and a collisional coupling matrix, or

$$I_{i,m,l,j}^{\text{LHS}}(\Theta_E, \Theta_S, \Theta_c) = I_{i,m,l,j}^{\text{STR}}(\Theta_E, \Theta_S) + I_{i,m,l,j}^{\text{COLL}}(\Theta_c), \quad (\text{A.1})$$

where  $I_{i,m,l,j}^{\text{STR}}(\Theta_E, \Theta_S)$  and  $I_{i,m,l,j}^{\text{COLL}}(\Theta_c)$  are given by

$$\begin{aligned} I_{i,m,l,j}^{\text{STR}}(\Theta_E, \Theta_S) &= M_{l,m}^{(t)} \delta_{i,j} - \Theta_E \tilde{E}_{||} \left[ M_{l,m}^{(s)} S_{i,j}^{(1)} + \frac{1}{s_i} M_{l,m}^{(B)} \delta_{i,j} \right] \\ &\quad - \frac{\Theta_S}{\gamma_i} \left[ \gamma_i^2 s_i M_{l,m}^{(F1)} S_{i,j}^{(1)} + \left( 4s_i^2 M_{l,m}^{(F1)} - M_{l,m}^{(F2)} + 2M_{l,m}^{(t)} \right) \delta_{i,j} \right] \end{aligned} \quad (\text{A.2})$$

$$\begin{aligned} I_{i,m,l,j}^{\text{COLL}}(\Theta_c) &= \frac{\Theta_c}{s_i} \left[ \left( 2A_s(s_i) + s_i \left( F_s(s_i) + \frac{\partial A_s}{\partial s} \Big|_{s=s_i} \right) \right) S_{i,j}^{(1)} + s_i A_s(s_i) S_{i,j}^{(2)} \right. \\ &\quad \left. + \left( 2F_s(s_i) + s_i \frac{\partial F_s}{\partial s} \Big|_{s=s_i} \right) \delta_{i,j} + \frac{\tilde{B}_s(s_i)}{s_i^2} M_{l,m}^{(c)} \delta_{i,j} \right]. \end{aligned} \quad (\text{A.3})$$

The total coupling matrix for the RHS of (5.47) is simply  $I_{i,m,l,j}^{\text{RHS}} = -I_{i,m,l,j}^{\text{LHS}}(1, 1, 1)$ , regardless of the value for the three centering parameters.

## A.2 Beliaev-Budker Operator Coupling

The coupling for the LHS using (4.57) is exactly the same as in (A.1) with the exception of  $I_{i,m,l,j}^{\text{COLL}}(\Theta_c)$ . To determine this, we introduce the following subset of coupling matrices:

$$I_{i,m,l,n,j}^{(s^2)} = \left[ \left( \gamma_i (8\Upsilon_{2,n,i} - \Upsilon_{0,n,i}) - \frac{2\gamma_i^3}{s_i} \frac{\partial \Upsilon_{-,n}}{\partial s} \Big|_{s=s_i} \right) M_{l,m,n}^{(aa)} + \left( \frac{2\gamma_i}{s_i^2} M_{l,m,n}^{(ab)} - \frac{\gamma_i}{s_i^2} M_{l,m,n}^{(ac)} \right) \Upsilon_{-,n,i} \right] S_{i,j}^{(2)} \quad (\text{A.4})$$

$$I_{i,m,l,n,j}^{(s)} = \left[ \left( \frac{1}{\gamma_i s_i} (8\Upsilon_{2,n,i} - \Upsilon_{0,n,i}) + \left( -16\gamma_i \frac{\partial \Upsilon_{2,n}}{\partial s} \Big|_{s=s_i} + 6\gamma_i \frac{\partial \Upsilon_{1,n}}{\partial s} \Big|_{s=s_i} - \gamma_i \frac{\partial \Upsilon_{0,n}}{\partial s} \Big|_{s=s_i} \right) - \frac{2\gamma_i^3}{s_i} \left( \frac{\partial^2 \Upsilon_{-,n}}{\partial s^2} \Big|_{s=s_i} + \frac{1}{s_i} \frac{\partial \Upsilon_{-,n}}{\partial s} \Big|_{s=s_i} \right) - \gamma_i \frac{\partial \Pi_n}{\partial s} \Big|_{s=s_i} \right) M_{l,m,n}^{(aa)} + \frac{1}{\gamma_i s_i} \left( 2 + \frac{1}{s_i^2} \right) \left( 2M_{l,m,n}^{(ab)} - M_{l,m,n}^{(ac)} \right) \Upsilon_{-,n,i} \right] S_{i,j}^{(1)} \quad (\text{A.5})$$

$$I_{i,m,l,n,j}^{(\xi^2)} = \frac{1}{\gamma_i s_i^2} \left[ \left( \frac{\gamma_i^2}{s_i} \frac{\partial \Upsilon_{-,n}}{\partial s} \Big|_{s=s_i} - \Upsilon_{+,n,i} \delta_{i,r} \right) M_{l,m,n}^{(ca)} + \frac{1}{s_i^2} \left( M_{l,m,n}^{(cc)} - M_{l,m,n}^{(cb)} \right) \Upsilon_{-,n,i} \right] \delta_{i,j} \quad (\text{A.6})$$

$$I_{i,m,l,n,j}^{(\xi)} = \frac{1}{\gamma_i s_i^4} \left[ \left( \left( 2M_{l,m,n}^{(bb1)} - 3s_i^2 M_{l,m,n}^{(bb2)} - \gamma_i M_{l,m,n}^{(bc)} \right) \Upsilon_{-,n,i} - s_i^2 M_{l,m,n}^{(bb2)} (4\Upsilon_{2,n,i} - 3\Upsilon_{1,n,i} + \Upsilon_{0,n,i} + \Pi_{n,i}) + 2s_i^2 M_{l,m,n}^{(ba)} \Upsilon_{+,n,i} \right) - 2\gamma_i^2 s_i \left( M_{l,m,n}^{(bb2)} + M_{l,m,n}^{(ba)} \right) \frac{\partial \Upsilon_{-,n}}{\partial s} \Big|_{s=s_i} \right] \delta_{i,j} \quad (\text{A.7})$$

$$I_{i,m,l,n,j}^{(s\xi)} = \frac{2\gamma_i}{s_i^2} M_{l,m,n}^{(bb2)} \left( s_i \frac{\partial \Upsilon_{-,n}}{\partial s} \Big|_{s=s_i} - \Upsilon_{-,n,i} \right) S_{i,j}^{(1)} \quad (\text{A.8})$$

$$I_{i,m,l,n,j}^{(f)} = \left[ - \left( \gamma_i \frac{\partial^2 \Pi_n}{\partial s^2} \Big|_{s=s_i} + \frac{1}{\gamma_i s_i} (2 + s_i^2) \frac{\partial \Pi_n}{\partial s} \Big|_{s=s_i} \right) M_{l,m,n}^{(aa)} + \frac{1}{\gamma_i s_i^2} \left( 2M_{l,m,n}^{(ab)} - M_{l,m,n}^{(ac)} \right) \Pi_{n,i} \right] \delta_{i,j}. \quad (\text{A.9})$$

Equations (A.4)-(A.9) are the discretized versions of the coefficients from (6.21)-(6.26). Note that the presence of BK potentials in the coupling matrices introduces an additional index due to its expansion in terms of Legendre polynomials. Therefore, we can simply add (A.4)-(A.9), take the sum over  $n$ , and include the collisional centering parameter  $\Theta_c$  to get

$$I_{i,m,l,j}^{\text{COLL}}(\Theta_c) = -\Theta_c \sum_{n=0}^{N_\xi} \left[ I_{i,m,l,n,j}^{(s^2)} + I_{i,m,l,n,j}^{(s)} + I_{i,m,l,n,j}^{(\xi^2)} + I_{i,m,l,n,j}^{(\xi)} + I_{i,m,l,n,j}^{(s\xi)} + I_{i,m,l,n,j}^{(f)} \right]. \quad (\text{A.10})$$

Derivatives of potentials in (A.4)-(A.9) can be evaluated at the collocation points using (B.24)-(B.33). Equation (A.10) can then be plugged into (A.1) to get the full LHS coupling. The RHS coupling is once again  $I_{i,m,l,j}^{\text{RHS}} = -I_{i,m,l,j}^{\text{LHS}}(1, 1, 1)$ .

APPENDIX B  
BRAAMS-KARNEY POTENTIALS

**B.1 BK Potentials and Their First and Second Derivatives**

First, let us define the Legendre coefficients of each potential in (6.61) in their fully explicit forms. Suppressing the  $k$ th time-step index, the potential coefficients are given by

$$\Upsilon_{0,l}(s) = y_{l,0}(s)R_l^{(1)}(s) + j_{l,0}(s)R_l^{(2)}(s, t) \quad (\text{B.1})$$

$$\Upsilon_{1,l}(s) = y_{l,0}(s)R_l^{(3)}(s) + y_{l,02}(s)R_l^{(4)}(s) + j_{l,02}(s)R_l^{(5)}(s) + j_{l,2}(s)R_l^{(6)}(s) \quad (\text{B.2})$$

$$\begin{aligned} \Upsilon_{2,l}(s) &= y_{l,0}(s)R_l^{(7)}(s) + y_{l,02}(s)R_l^{(8)}(s) + y_{l,022}(s)R_l^{(9)}(s) + j_{l,022}(s)R_l^{(10)}(s) \\ &+ j_{l,22}(s)R_l^{(11)}(s) + j_{l,2}(s)R_l^{(12)}(s) \end{aligned} \quad (\text{B.3})$$

$$\Pi_{0,l}(s) = y_{l,1}(s)R_l^{(13)}(s) + j_{l,1}(s)R_l^{(14)}(s) \quad (\text{B.4})$$

$$\Pi_{1,l}(s) = y_{l,1}(s)R_l^{(15)}(s) + y_{l,11}(s)R_l^{(16)}(s) + j_{l,11}(s)R_l^{(17)}(s) + j_{l,1}(s)R_l^{(18)}(s), \quad (\text{B.5})$$

where the terms  $R_l^{(r)}$  are the results of the Romberg integration for a particular value of  $s$  that correspond to each potential's integrals in (6.61). These are defined by

$$R_l^{(1)}(s) = \int_0^s j_{l,0}(s') \frac{s'^2}{\gamma'} f_{e,l}(s') ds' \quad (\text{B.6})$$

$$R_l^{(2)}(s) = \int_s^\infty y_{l,0}(s') \frac{s'^2}{\gamma'} f_{e,l}(s') ds' \quad (\text{B.7})$$

$$R_l^{(3)}(s) = \int_0^s j_{l,02}(s') \frac{s'^2}{\gamma'} f_{e,l}(s') ds' \quad (\text{B.8})$$

$$R_l^{(4)}(s) = \int_0^s j_{l,2}(s') \frac{s'^2}{\gamma'} f_{e,l}(s') ds' \quad (\text{B.9})$$

$$R_l^{(5)}(s) = \int_s^\infty y_{l,0}(s') \frac{s'^2}{\gamma'} f_{e,l}(s') ds' \quad (\text{B.10})$$

$$R_l^{(6)}(s) = \int_s^\infty y_{l,02}(s') \frac{s'^2}{\gamma'} f_{e,l}(s') ds' \quad (\text{B.11})$$

$$R_l^{(7)}(s) = \int_0^s j_{l,022}(s') \frac{s'^2}{\gamma'} f_{e,l}(s') ds' \quad (\text{B.12})$$

$$R_l^{(8)}(s) = \int_0^s j_{l,22}(s') \frac{s'^2}{\gamma'} f_{e,l}(s') ds' \quad (\text{B.13})$$

$$R_l^{(9)}(s) = \int_0^s j_{l,2}(s') \frac{s'^2}{\gamma'} f_{e,l}(s') ds' \quad (\text{B.14})$$

$$R_l^{(10)}(s) = \int_s^\infty y_{l,0}(s') \frac{s'^2}{\gamma'} f_{e,l}(s') ds' \quad (\text{B.15})$$

$$R_l^{(11)}(s) = \int_s^\infty y_{l,02}(s') \frac{s'^2}{\gamma'} f_{e,l}(s') ds' \quad (\text{B.16})$$

$$R_l^{(12)}(s) = \int_s^\infty y_{l,022}(s') \frac{s'^2}{\gamma'} f_{e,l}(s') ds' \quad (\text{B.17})$$

$$R_l^{(13)}(s) = \int_0^s j_{l,1}(s') \frac{s'^2}{\gamma'} f_{e,l}(s') ds' \quad (\text{B.18})$$

$$R_l^{(14)}(s) = \int_s^\infty y_{l,1}(s') \frac{s'^2}{\gamma'} f_{e,l}(s') ds' \quad (\text{B.19})$$

$$R_l^{(15)}(s) = \int_0^s j_{l,11}(s') \frac{s'^2}{\gamma'} f_{e,l}(s') ds' \quad (\text{B.20})$$

$$R_l^{(16)}(s) = \int_0^s j_{l,1}(s') \frac{s'^2}{\gamma'} f_{e,l}(s') ds' \quad (\text{B.21})$$

$$R_l^{(17)}(s) = \int_s^\infty y_{l,1}(s') \frac{s'^2}{\gamma'} f_{e,l}(s') ds' \quad (\text{B.22})$$

$$R_l^{(18)}(s) = \int_s^\infty y_{l,11}(s') \frac{s'^2}{\gamma'} f_{e,l}(s') ds'. \quad (\text{B.23})$$

Using (B.6)-(B.23), the first derivatives with respect to  $s$  for (B.1)-(B.5) are given by

$$\frac{\partial \Upsilon_{0,l}}{\partial s} = \frac{\partial y_{l,0}}{\partial s} R_l^{(1)}(s) + \frac{\partial j_{l,0}}{\partial s} R_l^{(2)}(s) \quad (\text{B.24})$$

$$\frac{\partial \Upsilon_{1,l}}{\partial s} = \frac{\partial y_{l,0}}{\partial s} R_l^{(3)}(s) + \frac{\partial y_{l,02}}{\partial s} R_l^{(4)}(s) + \frac{\partial j_{l,02}}{\partial s} R_l^{(5)}(s) + \frac{\partial j_{l,2}}{\partial s} R_l^{(6)}(s) \quad (\text{B.25})$$

$$\begin{aligned} \frac{\partial \Upsilon_{2,l}}{\partial s} &= \frac{\partial y_{l,0}}{\partial s} R_l^{(7)}(s) + \frac{\partial y_{l,02}}{\partial s} R_l^{(8)}(s) + \frac{\partial y_{l,022}}{\partial s} R_l^{(9)}(s) + \frac{\partial j_{l,022}}{\partial s} R_l^{(10)}(s) \\ &+ \frac{\partial j_{l,22}}{\partial s} R_l^{(11)}(s) + \frac{\partial j_{l,2}}{\partial s} R_l^{(12)}(s) \end{aligned} \quad (\text{B.26})$$

$$\frac{\partial \Pi_{0,l}}{\partial s} = \frac{\partial y_{l,1}}{\partial s} R_l^{(13)}(s) + \frac{\partial j_{l,1}}{\partial s} R_l^{(14)}(s) \quad (\text{B.27})$$

$$\frac{\partial \Pi_{1,l}}{\partial s} = \frac{\partial y_{l,1}}{\partial s} R_l^{(15)}(s) + \frac{\partial y_{l,11}}{\partial s} R_l^{(16)}(s) + \frac{\partial j_{l,11}}{\partial s} R_l^{(17)}(s) + \frac{\partial j_{l,1}}{\partial s} R_l^{(18)}(s) \quad (\text{B.28})$$

and the second derivatives are given by

$$\frac{\partial^2 \Upsilon_{0,l}}{\partial s^2} = \frac{\partial^2 y_{l,0}}{\partial s^2} R_l^{(1)}(s) + \frac{\partial^2 j_{l,0}}{\partial s^2} R_l^{(2)}(s) + \left( \frac{\partial y_{l,0}}{\partial s} j_{l,0} - \frac{\partial j_{l,0}}{\partial s} y_{l,0} \right) \frac{s^2}{\gamma} f_{e,l}(s) \quad (\text{B.29})$$

$$\begin{aligned} \frac{\partial^2 \Upsilon_{1,l}}{\partial s^2} &= \frac{\partial^2 y_{l,0}}{\partial s^2} R_l^{(3)}(s) + \frac{\partial^2 y_{l,02}}{\partial s^2} R_l^{(4)}(s) + \frac{\partial^2 j_{l,02}}{\partial s^2} R_l^{(5)}(s) + \frac{\partial^2 j_{l,2}}{\partial s^2} R_l^{(6)}(s) \\ &+ \left( \frac{\partial y_{l,0}}{\partial s} j_{l,02} - \frac{\partial j_{l,02}}{\partial s} y_{l,0} + \frac{\partial y_{l,02}}{\partial s} j_{l,2} - \frac{\partial j_{l,2}}{\partial s} y_{l,02} \right) \frac{s^2}{\gamma} f_{e,l}(s) \end{aligned} \quad (\text{B.30})$$

$$\begin{aligned} \frac{\partial^2 \Upsilon_{2,l}}{\partial s^2} &= \frac{\partial^2 y_{l,0}}{\partial s^2} R_l^{(7)}(s) + \frac{\partial^2 y_{l,02}}{\partial s^2} R_l^{(8)}(s) + \frac{\partial^2 y_{l,022}}{\partial s^2} R_l^{(9)}(s) + \frac{\partial^2 j_{l,022}}{\partial s^2} R_l^{(10)}(s) \\ &+ \frac{\partial^2 j_{l,22}}{\partial s^2} R_l^{(11)}(s) + \frac{\partial^2 j_{l,2}}{\partial s^2} R_l^{(12)}(s) \\ &+ \left( \frac{\partial y_{l,0}}{\partial s} j_{l,022} - \frac{\partial j_{l,022}}{\partial s} y_{l,0} + \frac{\partial y_{l,02}}{\partial s} j_{l,22} - \frac{\partial j_{l,22}}{\partial s} y_{l,02} \right. \\ &\left. + \frac{\partial y_{l,022}}{\partial s} j_{l,2} - \frac{\partial j_{l,2}}{\partial s} y_{l,022} \right) \frac{s^2}{\gamma} f_{e,l}(s) \end{aligned} \quad (\text{B.31})$$

$$\frac{\partial^2 \Pi_{0,l}}{\partial s^2} = \frac{\partial^2 y_{l,1}}{\partial s^2} R_l^{(13)}(s) + \frac{\partial^2 j_{l,1}}{\partial s^2} R_l^{(14)}(s) + \left( \frac{\partial y_{l,1}}{\partial s} j_{l,1} - \frac{\partial j_{l,1}}{\partial s} y_{l,1} \right) \frac{s^2}{\gamma} f_{e,l}(s) \quad (\text{B.32})$$

$$\begin{aligned}
\frac{\partial^2 \Pi_{1,l}}{\partial s^2} &= \frac{\partial^2 y_{l,1}}{\partial s^2} R_l^{(15)}(s) + \frac{\partial^2 y_{l,11}}{\partial s^2} R_l^{(16)}(s) + \frac{\partial^2 j_{l,11}}{\partial s^2} R_l^{(17)}(s) + \frac{\partial^2 j_{l,1}}{\partial s^2} R_l^{(18)}(s) \\
&+ \left( \frac{\partial y_{l,1}}{\partial s} j_{l,11} - \frac{\partial j_{l,11}}{\partial s} y_{l,1} + \frac{\partial y_{l,11}}{\partial s} j_{l,1} - \frac{\partial j_{l,1}}{\partial s} y_{l,11} \right) \frac{s^2}{\gamma} f_{e,l}(s). \tag{B.33}
\end{aligned}$$



CURRICULUM VITAE

# TYLER MARKHAM

(919) 559-9053 ◊ tyler.markham@usu.edu

I am a graduate student at Utah State University studying theoretical and computational plasma physics. I am passionate about everything I do, and enjoy coming up with new solutions to complicated problems.

## EDUCATION

---

**Doctor of Philosophy in Physics** August 2018 - December 2022  
*Utah State University* Logan, UT

Overall GPA: 4.00

**Master of Science in Physics** August 2016 - July 2018  
*Auburn University* Auburn, AL

Overall GPA: 3.33

**Bachelor of Science in Physics (Physics/Math Double Major)** August 2010 - December 2014  
*University of North Carolina at Asheville* Asheville, NC

Overall GPA: 3.39

## RESEARCH EXPERIENCE

---

**Graduate Research Assistant: Computational Plasma Physics** August 2018 - Present  
*Advisor: Eric D. Held, Ph.D* Logan, UT

- Doctoral Thesis Research
- Created a 2D relativistic non-linear kinetic equation solver for the purposes of simulating relativistic runaway electrons in tokamak environments.
- Implemented this solver into the MHD code NIMROD to allow the relativistic kinetic effects of to couple to MHD simulations.

**Graduate Research Assistant: Computational Plasma Physics** August 2016 - July 2018  
*Advisor: Luca Guazzotto, Ph.D* Auburn, AL

- Master's Thesis Research
- Modified existing NIMROD MHD code to allow for hydrodynamic equilibrium calculations.
- Used FLOW code, written by Dr. Guazzotto, to benchmark new hydrostatic equilibrium capabilities in NIMROD.

**Undergraduate Researcher: Theoretical Wave Physics** August 2013 - December 2014  
*Advisor: James Perkins, Ph.D* Asheville, NC

- Developed ab initio theory based on the Feynman derivation of standing waves in a cylinder to account for small fluctuations in cross-sectional area.
- Created numerical solution to variable cross-section wave equation and created time-dependent simulation showing self-interference of waves generated from a point source in the center of the enclosure.

**Pisgah Astronomical Research Institute: Astrophysics Internship** May 2013 - August 2013  
*Supervisors: Brian Dennison, Ph.D and Charles Bennett, Ph.D* Brevard, NC

- Developed the Master Offset Program (MOP) which diagnosed counter-balance issues for two radio telescopes that comprised the Dedicated Interferometer for Rapid Variability (DIRV).
- Determined that new offsets for rastering was needed due to seasonal thermal expansion of the radiotelescopes.

## HONORS/AWARDS

---

- W. Farrell Edward Award
- Blood/Taylor Fellowship
- Sigma Pi Sigma (Physics Honors Society: UNCA)

## PEER-REVIEWED PAPERS

---

**Maxwell-Boltzmann statistics of the quantum ideal gas in the canonical ensemble** October 2020  
*Tyler Markham et al J. Stat. Mech. (2020) 103103*

- Authors: Tyler Markham, Jeong-Young Ji, and Eric D. Held

## NOT PEER-REVIEWED PAPERS

---

**Equilibrium Calculation with Toroidal Flow in NIMEQ** July 2018  
*Master's Thesis/Talk: Auburn University*

- Authors: Tyler Markham, Luca Guazzotto, Eric Howell

**Correcting the Pointing Model** July 2013  
*Paper: 2013 PARI Summer Student Proceedings*

- Authors: Tyler Markham and Adam Shelley

## TALKS

---

**Progress and Plans for the Nonlinear Relativistic Collision Operator** May 2021  
*Talk: NIMROD team meeting*

- Tyler Markham, Eric D. Held, Jeong-Young Ji, and Andrew Spenser

**Relativistic, Continuum DKE: RE Test Particle Operator** October 2020  
*Talk: APS 4CS Conference*

- Tyler Markham, Eric D. Held, Jeong-Young Ji, and Andrew Spenser

**Relativistic, Continuum DKE: RE Test Particle Operator** June 2020  
*Talk: NIMROD team meeting*

- Tyler Markham, Eric D. Held, Jeong-Young Ji, and Andrew Spenser

**Equilibrium Calculation with Toroidal Flow in NIMEQ: Results** May 2018  
*Talk: NIMROD team meeting*

- Tyler Markham, Luca Guazzotto, Eric Howell

**Inhomogeneous Wave Equation Simulation for Variable Cross-Section** December 2014  
*Talk: University of North Carolina at Asheville*

- Tyler Markham and James Perkins